2008

Development of a New Storm Surge Index for Global Prediction of Tropical Cyclone Generated Storm Surge

Mark Rickman Jordan

FLORIDA STATE UNIVERSITY

COLLEGE OF ARTS AND SCIENCES

DEVELOPMENT OF A NEW STORM SURGE INDEX FOR GLOBAL PREDICTION OF TROPICAL CYCLONE GENERATED STORM SURGE

By

MARK RICKMAN JORDAN II

A Dissertation submitted to the
Department of Meteorology
in partial fulfillment of the
requirements for the degree of
Doctor of Philosophy

Degree Awarded:
Summer Semester, 2008

The members of the committee approve the dissertation of Mark R. Jordan II defended on 23 April 2008.

_____
Carol Anne Clayson
Professor Directing Dissertation

_____
Jennifer Georgen
Outside Committee Member

_____
Robert Hart
Committee Member

_____
Paul Ruscher
Committee Member

_____
Peter Ray
Committee Member

_____
Steven Cocke
Committee Member

The Office of Graduate Studies has verified and approved the above named committee members.

ACKNOWLEDGEMENTS

First and foremost, I would like to thank my major professor, Dr. Carol Anne Clayson, for giving me the opportunity to pursue a dream that seemed all but dead two and a half years ago. Thank you for your unending kindness and generosity and for teaching me how to be a respected scientist. You are a saint, and I will never forget what you have done for me. I would also like to thank the other members of my committee, Dr. Robert Hart, Dr. Paul Ruscher, Dr. Peter Ray, Dr. Steve Cocke, and Dr. Jen Georgen for all of their suggestions and support over the years. Each one of you has contributed in your own way toward my success in graduate school, and I am eternally grateful for everything you have done. Furthermore, thank you Dr. Maria (Masha) Luneva for all of your help with this project. I have learned so much from you, and I am fortunate to have been able to collaborate with someone whose passion for her subject is so intense. Finally, I would like to thank my family and friends here and elsewhere, for all of you have provided an endless supply of love and support over the years. I would not be where I am today if it had not been for all of you.

TABLE OF CONTENTS

LIST OF FIGURES vi
LIST OF TABLES x
ABBREVIATIONS AND ACRONYMS xi
ABSTRACT xii
1. INTRODUCTION 1
1.1 Motivation 1
1.2 Literature Review 2
1.3 Physics of Storm Surge 6
1.4 Organization of Dissertation 7
2. OCEAN MODEL DESCRIPTION AND VERIFICATION 9
2.1 Overview 9
2.2 Governing Equations and Forcing 9
2.3 Model Description and Characteristics 10
2.4 Vortex Parameterization 12
2.5 Model Verification and Analysis 13
3. DATA AND METHODOLOGY 18
3.1 Overview 18
3.2 Power-Law Analysis and Theory 18
3.3 Determination of the Appropriate Scaling Parameter 19
3.4 Polynomial Curve Fitting 20
3.5 Verification Data Sets 21
4. RESULTS 25
4.1 Overview 25
4.2 Parameterization of Maximum Wind Speed 25
4.3 Oceanic Response Time and Wind Speed 35
4.4 Radius of Maximum Winds 41
4.5 Translation Speed 46
4.6 Maximum Water Depth 52
4.7 Shelf Length 57
4.8 Pressure 62

4.9 Determination of Final Storm Surge Index....63
5. ERROR ANALYSIS....67
5.1 Overview of Possible Errors....67
5.2 Calculation of Possible Storm Surge Index Error....68
6. CONCLUSIONS....74
6.1 Scientific Value of Dissertation....74
6.2 Societal Value of Dissertation....75
6.3 Future Work....76
REFERENCES....78
BIOGRAPHICAL SKETCH....83

LIST OF FIGURES

1. Map of model domain with bathymetric contours and tracks of tropical cyclones considered in model verification....15

2. Scatter plot of maximum winds at landfall versus areal-averaged observed storm surge heights and model-simulated storm surge heights....16

3. Scatter plot of maximum winds at landfall versus model-simulated storm surge and maximum observed storm surge....17

4. Logarithmic Plot of Maximum Wind vs. Maximum Surge (RMW = 10 km, TS = 2 ms^{-1}, MWD = 20 m, SL = 111 km)....31

5. Logarithmic Plot of Maximum Wind vs. Maximum Surge (RMW = 76.5 km, TS = 2 ms^{-1}, MWD = 20 m, SL = 111 km)....32

6. Logarithmic Plot of Maximum Wind vs. Maximum Surge (RMW = 10 km, TS = 14 ms^{-1}, MWD = 20 m, SL = 111 km)....32

7. Logarithmic Plot of Maximum Wind vs. Maximum Surge (RMW = 10 km, TS = 2 ms^{-1}, MWD = 140 m, SL = 111 km)....33

8. Logarithmic Plot of Maximum Wind vs. Maximum Surge (RMW = 10 km, TS = 2 ms^{-1}, MWD = 20 m, SL = 333 km)....33

9. Logarithmic Plot of Maximum Wind vs. Maximum Surge (RMW = 76.5 km, TS = 14 ms^{-1}, MWD = 140 m, SL = 333 km)....34

10. Sensitivity Experiments Varying MW with Different Constants of RMW, TS, MWD, and SL....34

11. Scatter Plot of Scaled, Maximum Wind Speed at Landfall vs. Observed Maximum Surge Heights....38

12. Scatter Plot of Scaled, 24-Hour, Pre-Landfall Wind Speed Average vs. Observed Maximum Surge Heights....38

13. Scatter Plot of Scaled, 12-Hour, Pre-Landfall Instantaneous Wind Speed vs. Observed Maximum Surge Heights....39

14. Pearson and Spearman Correlations of Scaled, Instantaneous Wind Speeds vs. Observed Storm Surge Heights....39

15. Logarithmic Plot of Radius of Maximum Wind vs. Maximum Surge (MW = 21 ms^{-1}, TS = 2 ms^{-1}, MWD = 20 m, SL = 111 km)....42

16. Logarithmic Plot of Radius of Maximum Wind vs. Maximum Surge (MW = 73 ms^{-1}, TS = 2 ms^{-1}, MWD = 20 m, SL = 111 km).....43

17. Logarithmic Plot of Radius of Maximum Wind vs. Maximum Surge (MW = 21 ms^{-1}, TS = 14 ms^{-1}, MWD = 20 m, SL = 111 km).....43

18. Logarithmic Plot of Radius of Maximum Wind vs. Maximum Surge (MW = 21 ms^{-1}, TS = 2 ms^{-1}, MWD = 140 m, SL = 111 km).....44

19. Logarithmic Plot of Radius of Maximum Wind vs. Maximum Surge (MW = 21 ms^{-1}, TS = 2 ms^{-1}, MWD = 20 m, SL = 333 km).....44

20. Logarithmic Plot of Radius of Maximum Wind vs. Maximum Surge (MW = 73 ms^{-1}, TS = 14 ms^{-1}, MWD = 140 m, SL = 333 km).....45

21. Sensitivity experiments varying RMW with a variety of constant values of MW, TS, MWD, and SL.....45

22. Plot of Translation Speed vs. Maximum Surge (MW = 21 ms^{-1}, RMW = 10 km, MWD = 20 m, SL = 111 km).....48

23. Plot of Translation Speed vs. Maximum Surge (MW = 21 ms^{-1}, RMW = 73 km, MWD = 20 m, SL = 111 km).....49

24. Plot of Translation Speed vs. Maximum Surge (MW = 48 ms^{-1}, RMW = 10 km, MWD = 20 m, SL = 111 km).....49

25. Plot of Translation Speed vs. Maximum Surge (MW = 48 ms^{-1}, RMW = 73 km, MWD = 20 m, SL = 111 km).....50

26. Plot of Translation Speed vs. Maximum Surge (MW = 73 ms^{-1}, RMW = 10 km, MWD = 20 m, SL = 111 km).....50

27. Plot of Translation Speed vs. Maximum Surge (MW = 73 ms^{-1}, RMW = 73 km, MWD = 20 m, SL = 111 km).....51

28. Sensitivity Experiments Varying TS at Different Constant Values of MW, RMW, MWD, and SL.....51

29. Logarithmic Plot of Maximum Water Depth vs. Maximum Surge (MW = 21 ms^{-1}, RMW = 10 km, TS = 2 ms^{-1}, SL = 111 km).....53

30. Logarithmic Plot of Maximum Water Depth vs. Maximum Surge (MW = 73 ms^{-1}, RMW = 10 km, TS = 2 ms^{-1}, SL = 111 km).....54

31. Logarithmic Plot of Maximum Water Depth vs. Maximum Surge (MW = 21 ms^{-1}, RMW = 76.5 km, TS = 2 ms^{-1}, SL = 111 km) 54

32. Logarithmic Plot of Maximum Water Depth vs. Maximum Surge (MW = 21 ms^{-1}, RMW = 10 km, TS = 14 ms^{-1}, SL = 111 km) 55

33. Logarithmic Plot of Maximum Water Depth vs. Maximum Surge (MW = 21 ms^{-1}, RMW = 10 km, TS = 2 ms^{-1}, SL = 333 km) 55

34. Logarithmic Plot of Maximum Water Depth vs. Maximum Surge (MW = 73 ms^{-1}, RMW = 76.5 km, TS = 14 ms^{-1}, SL = 333 km) 56

35. Sensitivity Experiments Varying MWD with Different Constants of MW, RMW, TS, and SL 56

36. Logarithmic Plot of Shelf Length vs. Maximum Surge (MW = 21 ms^{-1}, RMW = 10 km, TS = 2 ms^{-1}, MWD = 20 m) 58

37. Logarithmic Plot of Shelf Length vs. Maximum Surge (MW = 73 ms^{-1}, RMW = 10 km, TS = 2 ms^{-1}, MWD = 20 m) 59

38. Logarithmic Plot of Shelf Length vs. Maximum Surge (MW = 21 ms^{-1}, RMW = 76.5 km, TS = 2 ms^{-1}, MWD = 20 m) 59

39. Logarithmic Plot of Shelf Length vs. Maximum Surge (MW = 21 ms^{-1}, RMW = 10 km, TS = 14 ms^{-1}, MWD = 20 m) 60

40. Logarithmic Plot of Shelf Length vs. Maximum Surge (MW = 21 ms^{-1}, RMW = 10 km, TS = 2 ms^{-1}, MWD = 140 m) 60

41. Logarithmic Plot of Shelf Length vs. Maximum Surge (MW = 73 ms^{-1}, RMW = 76.5 km, TS = 14 ms^{-1}, MWD = 140 m) 61

42. Sensitivity Experiments Varying Shelf Length with Different Constants of MW, RMW, TS, and MWD 61

43. Error Due to Changes in MW (RMW=30 km, Pressure = 970 hPa, Translation Speed = 5 ms^{-1}) 72

44. Error Due to Changes in RMW (MW = 50 ms^{-1}, Pressure = 970 hPa, Translation Speed = 5 ms^{-1}) 72

45. Error Due to Changes in Translation Speed (MW = 50 ms^{-1}, RMW = 30 km, Pressure = 970 hPa) 73

46. Error Due to Changes in Pressure..73

LIST OF TABLES

1. Saffir-Simpson Scale. Categories and associated wind speeds, storm surges, and qualitative damage estimates. (Note: Saffir-Simpson categories are assigned by maximum sustained wind speed. Storm surge values and damage qualifications are just estimates.) 3

2. Hurricanes, landfall years, and associated maximum storm surge heights for each storm. The 1 and 2 following some of the hurricanes names indicates the first and second landfall for that storm, respectively. 22

3. Parameterized Variables along with Lower and Upper Bounds of Each Variable Considered in Model Simulations.....25

4. Landfall wind speeds, scaled landfall wind speeds, and scaled, 24-hour average wind speeds for all hurricane landfalls in the database. The 1, 2, and 3 after some of the storms names indicate multiple landfalls for the same storm. MW_o is 33 ms^{-1}. 28

5. Parabolic Curve Fits Associated With Ranges of Radii of Maximum Wind. TS_o is a normalization constant equal to 5 ms^{-1} 48

6. Various Statistical Parameters associated with the Parameters Determined to be Statistically Significant to the Surge Index Model 64

LIST OF ABBREVIATIONS

A.....normalizing constant
β.....scaling parameter
C_d.....drag coefficient
C_{dbot}.....bottom drag coefficient
η.....sea surface elevation
f.....Coriolis parameter
ft.....feet
g.....gravitational constant
H.....bottom topography
hPa.....hectopascals
IBC.....inverse barometric correction
km.....kilometers
m.....meters
ms^{-1}.....meters per second
MW.....maximum wind
MWD.....maximum water depth
P.....pressure
ρ_a.....air density
ρ_w.....density of water
r.....distance from cyclone's center
r_m.....radius of maximum winds
r_o.....radius where cyclone effects vanish
R^2.....variance
RMW.....radius of maximum winds
s.....seconds
SL.....shelf length
SLOSH.....Sea, Lake, and Overland Surges from Hurricanes
τ.....wind stress
TS.....translation speed
u.....zonal wind speed
U_{10}.....10-meter wind speed
v.....meridional wind speed
V_m.....maximum wind speed
Δz.....water level rise
Δp.....pressure anomaly

ABSTRACT

This research involves the creation of a new storm surge index that incorporates many variables important in storm surge generation like maximum winds, radius of maximum winds, pressure, translation speed, and bathymetry. Using a two-dimensional, barotropic ocean model, power laws have been developed that describe the relationship between storm surge and changes in maximum wind, radius of maximum winds, pressure, and bathymetry. Direct curve fitting is used to describe the relationship between storm surge and changes in translation speed since a power-law relationship does not exist in that case. A database of 39 landfalling, United States hurricanes between 1986 and 2007 is used to evaluate the quality of the index. Storm parameters for all database storms are compiled using the extended best track dataset, and an index value is calculated for each storm in the database. Correlation analysis is then performed using the index values and observed maximum storm surge heights. Finally, an extensive error analysis is presented to demonstrate uncertainties in the index in both forecast and post-analysis situations.

CHAPTER 1

INTRODUCTION

1.1 Motivation

Tropical cyclone generated storm surge is one of the most significant and devastating natural phenomena known to man. Over the past 50 years, storm surge has been responsible for more deaths worldwide than tornadoes, earthquakes, lightning, and fresh-water flooding events combined. In November 1970, the infamous Bhola cyclone made landfall in Bangladesh; the associated storm surge is estimated to have killed 500,000 people (Kabir et al. 2007). In 1991 another cyclone made landfall in Bangladesh, and the associated surge killed 138,000 people (Jones et al. 1993). More recently, Hurricane Katrina made landfall in Louisiana and Mississippi in August 2005. The right-front quadrant of the hurricane passed over the Mississippi coast and generated a 28-foot storm surge. The vast majority of the 238 deaths on the Mississippi coast was storm-surge related, and if only 238 people had died in Katrina, the hurricane would have been the deadliest U.S. hurricane since Hurricane Camille in 1969. Unfortunately, Katrina's storm surge breached levees near New Orleans, Louisiana, and eighty percent of the city flooded as a result of levee failures. Storm surge and related flooding killed 1,577 people in Louisiana, making Katrina the deadliest U.S. hurricane since Florida's Lake Okeechobee hurricane in 1928 (Hunter 2006).

Hurricane Katrina was an anomaly for the United States since hurricane-related deaths have significantly decreased during the last 50 years. The decrease in deaths is primarily due to improved hurricane track and intensity forecasting, which directly impacts predictions of coastal storm surge. Improvements in storm surge prediction have also occurred because of the development of numerical models that can account for various storm-related parameters as well as intricate coastal features. The most prominent storm surge model in the United States is the Sea, Lake, and Overland Surges from Hurricanes (SLOSH) model. The model incorporates storm-related parameters such as pressure, maximum wind speed, radius of maximum winds, and translation speed in addition to geographic parameters such as bathymetry and coastline shape in order to

derive storm surge predictions for specific tropical cyclones (Jarvinen and Neumann 1985). This model is used by the federal government, and model guidance is distributed to various emergency management agencies in coastal locations. However, the vast majority of coastal locations throughout the world does not have access to numerical storm surge models and have very little overall guidance for accurately predicting storm surge. These locations need a relatively simple method for surge prediction that incorporates central pressure, wind speed, radius of maximum winds, translation speed, and bathymetry.

Providing physical and numerical descriptions of the sensitivity of storm surge to changes in the previously mentioned variables would significantly aid surge-prone countries without access to numerical modeling. Such descriptions have led to the development of a new storm surge index that quantifies these sensitivities, and this normalization can provide many countries with their first-ever reliable method of storm surge prediction. Furthermore, with the significant concern today over whether the climate is substantially warming, such an index could be used to describe how storm surge heights could change in a world with stronger, larger storms and increased sea levels. Finally, a modified version of the index could be used in a post-analysis format, especially in situations where precise surge measurements are not available.

1.2 Literature Review

Several storm surge indices have been developed over the past several decades in an effort to simplify the complexities associated with storm surge prediction. Some methods are relatively simple, and other methods attempt to incorporate a wide variety of coastal and storm features. The first, and simplest, method of storm surge prediction, the Saffir-Simpson (SS) Scale, was introduced in the late 1960s and was presented as an easy way of categorizing hurricanes based on wind speed. Associated with the SS Scale are storm surge estimates for each category from one to five. An empirically-derived scale, the SS Scale has many drawbacks for storm surge estimation since it assigns surge estimates based on maximum sustained wind speed and does not account for other storm parameters (Kantha 2006). Furthermore, the SS Scale also does not take into account localized coastal features. To be fair, the U.S. government advocates categorizing storms

based on wind speed and does not encourage storm categorization based on storm surge estimates; official surge forecasts are based on the SLOSH model. However, American culture uses the facets of the SS Scale on a widespread basis for evaluating potential impacts associated with an impending tropical cyclone. Table 1 shows the different aspects of the SS Scale.

Table 1.1: Saffir-Simpson Scale. Categories and associated wind speeds, storm surges, and qualitative damage estimates. (Note: Saffir-Simpson categories are assigned by maximum sustained wind speed. Storm surge values and damage qualifications are just estimates.)

Category	Wind (m.p.h.)	Storm Surge Estimate (ft)	Qualitative Damage Estimate
1	74-95	4-5	Minimal
2	96-110	6-8	Moderate
3	111-130	9-12	Extensive
4	131-155	13-18	Extreme
5	156+	19+	Catastrophic

Another storm surge index that has been proposed incorporates both storm parameters and coastal parameters in order to more accurately account for the complexities of storm surge prediction. The surge index proposed in Russo (1998) incorporates storm features such as central pressure, radius of maximum winds, maximum winds, angle of approach to the coast, and coastal bathymetry. Russo's index appropriately acknowledges that storm surge varies linearly with central pressure; this relationship is due to the inverse barometric effect, which will be discussed later. However, many problems exist with portions of the index and the validation of the index. First, Russo uses curve fitting to simulate the bathymetry of the Atlantic and Gulf coasts. Undoubtedly, many important aspects of the continental shelf slope for individual

locations would be masked by curve fitting. Furthermore, continental shelf slope has been shown to significantly impact storm surge height at the coast. Instead of incorporating information about the entire continental shelf adjacent to a coastal location, Russo chose to only consider water depths up to 18 m. Since the average depth of water at the shelf break is approximately 140 m, it would be inappropriate to only consider a portion of continental shelf because of the assumption of continental slope similarity at all coastal locations beyond the 18 m depth contour. Second, radius of maximum wind information claims to have been included in the index; however, Russo provides no evidence as to how the information was used. There are indications that Russo multiplies the radius of maximum winds with other index terms; however, he provides no evidence that there is a linear relationship between radius of maximum winds and storm surge. Finally, Russo uses a database of landfalling hurricanes and associated surge values for storms between 1893 and 1957. Russo does not provide actual storm surge values or any other parameters associated with the storms he considers.

Next, Kantha (2006) proposes another form of a storm surge index, which he names the Hurricane Surge Index (HSI). The following is the equation for the HSI:

$$HSI = (R / R_o)(V_{\max} / V_{\max 0})^2, \tag{1.1}$$

where R = radius of hurricane-force winds for a particular storm, V_{max} is the maximum sustained winds for a particular storm, and R_o and V_{max0} are normalizing constants of 60 km and 33 ms^{-1}, respectively. Kantha argues that storm surge dependence on wind speed should scale like the square of the wind speed since wind stress is proportional to the square of wind speed. Furthermore, Kantha claims that storm surge should scale linearly with the radius of hurricane-force winds because of hydrostatics, but Kantha does not explain why he chose the radius term to represent radius of hurricane-force winds instead of radius of maximum winds. Jordan and Clayson (2008a) used a database of U.S. landfalling hurricanes between 1986 and 2005 for calculating HSI values and correlating those values with observed maximum storm surge heights. The calculated Pearson correlation is determined to be 0.75, not an insignificant correlation considering the limited number of parameters used in the index. Drawbacks of the index include the lack

of bathymetric information and questions of whether the radius of hurricane-force winds is really a key parameter for determining surge impact.

An outgrowth of Kantha's HSI, the Carville Hurricane Index (CHI), attempts to account for all the destructive forces in a hurricane. Below is the equation for the CHI:

$$CHI = (V_{\max} / V_{\max 0})^3 + 1.5(R / R_o)(V_{\max} / V_{\max 0})^2, \quad (1.2)$$

where all variables and constants are the same as in the HSI. CHI incorporates the effect of wind and storm surge together to evaluate total destructive potential for a given landfalling tropical cyclone (Smith 2006). No explanation is given as to why the cube of wind speed is chosen to represent the destructive potential of wind, but another of Kantha's indices, the Hurricane Damage Index (HDI), incorporates the same term to describe how hurricane damage would scale as a function of wind speed (Kantha 2006). There is no explanation provided as to why the CHI modifies Kantha's HSI by a factor of 3/2. Either way, the CHI has the same problems with accurate surge estimation as Kantha's HSI.

Next, another form of storm surge estimation is suggested by Powell (2007), where tropical cyclone integrated kinetic energy is calculated and related to predictions of storm surge. Powell defines a function, the surge damage potential (S_{DP}), as the following:

$$S_{DP} = 0.676 + 0.43\sqrt{IKE_{TS}} - 0.0176(\sqrt{IKE_{TS}} - 6.5)^2, \quad (1.3)$$

where IKE_{TS} represents the integrated kinetic energy at radii where the maximum sustained winds are at least tropical-storm force. Powell (2007) includes a table that shows S_{DP} for various landfalling tropical cyclones over the past 50 years. The index performs well for many systems, but the order of the index magnitudes frequently does not correspond to the order of storm surge heights, particularly for stronger hurricanes. While the methodology of this index takes into account distribution of winds, this index, like HSI and CHI, does not take into account localized bathymetry issues, which also have a significant role in determining maximum surge for a particular cyclone.

Finally, Hebert (2008) describes the development of another index meant to estimate the destructive potential of a landfalling tropical cyclone through assigning

points based on intensity and wind-field distribution. The Hurricane Severity Index, like the CHI, is meant to describe the destructive potential of both wind and storm surge. The technique assigns a maximum of 25 points for intensity and 25 points for wind-field distribution, making a storm with a total of 50 points, theoretically, the most destructive type of storm. Intensity points are determined by the following formula:

$$SeverityIndex = (V_{\max} / 30kts)^2, \tag{1.4}$$

where V_{max} is the maximum sustained wind speed of the tropical cyclone. Cyclones with less than 30-knot winds are given no points, and cyclones with winds equal to or greater than 150 knots are given the maximum possible 25 points. Distribution of points with respect to wind radii is a bit more complicated. Four different wind radii are considered: 35 kt, 50 kt, 65 kt, and 87 kt. Based on wind radii distribution for all storms in the extended best track database, storms are assigned a number of points based on the size of their wind radii. Maximum points possible for each of the wind radii examined are three, four, eight, and ten, respectively. Therefore, a storm with maximum winds of at least 150 kts and abnormally large wind fields can achieve the 50-point ranking. It is important to note that this index does not provide an actual storm surge height forecast, just a point-system ranking for destructive potential of tropical cyclones. With regards to surge estimation, this index, like many previous indices, ignore the effects of coastal bathymetry, pressure, and translation speed. In a situation where one attempts to quantify surge potential based on scaling parameters, choosing to parameterize only one or two variables can risk ignoring valuable information important in forecasting. Without such information, surge indices will often be plagued with excess scatter and be virtually useless to the scientific community and public.

1.3 Physics of Storm Surge

Tropical cyclone generated storm surge is primarily a function of the transfer of momentum from the atmosphere to the ocean during periods of exceptionally high winds. The increase in water level due to momentum transfer is estimated to account for the vast majority of the realized storm surge at the coast (Hunter 1963). Based on the definition of wind stress curl, momentum is transferred from the atmosphere to the ocean proportional

to the square of the wind speed. Therefore, assuming current estimates of drag coefficients at high wind speeds are reasonable, a tropical cyclone with maximum winds of 33 ms^{-1} will impart significantly less momentum to the ocean as compared to a tropical cyclone with maximum winds of 60 ms^{-1}. The exact percentage of momentum that contributes to realized surge is unknown at this time, as is the time necessary to reach equilibrium under a given sustained wind speed. However, observations and modeling both confirm that storm surge increases when wind increases. Furthermore, this across-shore wind stress enhances the across-shore sea surface slope. Since the sea surface slope is directly proportional to wind stress and inversely proportional to water depth, shallow water tends to enhance surge height farther upslope (Hunter 1963). Additional research that will be discussed in Chapter 4 indicates that the winds need to be blowing over a given area for an extended period in order to generate the equilibrium surge for a given sustained wind speed. In this instance, and throughout this dissertation, equilibrium refers to the maximum possible storm surge associated with a given wind speed, assuming all other factors are constant.

Another factor impacting the height of storm surge is the inverse barometric effect. The inverse barometric effect indicates that for every hPa drop in pressure from mean sea-level pressure (1013.25 hPa), sea level increases about 1 centimeter. This effect is consistent at both lower and higher pressures. For a given tropical cyclone, the average contribution to storm surge from the inverse barometric effect is approximately 40-50 cm. Even for the most intense storms, the contribution is rarely greater than 80 cm. Therefore, the pressure contribution to storm surge is usually around 10 percent of the total storm surge (Hunter 1963).

Other tropical cyclone related parameters and coastal parameters have a significant role in the storm surge realized during a particular tropical cyclone. The importance of factors such as radius of maximum winds, translation speed, pressure, and coastal bathymetry will be discussed in detail later in the dissertation.

1.4 Organization of Dissertation

The dissertation is divided into six chapters. Chapter 1 has discussed the need for a comprehensive storm surge index, provided an overview of various damage and surge

indices, and explained the basic physics behind storm surge. Chapter 2 details the model used for numerical simulations and provides verification of the model's storm surge output. Chapter 3 discusses the methodology used for evaluating numerical simulations and explains the various data sets used for validation of the derived storm surge index. Chapter 4 presents results of all numerical simulations and statistically analyzes those results. Chapter 5 presents a detailed error analysis of the newly-derived storm surge index and discusses possible sources of error associated with the validation data sets. Finally, Chapter 6 discusses conclusions of the dissertation and various areas for future work in storm surge modeling and storm surge index development.

CHAPTER 2
OCEAN MODEL DESCRIPTION AND VERIFICATION

2.1 Overview

This chapter describes the forcing behind tropical cyclone generated storm surge and provides a description of the ocean model used for sensitivity experiments in this project. Furthermore, a description and justification of the vortex parameterization used for this research is provided. Finally, a detailed model verification is provided to show that the ocean model can reasonably reproduce storm surge heights associated with previous tropical cyclones. Such a verification is important to confirm that the model has a reasonable chance at describing the sensitivity of storm surge to changes in governing variables.

2.2 Governing Equations and Forcing

The governing equations are the depth-integrated shallow water equations representing the conservation laws for mass and momentum:

$$\frac{\partial \eta(x,y)}{\partial t} + \frac{\partial u(H(x,y)+\eta(x,y))}{\partial x} + \frac{\partial v(H(x,y)+\eta(x,y))}{\partial y} = 0 \tag{2.1}$$

$$\frac{Du}{Dt} = -g\frac{\partial \eta}{\partial x} - c_{dbot}u + fv \tag{2.2}$$

$$\frac{Dv}{Dt} = -g\frac{\partial \eta}{\partial y} - c_{dbot}v - fu\,, \tag{2.3}$$

where $H(x,y,)$ is the bottom topography, $\eta(x,y)$ is sea surface elevation, f is Coriolis parameter, C_{dbot} is the operator describing bottom friction, g is gravity, u is the zonal wind speed, and v is the meridional wind speed (Kantha and Clayson 1999).

Forcing induced by a hurricane itself, neglecting the effect of waves, can be described by two different terms: the inverse barometric effect and wind shear stresses. The inverse barometric effect describes the rise or fall in sea-surface height due to changes in atmospheric pressure. Once a change in atmospheric pressure occurs, a readjustment of the sea occurs through long gravity waves propagating at a phase speed

of $(gH)^{0.5}$, where g is the gravitational constant, and H is the sea-surface height. The following relationship describes the inverse barometric effect:

$$\Delta z = \frac{\Delta p}{\rho_w g}, \tag{2.4}$$

where Δz is water level rise, Δp is pressure anomaly, and ρ_w is water density. Equation 2.4 shows that, assuming ρ_w and g, remain constant over time and space, the change in sea-surface height due to pressure readjustment is directly proportional to size of the pressure rise or pressure fall (Hunter 1963). This relationship will be important later in developing the pressure term for the new storm surge index. The second forcing mechanism affecting storm surge, wind shear stresses, is described by the following relationship:

$$\tau = C_d \rho_a U_{10}^2, \tag{2.5}$$

where ρ_a is air density; U_{10} is 10-meter wind speed, and C_d is the drag coefficient. This relationship formalizes the explanation as to how wind imparts momentum to the ocean. Assuming that air density remains constant through time and space, the drag coefficient and the square of the wind speed are believed to totally describe momentum transport from the air to the sea. Therefore, the overall factors which would lead to the highest possible storm surge in a particular situation are a large drag coefficient, a large wind speed, and a low atmospheric pressure.

2.3 Model Description and Characteristics

For the purposes of this project, it is necessary to use a model that can reproduce the nonlinearity associated with high storm surges, a model that is adaptive to changes in bottom topography, and a model that is relatively fast in order to permit thousands of sensitivity experiments. The model used for this research is a two-dimensional, barotropic, sigma coordinate, regional ocean model. This model's numerics are derived from the University of Colorado version of the Princeton sigma-coordinate model (Kantha and Clayson, 2000; see also Blumberg and Mellor, 1987). The mixed layer model uses second moment turbulence closure (Kantha and Clayson 1994; Kantha and Clayson 2004), and includes recent developments in turbulence (Kantha 2003). The

CUPOM model has been extensively verified in a number of regions (e.g. Clayson and Luneva, 2004 in the Sea of Japan; Toner et al. 2001, 2003 in the Gulf of Mexico, and in the Indian Ocean as described in Kantha et al. 2007). The modifications made to this basic model for this research are described in the next paragraph.

Baroclinicity is disregarded by solving a shallow-water system of equations (as discussed in Section 2.1). The barotropic forms of the governing equations used in the model are derived by integrating the continuity and momentum equations vertically over the depth of the entire water column. The model uses a horizontal adaptive grid with a resolution of 10 km far from the cyclone's path, decreasing to approximately 2 km along the pre-defined continental shelf and along the cyclone's path. The model allows for the shelf width, bottom topography, and shore curvature to be easily varied. For purposes of time differencing, the model uses a high order predictor-corrector scheme since this scheme resulted in computational stability more often that when using either the Adams-Bashforth or Runge-Kutta time differencing schemes. Furthermore, in an effort to enhance computational efficiency, mode splitting is used for various processes, which allows the use of larger time steps for advection and horizontal diffusion (about 5 min.) and smaller time steps for other terms. For purposes of spatial differencing, second-order, centered finite differencing is used. The model uses the Smagorinsky operator for horizontal viscosity with a horizontal viscosity parameter of 0.07 and background viscosity of 4 m^2s^{-1}.

Boundary conditions include the bottom drag coefficient, which is increased in the shelf zone from 2.5 x 10^{-3} to 5 x 10^{-3}, depending on the strength of the cyclone and the depth of the shelf. The wind-dependent drag coefficient is assigned according to the drag coefficient parameterization proposed by Donelan et al. (2004), where the drag coefficient increases for winds up to approximately 33 ms^{-1} and then levels off in higher wind speeds. A more detailed discussion of drag coefficients is presented in Chapter 3. The model's domain represents the semi-square ocean with size of approximately 10^o latitude by 18^o longitude, with the ability to shape the northern boundary. The interior ocean has a depth of 4000 m, and the shelf is located at the northern boundary.

2.4 Vortex Parameterization

The vortex parameterization used for all model simulations in this research is the Emanuel et al. (2006) cyclone parameterization. This parameterization describes the radial evolution of winds in an ideal cyclone at a level above the friction layer. While this vortex parameterization has not been widely used in meteorological research during the last few years, a comparison with a well-known parameterization, Holland (1980), reveals significant similarities in the wind fields generated by both parameterizations. Furthermore, the Emanuel et al. (2006) parameterization is likely superior to a modified Rankin vortex because of the lack of discontinuity in the derivative of the radial wind profile at the radius of maximum winds. Equation 2.6 shows the Emanuel et al. (2006) vortex parameterization:

$$V^2 = V_m^2 \left(\frac{r_o - r}{r_o - r_m}\right)^2 \left(\frac{r}{r_m}\right)^{2m} \left[\frac{(1-b)(n+m)}{n + m\left(\frac{r}{r_m}\right)^{2(n+m)}} + \frac{b(1+2m)}{1 + 2m\left(\frac{r}{r_m}\right)^{2m+1}}\right], \tag{2.6}$$

where V_m is the maximum wind speed (which includes the effects of the translation speed), r is the distance from the center of the cyclone, r_m is the radius of maximum winds, r_o is a distance from the cyclone's center at which the cyclone's effects vanish, and b, m, and n are parameters that control the shape of the wind profile. For experimentation purposes, b = 0.25, m = 1.6, n = 0.9, and r_o = 1200 km, in accordance with Emanuel et al. (2006). It should be noted, however, that even though the preceding values are held constant for all sensitivity experiments, varying these constants would result in different results compared to the results shown in Chapter 4. Near the center of the hurricane velocity near linearly increases with distance up to a maximum value V_m at the radius of maximum winds and then decays approximately inversely with distance. The vortex is held in gradient wind balance through determining radial pressure gradients in accordance with the gradient wind equation. There is no reduction of the gradient wind to a surface-based wind because this research primarily examines how storm surge scales with respect to changes in variables. Applying a common reduction factor to gradient layer winds does not change the scaling parameters derived later in this dissertation.

Furthermore, even though the radius of maximum winds is generally found at a larger radius above the friction layer, as compared to in the friction layer, no adjustment is attempted to correct for the deficiency for the same reason no adjustment is made to the derived gradient wind.

2.5 Model Verification and Analysis

In order to verify that the model can produce comparable storm surge heights for actual situations, 12 Atlantic tropical cyclones were chosen, and simulations were conducted using wind, size, and translation speed information in the extended best track data from the National Hurricane Center. The tropical cyclones used in the verification are Bonnie (1986), Florence (1988), Chantal (1989), Erin (1995), Opal (1995), Allison (1995), Josephine (1996), Charley (2004), Ivan (2004), Cindy (2005), Wilma (2005), and Humberto (2007) (Gerrish 1986, Guiney 1988, Gerrish 1989, Rappaport 1995, Mayfield 1995, Pasch 1996a, Pasch 1996b, Pasch et al. 2005, Stewart 2005, Stewart 2006, Pasch et al. 2006, Blake 2007). Considering all times during the lives of these storms, maximum wind speeds ranged from 17 ms^{-1} to 75 ms^{-1}, and radii of maximum winds ranged from 7 km to 75 km. Bottom topography was derived from the 1/12 ETOPO database, for which the resolution is $1/36^{o}$. It is important to remember that because a finite differencing technique is employed with the adjustable continental shelf in the model, individual features that are present in the ETOPO dataset are often smoothed out in simulations including adjustable shelf length since the shelf is described by a linear function that increases farther from shore. Minimum depth of the undisturbed sea is set at 1 m, and spin-up time for all tropical cyclones considered in these simulations is 12 hrs.

Figure 2.1 shows the model domain, tracks of all hurricanes used in the verification, and ocean depth contours. Figure 2.2 shows a comparison between the areal-averaged storm surge heights for the hurricanes considered and simulated heights produced by the model. Areal-averaged storm surge heights are initially used for comparison because of the two kilometer spatial resolution of the model near the coastline. The distribution of observed storm surge heights is examined, and if more than one surge height is reported within a km of the maximum surge height location, those observations are averaged. It is important to note than in some situations, there is only

one storm surge observation within the area of the grid cell, so only the maximum surge is used. As is seen in Figure 2.2, the simulated storm surge heights closely resembled the areal-averaged storm surge heights provided in storm reports by the National Hurricane Center. Based on these hurricanes and other tropical storm simulations (not provided), the accuracy of this ocean model is +/- 21 percent. Figure 2.3 shows a comparison between the maximum observed storm surge heights and simulated heights produced by the model. Since verification of a model is generally based on this parameter, it is necessary to show this comparison in addition to the comparison in Figure 2.2. Based on these hurricanes and other tropical storm simulations (not provided), the accuracy of the ocean model using this metric is +/- 40 percent. No other model has published comparisons of storm surges over a large number of hurricanes; however, another widely used storm surge model by the United States government, SLOSH, is claimed to produce storm surge heights that are accurate to +/- 20 percent (Jarvinen and Neumann 1985). The accuracy metric used to describe the SLOSH model is different from the accuracy metric used to describe the ocean model in this project because SLOSH considers distribution of storm surge heights in addition to maximum surge heights. Evaluation of the ocean model for this project only considers maximum surge heights, not distribution of storm surge heights. Based on these comparisons of simulations versus actual storm surge heights it is reasonable to conclude that the model used in this study is capturing the main dynamics of the system, and compares favorably with the government's SLOSH model. Further comparisons of the resulting parameterization are shown in Chapter 5, which demonstrates the capabilities of both the model and the index in reproducing storm surge estimates.

For the purposes of model simulations in the research, two variables are not considered for scaling purposes: shape of the coastline and landfall angle. The shape of the coastline is set as a flat coastline on the northern Gulf of Mexico, and the tropical cyclone intersects the coastline at a 90 degree angle, with no other angles considered. The track of the hurricane is dictated by the starting point and the ending point, and the simulated tropical cyclone propagates with constant characteristics of maximum wind speed, radius of maximum winds, and translation speed until reaching a point three times the radius of maximum winds inland from the coastline. Bathymetry is a more important

consideration compared to either shape of the coastline or landfall angle because without a gradual rise in the seafloor near the coast and associated increase in bottom friction, observed storm surge would always be minimal. On the other hand, while varying shapes of the coastline and landfall angles can cause modest changes in observed surge heights, neither variable is as vital to storm surge production as the bathymetric profile adjacent to the coastline (Harris 1963). Therefore, the only cyclone parameters considering for scaling purposes are the maximum wind speed, radius of maximum winds, and the translation speed.

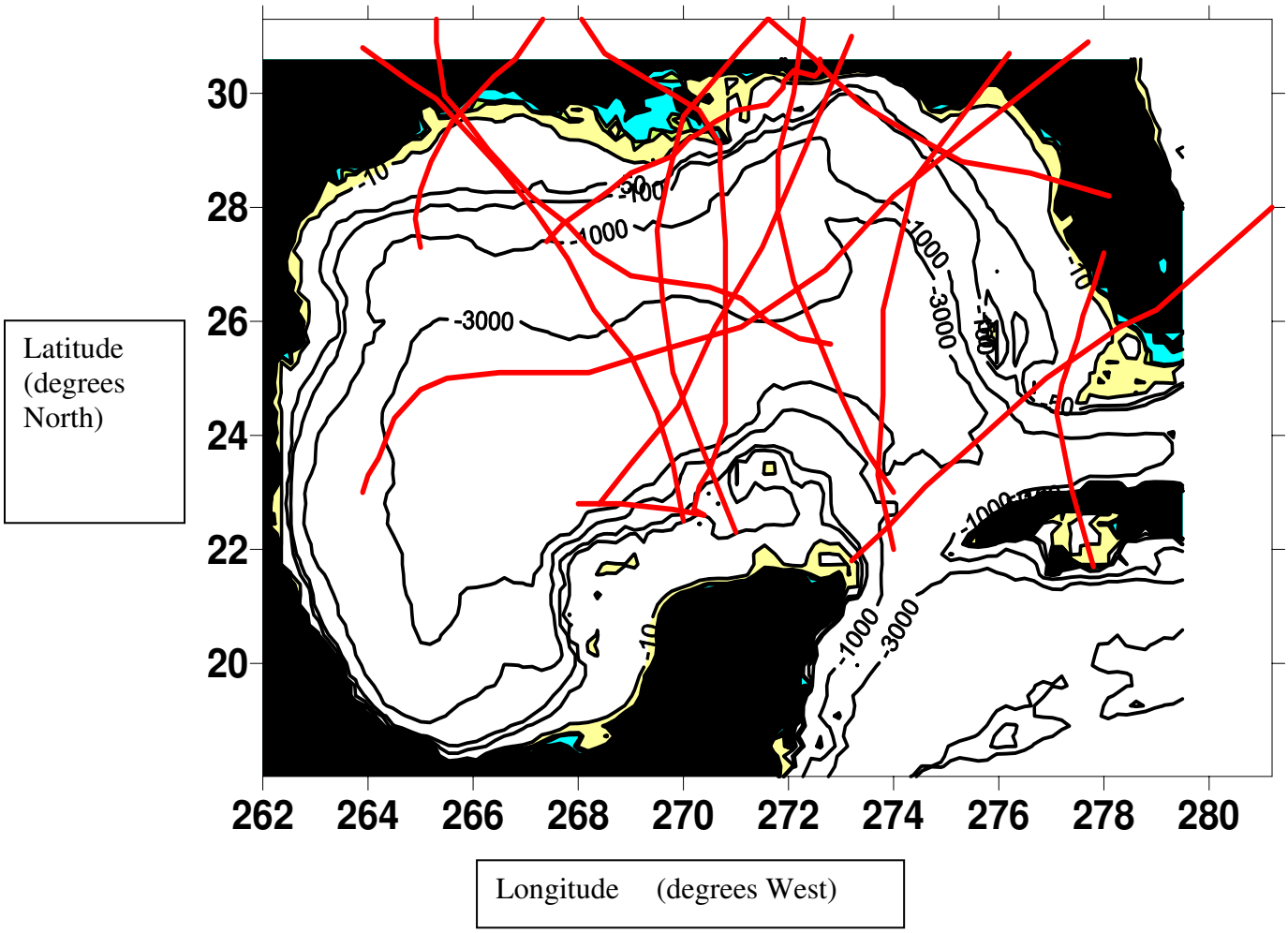

Figure 2.1: Map of model domain with bathymetric contours and tracks of tropical cyclones considered in model verification

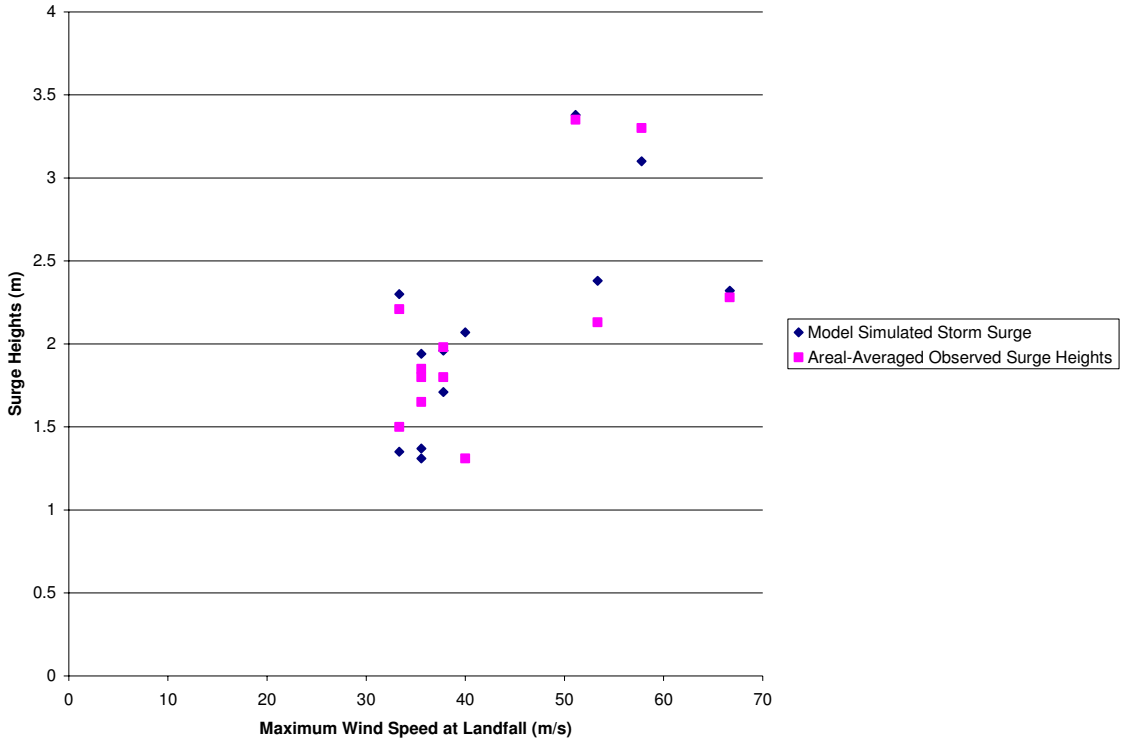

Figure 2.2: Scatter plot of maximum winds at landfall versus areal-averaged observed storm surge heights and model-simulated storm surge heights

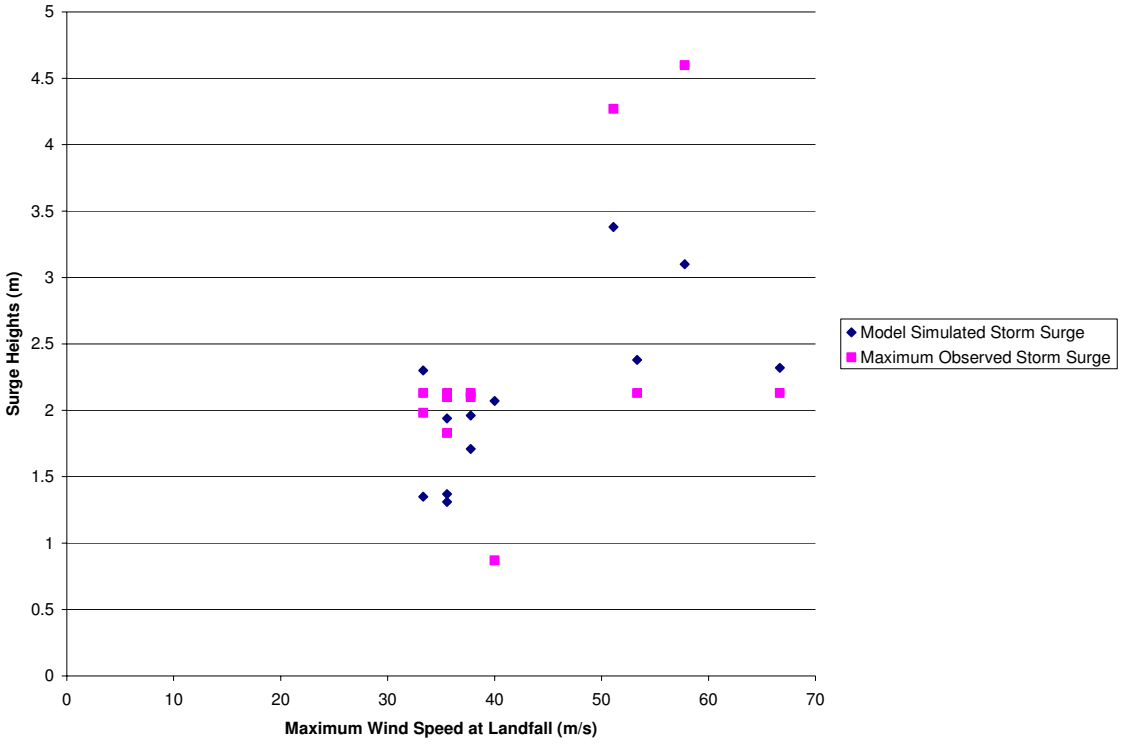

Figure 2.3: Scatter plot of maximum winds at landfall versus model-simulated storm surge and maximum observed storm surge

CHAPTER 3

METHODOLOGY AND DATA SETS

3.1 Overview

The procedure for developing the new storm surge index involves using the numerical model described in Chapter 2 to conduct thousands of sensitivity experiments where power-law relationships are determined that relate changes in storm surge height to changes in maximum wind speed, radius of maximum winds, and bathymetry characteristics. The sensitivity of storm surge to changes in pressure will be discussed separately, and a physically-derived relationship will be presented that simplifies the storm surge/pressure relationship. Finally, it is impossible to derive a power-law relationship to quantify the changes in storm surge to changes in translation speed; therefore, curve fitting was employed in that case to describe the sensitivity relationship.

In order to determine how the storm surge index compares to reality, it is necessary to compile a number of landfalling tropical cyclones that have reliable information concerning maximum wind speed, radius of maximum winds, pressure, translation speed available for data analysis. Furthermore, reliable bathymetry information for the landfall locations needs to be acquired for incorporation into the index. This chapter will detail the theory behind power-law analysis, along with assumptions pertaining to this research, polynomial curve fitting theory, and a description of the various data sets used for comparison of cyclone index values to observed storm surge values.

3.2 Power-Law Analysis and Theory

Power-law analysis is a form of data analysis in the physical sciences; however, many uncertainties exist with assigning power-law relationships to phenomena. In general, a measured quantity x follows a power-law relationship if it is associated with a probability distribution such that

$$p(x) \alpha Ax^{\beta}, \qquad (3.1)$$

where β is the scaling parameter, and A is a scaling constant. The type of power-law distribution that will be considered for purposes of this research is the continuous power-law distribution since all real numbers need to be considered instead of just integers (as is the case with discrete power-law distributions). A continuous power-law distribution is described by the probability distribution ($p(x)$) where

$$p(x)\,dx = \Pr(x \le X \le x + dx) = Ax^{\beta}\,dx\,. \qquad (3.2)$$

In the previous equation, X represents the numerically simulated/measured value. It should be noted that there are two separate bounds on X in Equation 3.2, a maximum and a minimum bound. In a normal continuous power-law distribution, only a minimum bound is set, not a maximum bound (Clauset 2007). In the case of this research, a wide variety of ranges are considered for the variables used in the storm surge index. For example, maximum wind speeds of between 21 ms^{-1} and 73 ms^{-1} are considered. Wind speeds below 21 ms^{-1} are not considered in this research since the focus is on storm surge heights associated with significant storms, not weak tropical storms and tropical depressions. Furthermore, wind speeds in excess of 73 ms^{-1} are not considered, as, through observation, most landfalling tropical cyclones have maximum winds of 73 ms^{-1} or less. Therefore, there is no guarantee that the power-law relationships relating the variables and storm surge are valid beyond the tested values.

3.3 Determination of the Appropriate Scaling Parameter

When the natural logarithm is taken of both sides of Equation 3.1, the following equation is the result:

$$\ln p(x) = \beta \ln x + \ln A\,, \qquad (3.3)$$

When examining a frequency distribution plot produced by Equations 3.1 and 3.3 for an array of variables, if it appears that the distribution is aligned approximately along a straight line, it is reasonable to assume that a power-law relationship exists between the plotted variables (Clauset 2007). In this case, β represents the slope of the line and quantifies the power-law relationship between the two variables. Instead of developing frequency distribution histograms to determine whether power-law relationships are valid

for relating the storm surge index variables and storm surge heights, the natural logarithm of modeled surge values is plotted against the natural logarithm of the chosen variable. Least-squares linear regression is then performed, and the R^2 value of the resultant line is examined. For all linear regressions performed in this research, R^2 values are at least 0.95. Therefore, it is likely, at least for the bounds chosen for the individual variables, that establishing power-law relationships is reasonable where they are considered.

One main concern is noted in the literature regarding the assignment of power-law relationships through using least-squares linear regression. It is possible that for a given set of measurements over many scales of magnitude, a simple linear regression could lead to a high R^2 value even though the relationship between two variables is not a true power law (Clauset 2007). In this research, the range of the variables considered does not span over many orders of magnitude. In fact, none of the variable ranges considered span over even one order of magnitude. Furthermore, there is no assumption that power-law relationships derived in this research are applicable outside of the variable ranges considered in the various experiments. Therefore, while the basic premise of power-law analysis involves deriving universal relationships between variables, there is no assumption of universality for any of the relationships derived in this research.

3.4 Polynomial Curve Fitting

The purpose of curve fitting is to find a polynomial that minimizes the distance between the distribution of data and the polynomial itself. The most appropriate curve fit to a given set of data could be linear, quadratic, cubic, or an even higher-order polynomial. Generally, the desire is to find a fit with as few roots as possible because multiple solutions to a curve-fit equation may exist with higher-order curves. Furthermore, attempting to find a curve that can fit every point in a distribution is not always wise because model noise and measurement error can be the reason for small deviations from a lower-order curve fit. In this research, translation speed is the only variable for which a direct curve fit is attempted, and the curve fit chosen is based on these guidelines and visual inspection (Johnson 2000).

3.5 Verification Data Sets

A quantification of the errors of the storm surge index is achieved by compiling a database of United States landfalling hurricanes between 1986 and 2007. 39 hurricane landfalls are included in the database. Table 3.1 provides a list of hurricanes in the database along with their corresponding maximum storm surge heights. Three hurricane landfalls were excluded from the database because of a lack of maximum observed storm surge data for those storms. The maximum storm surge data for the storms was obtained through tropical cyclone summary reports provided by the National Hurricane Center. The summary reports include reports of maximum wind speed, storm surge, storm tide, and high water mark levels at many locations near the point of landfall (Gerrish 1986, Guiney 1988, Gerrish 1989, Lawrence 1989, Mayfield 1989, Mayfield 1991, Rappaport 1993, Rappaport 1995, Mayfield 1995, Lawrence 1996, Mayfield 1996, Pasch 1997, Avila 1998, Mayfield 1998, Guiney 1998, Pasch et al. 1999, Avila 1999, Lawrence 2003, Beven 2003, Beven and Cobb 2004, Pasch et al. 2004, Beven 2004, Franklin et al. 2005, Stewart 2005, Lawrence and Cobb 2005, Stewart 2006, Beven 2006, Knabb et al. 2006a, Knabb et al. 2006b, Pasch et al. 2006, Blake 2007). Information about maximum winds, radius of maximum winds, pressure, and translation speed is obtained through the extended best track database. Information about those same variables at the time of landfall, however, is obtained through the best track data since the extended best track database only provides 6-hour information, in general, about tropical cyclones (Demuth et al. 2006). One tropical cyclone, Hurricane Humberto, is not included in the most recent version of the extended best track database; storm information parameters for Humberto, therefore, are based on experimental tropical cyclone surface wind analyses provided by the Hurricane Research Division (Powell et al. 1998). Since best track data is available for Humberto, landfall information is available through that data. Bathymetry information is provided by the National Geophysical Data Center's ETOPO2v2 data sets. The results of the error analysis are shown in Chapter 5.

Table 3.1: Hurricanes, landfall years, and associated maximum storm surge heights for each storm. The 1 and 2 following some of the hurricanes names indicates the first and second landfall for that storm, respectively.

Storm Name and Year	Observed Storm Surge Heights (m)
Bonnie-1986	1.58
Florence-1988	1.83
Chantal-1989	1.68
Hugo-1989	6.10
Jerry-1989	1.52
Bob1-1991	1.98
Bob2-1991	2.04
Andrew1-1992	5.21
Andrew2-1992	2.74
Erin1-1995	0.91
Erin2-1995	1.52
Opal-1995	4.27

Table 3.1 (continued)

Storm Name and Year	Observed Storm Surge Heights (m)
Bertha-1996	2.44
Fran-1996	3.66
Danny1-1997	1.52
Danny2-1997	1.22
Danny3-1997	1.22
Bonnie-1998	2.44
Earl-1998	2.44
Georges1-1998	1.52
Georges2-1998	3.63
Floyd-1999	3.14
Irene1-1999	0.61
Irene2-1999	0.91

Table 3.1 (continued)

Storm Name and Year	Observed Storm Surge Heights (m)
Lili-2002	3.35
Claudette-2003	2.80
Isabel-2003	3.20
Charley1-2004	2.13
Frances-2004	2.44
Gaston-2004	2.13
Ivan-2004	4.57
Jeanne-2004	2.90
Cindy-2005	2.16
Dennis-2005	3.05
Katrina1-2005	1.16
Katrina3-2005	8.47
Rita-2005	4.57
Wilma-2005	2.13
Humberto-2007	0.87

CHAPTER 4

RESULTS

4.1 Overview

As mentioned in Chapter 3, the method of determining the sensitivity of storm surge to changes in maximum wind speed, radius of maximum winds, translation speed, bathymetry characteristics, and central pressure is power-law analysis. Each variable and associated analysis will be presented in this chapter along with an examination of how each parameterization affects the overall quality of the storm surge index. This storm surge index will be used to evaluate maximum storm surge, not storm surge distribution. Model simulations are conducted for the ranges of each variable shown in Table 4.1.

Table 4.1: Parameterized Variables along with Lower and Upper Bounds of Each Variable Considered in Model Simulations

Variable	Lower Bound	Upper Bound
Maximum Wind (MW)	21 ms^{-1}	73 ms^{-1}
Radius of Maximum Wind (RMW)	10 km	76.5 km
Translation Speed (TS)	2 ms^{-1}	14 ms^{-1}
Maximum Water Depth (MWD)	20 m	140 m
Shelf Length (SL)	28 km	333 km

4.2 Parameterization of Maximum Wind Speed

Determining the proper power law relationship between maximum wind speed and maximum storm surge involves conducting several hundred experiments varying MW while RMW, TS, MWD, and SL are held constant at lower bound values. Subsequent experiments involve setting each of the constants at its respective upper bound one at a time while varying MW. Finally, all constants are set to their respective upper bounds, and MW is, again, varied. Figures 4.1-4.7 show some representative logarithmic plots of maximum wind speed versus maximum storm surge produced by the model. Linear regression is then performed, and the slope of the individual lines is accepted as the appropriate power-law relationship between wind speed and storm surge in each situation.

For the experiments presented in the figures, the slopes of the lines range from 1.43 to 1.76. For all experiments conducted, the slopes of the lines range from 1.43 to 1.86. These results are encouraging, for, while there is some spread in power-law relationships in different regimes, the spread is not across several orders of magnitude. Furthermore, the R^2 values for all regressed lines are very close to 1. Therefore, it is reasonable to assume that the power-law relationships presented for the different regimes are valid for the ranges of values considered given the limited nature of the range of values. Instead of maintaining the individual power-law relationships for all of the regimes, a multiple linear regression of MW, RMW, MWD, and SL vs. simulated surge heights is performed. For all 7130 experiments conducted, the power law relating MW to simulated storm surge is 1.60. The cost of preserving the power-law relationships for each regime outweighs the benefit, especially considering the small spread in slopes and the desire for the general public to be able to conveniently use the index. Therefore the storm surge will be described as scaling like $MW^{1.60}$.

This numerically-derived, power-law relationship differs from previously published "physically-derived" relationships describing how storm surge varies with wind speed. Kantha (2006), Smith (2006), and Hebert (2008) all describe a quadratic relationship between storm surge and wind speed. Kantha (2006) justifies choosing a quadratic relationship in this instance because the method in which atmospheric momentum is transferred to the ocean is proportional to the square of wind speed; therefore, he reasons that the subsequent response in storm surge height should be proportional the square of wind speed also. This assumption is difficult to justify as very little research has been published that quantifies how oceanic momentum is distributed at various wind speeds, although there is evidence that the distribution of momentum input from the atmosphere between waves and currents alters as wave equilibrium is reached (Moon 2004). Therefore, while the numerical simulations presented in this research show that the relationship varies somewhat depending on other factors, the simulations are consistent in showing that storm surge does not scale like the square of wind speed. Thus, it is felt that it is preferable to use the data from these simulations which can be tested and compared rather than an ad-hoc number based on untested generalizations.

Next, landfall wind speeds for all 39 landfalling hurricanes in the verification database are compiled and used in the calculation of the expression $(MW/MW_o)^{1.60}$, where MW_o is 33 ms^{-1}, to develop a non-dimensional index quantity. An index value is calculated for each storm, and that is value is correlated with the maximum observed storm surge for that particular storm. The resulting Pearson correlation is 0.61, and the Spearman correlation is 0.70. Landfall wind speeds and scaled landfall wind speeds can be found in Table 4.2. Out of instinct, these correlations seem surprisingly low considering that wind is generally regarded as the most important factor in generating storm surge. Ultimately, landfall wind speed only accounts for 37 percent of surge variance when considering a linear relationship, and the metric accounts for 49 percent of surge variance by rank. In order to shed some light on these results, the next section focuses on the effects of the response time of the ocean to changes in wind speed.

To determine whether the correlations calculated are statistically significant, a two-tailed probability test must be conducted. The sample considered in this study has 37 degrees of freedom, and a 0.61 Pearson correlation indicates that there is a greater than 99 percent chance that the relationship between scaled, landfall wind speed and maximum observed storm surge shown here is not a result of chance. The critical correlation value for the 99 percent confidence interval is 0.405. For the Spearman correlation, there is also a greater than 99 percent chance that the relationship is not a result of chance.

Table 4.2: Landfall wind speeds, scaled landfall wind speeds, and scaled, 24-hour average wind speeds for all hurricane landfalls in the database. The 1, 2, and 3 after some of the storms names indicate multiple landfalls for the same storm. MW_o is 33 ms^{-1}.

Storm Name and Year	$MW_{landfall}$ (ms^{-1})	$(MW_{landfall}/MW_o)^{1.60}$	$(\sum_{i=1}^{5} MWi^{1.60}_{avg})/(MW_o^{1.60})$ where MWi refers to the following 5 different intensities: 0, 6, 12, 18, and 24 hours prior to landfall
Bonnie-1986	38.58	1.29	1.07
Florence-1988	36.01	1.15	0.90
Chantal-1989	36.01	1.15	0.97
Hugo-1989	61.73	2.78	2.47
Jerry-1989	38.58	1.29	0.96
Bob1-1991	46.30	1.74	1.81
Bob2-1991	43.73	1.58	1.78
Andrew1-1992	74.59	3.78	3.40
Andrew2-1992	64.31	2.97	2.77
Erin1-1995	38.58	1.29	1.28

Table 4.2 (continued)

Storm Name and Year	$MW_{landfall}$ (ms^{-1})	$(MW_{landfall}/MW_o)^{1.60}$	$(\sum_{i=1}^{5} MWi^{1.60}{}_{avg})/(MW_o^{1.60})$ where MWi refers to the following 5 different intensities: 0, 6, 12, 18, and 24 hours prior to landfall
Erin2-1995	43.73	1.58	1.10
Opal-1995	51.44	2.06	2.30
Bertha-1996	46.30	1.74	1.38
Fran-1996	51.44	2.06	2.09
Danny1-1997	33.44	1.02	0.72
Danny2-1997	36.01	1.15	0.84
Danny3-1997	33.44	1.02	1.10
Bonnie-1998	48.87	1.90	1.98
Earl-1998	36.01	1.15	1.19
Georges 1-1998	46.30	1.74	1.49

Table 4.2 (continued)

Storm Name and Year	$MW_{landfall}$ (ms^{-1})	$(MW_{landfall}/MW_o)^{1.60}$	$(\sum_{i=1}^{5} MWi^{1.60}{}_{avg})/(MW_o^{1.60})$ where MWi refers to the following 5 different intensities: 0, 6, 12, 18, and 24 hours prior to landfall
Georges 2-1998	46.30	1.74	1.81
Floyd-1999	46.30	1.74	1.93
Irene1-1999	33.44	1.02	0.95
Irene2-1999	36.01	1.15	1.01
Lili-2002	41.16	1.43	2.28
Claudette-2003	41.16	1.43	1.04
Isabel-2003	46.30	1.74	1.72
Charley1-2004	66.88	3.16	2.26
Frances-2004	46.30	1.74	1.70
Gaston-2004	33.44	1.02	0.82
Ivan-2004	54.02	2.23	2.46

Table 4.2 (continued)

Storm Name and Year	$MW_{landfall}$ (ms^{-1})	$(MW_{landfall}/MW_o)^{1.60}$	$(\sum_{i=1}^{5} MWi^{1.60}{}_{avg})/(MW_o^{1.60})$ where MWi refers to the following 5 different intensities: 0, 6, 12, 18, and 24 hours prior to landfall
Jeanne-2004	54.02	2.23	2.02
Cindy-2005	33.44	1.02	0.71
Dennis-2005	54.02	2.23	2.42
Katrina1-2005	36.01	1.15	0.79
Katrina3-2005	54.02	2.23	3.16
Rita-2005	51.44	2.06	2.31
Wilma-2005	54.02	2.23	1.90
Humberto-2007	38.58	1.29	0.71

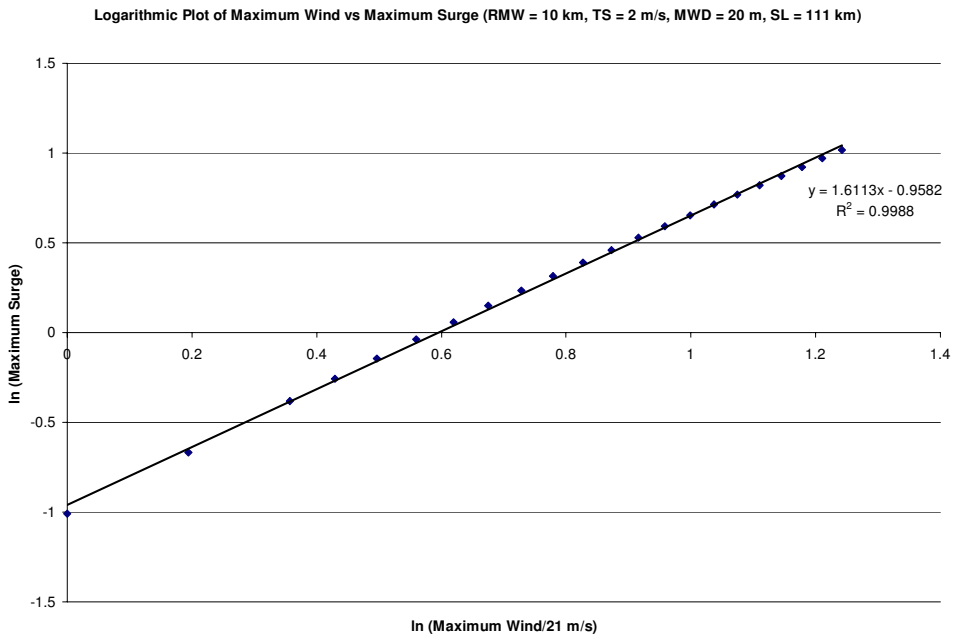

Figure 4.1: Logarithmic Plot of Maximum Wind vs. Maximum Surge (RMW = 10 km, TS = 2 ms^{-1}, MWD = 20 m, SL = 111 km)

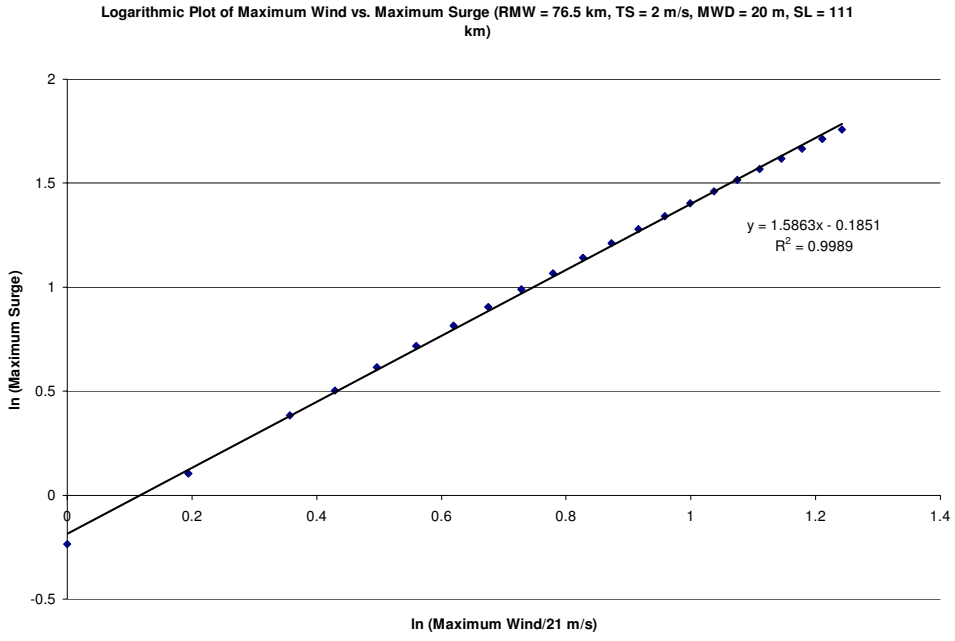

Figure 4.2: Logarithmic Plot of Maximum Wind vs. Maximum Surge (RMW = 76.5 km, TS = 2 ms^{-1}, MWD = 20 m, SL = 111 km)

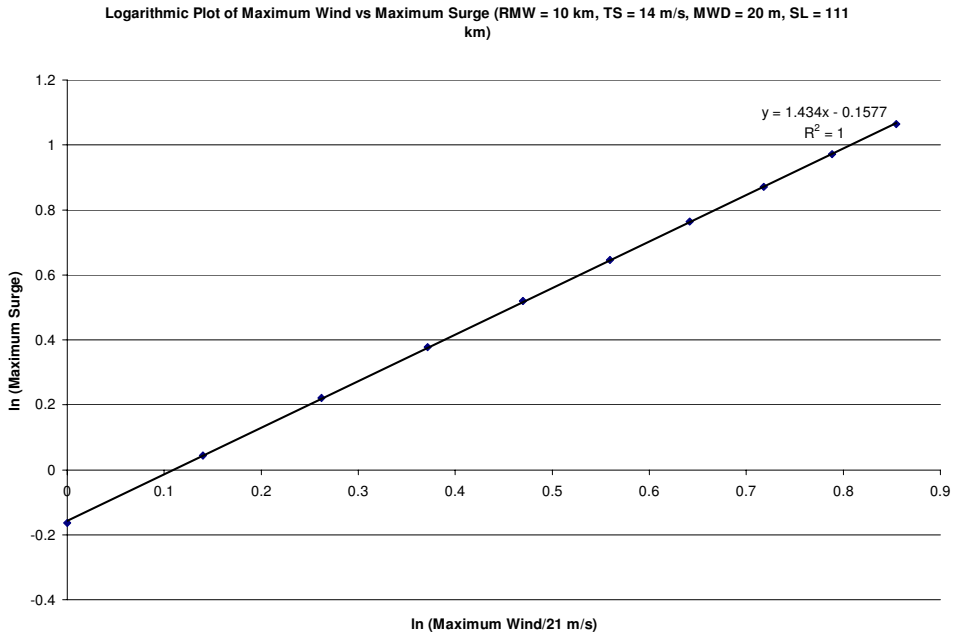

Figure 4.3: Logarithmic Plot of Maximum Wind vs. Maximum Surge (RMW = 10 km, TS = 14 ms^{-1}, MWD = 20 m, SL = 111 km)

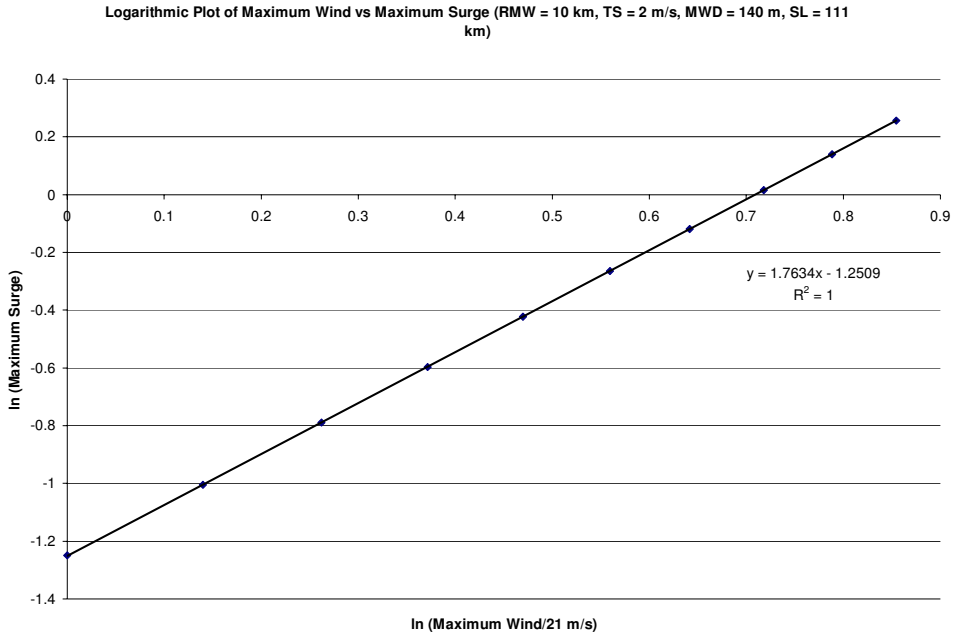

Figure 4.4: Logarithmic Plot of Maximum Wind vs. Maximum Surge (RMW = 10 km, TS = 2 ms^{-1}, MWD = 140 m, SL = 111 km)

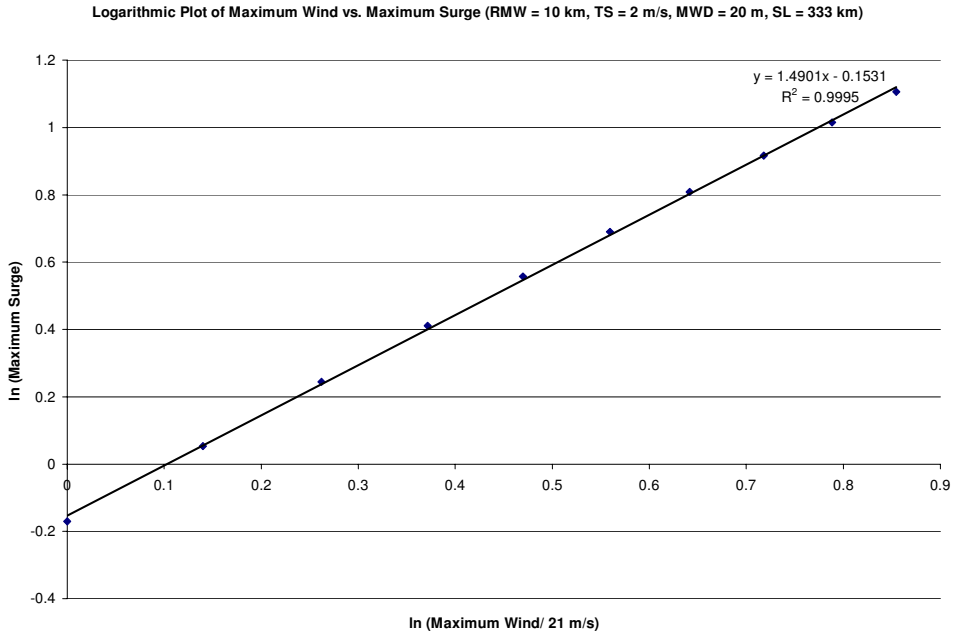

Figure 4.5: Logarithmic Plot of Maximum Wind vs. Maximum Surge (RMW = 10 km, TS = 2 ms^{-1}, MWD = 20 m, SL = 333 km)

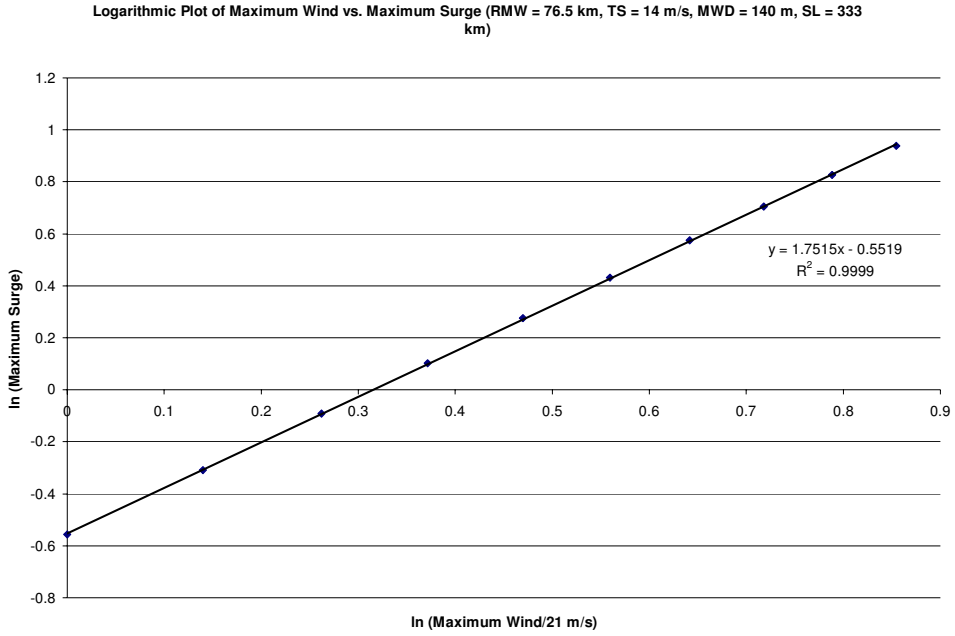

Figure 4.6: Logarithmic Plot of Maximum Wind vs. Maximum Surge (RMW = 76.5 km, TS = 14 ms^{-1}, MWD = 140 m, SL = 333 km)

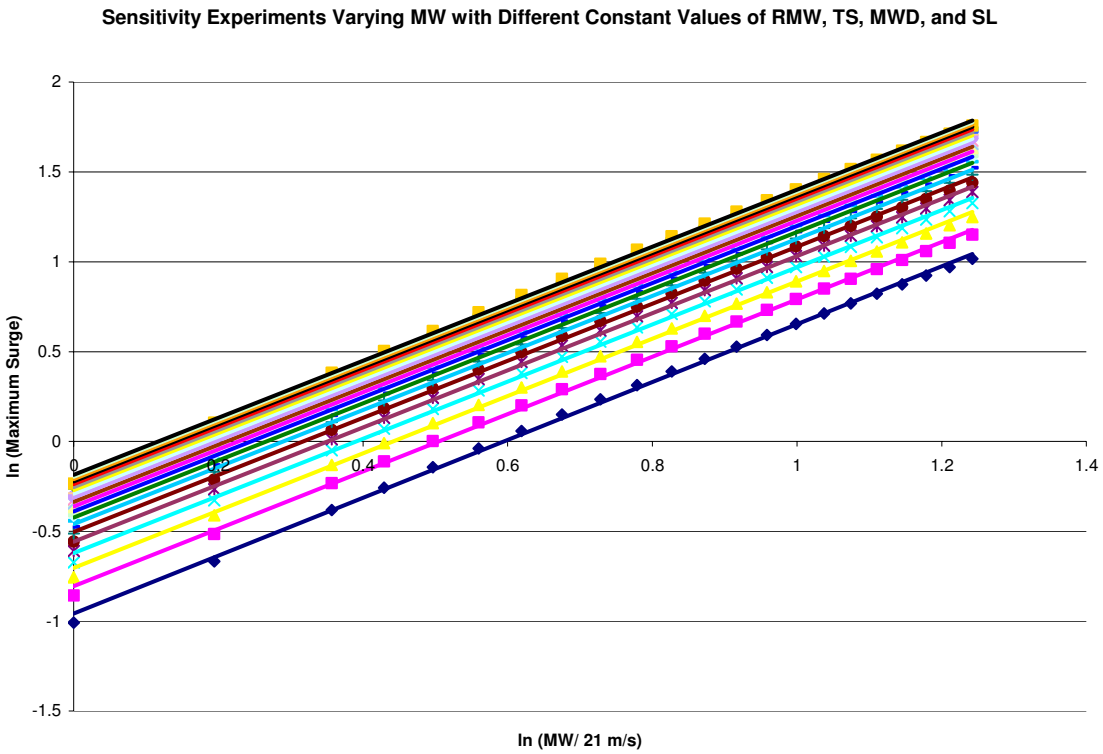

Figure 4.7: Sensitivity Experiments Varying MW with Different Constants of RMW, TS, MWD, and SL

4.3 Oceanic Response Time and Wind Speed

During the past several years, many hurricanes that have quickly strengthened or weakened within hours of landfall have significantly trailed/exceeded official government storm surge forecasts. For example, Hurricane Katrina in 2005 weakened significantly during the 12 hours prior to landfall in Mississippi. As the storm began to weaken, NHC storm surge forecasts were lowered from 28 feet to 15-20 feet (http://www.nhc.noaa.gov/archive/2005/pub/al122005.public.027.shtml?). However, Hurricane Katrina produced a maximum storm surge of 28 feet on the Mississippi coast even though the storm had weakened from a strong Category 5 storm to a Category 3 storm. Hurricanes Charley and Wilma, on the other hand, significantly strengthened within the 12 hours prior to landfall. Official storm surge forecasts stated a 15-18 foot storm surge was expected from each storm (http://www.nhc.noaa.gov/archive/2004/pub/al032004.public.018.shtml?;

http://www.nhc.noaa.gov/archive/2005/pub/al242005.public.036.shtml?). However, both storms produced significantly less storm surge than expected, as each storm produced a maximum storm surge of around 7 feet. Other instances of these trends are noted in historical databases, and this observation prompts the question of whether pre-landfall intensity is a major factor in realized storm surge at the coast.

The methodology for evaluating the effects of pre-landfall intensity on storm surge is as outlined in Jordan and Clayson (2008b), and is reproduced here. The first test to determine whether pre-landfall intensity is important in producing storm surge at the coast involves pre-landfall intensity averaging. For all 39 storms in the database, landfall intensity, 6-hour, pre-landfall intensity, 12-hour, pre-landfall intensity, 18-hour, pre-landfall intensity, and 24-hour, pre-landfall intensity is obtained, and each intensity is scaled based on the power-law relationship between surge and wind speed that was derived in Section 4.2. The scaled intensities are averaged and normalized, as in Section 4.2, and correlations of the scaled and normalized average intensities and observed maximum storm surges are calculated. The Pearson correlation using this new metric is 0.80, and the Spearman correlation is 0.79. Therefore, using an average of pre-landfall intensities explains 64 percent of the variance in storm surge using a linear relationship while the new metric explains 62 percent of storm surge variance by rank. Scatter plots of landfall intensity vs. observed surge and pre-landfall intensity averages vs. surge are found in Figures 4.8 and 4.9, respectively. It is important to consider that using pre-landfall intensity averages improves surge variance explanation by 27 percent when using a linear relationship, and the pre-landfall intensity averages improve variance explanation by 13 percent when considering rank. Using pre-landfall intensity averages also decreases the standard deviation of the error compared to using landfall intensity. The standard deviation of the surge height error when using landfall intensity is 0.46 m while using pre-landfall intensity averages produces a surge-height error standard deviation of 0.33 m.

Next, in an attempt to make sure that outliers are not skewing the previous Pearson correlations, the three storms with the highest observed storm surge (Hugo, Andrew, and Katrina) are removed from the database, resulting in 36 samples. Landfall intensities and pre-landfall intensity averages are scaled and normalized, and the resulting

Pearson correlations are 0.55 and 0.76, respectively. Therefore, even though both correlations decreased by removing extreme outliers, strong evidence exists that pre-landfall intensity provides a better estimate of observed maximum storm surge. In fact, as is the case when the outliers are included, 27 percent more of the surge variance is explained using the pre-landfall intensity averages, as compared to landfall intensity.

Finally, other correlations were performed to determine whether another pre-landfall wind speed average would correlate better than the scaled and normalized, 24-hour, pre-landfall wind speed average. Furthermore, instantaneous wind speeds from 6 to 36 hours prior to landfall were also correlated with observed surges to determine whether the averages were masking a higher correlation with one of the instantaneous wind speeds. First, scaled and normalized 12-hour and 36-hour pre-landfall wind speed averages were correlated with observed storm surges. Pearson correlations for these scenarios are 0.76 and 0.73, respectively. Therefore, it appears that the scaled and normalized, 24-hour, pre-landfall wind speed average best represents the potential maximum storm surge with a landfalling tropical cyclone. Pearson correlations of instantaneous cyclone intensity at 6-hour intervals from 6 to 36 hours prior to landfall and observed storm surges indicate that the 12-hour, pre-landfall instantaneous wind speed has the highest correlation at 0.8. Standard deviation of the surge-height error using the 12-hour, pre-landfall instantaneous wind speed is 0.34 m, almost identical to the standard deviation of the surge-height error using the 24-hour, pre-landfall average. Figure 4.10 shows a scatter plot of scaled and normalized 12-hour, pre-landfall wind speed versus observed storm surge. Figure 4.11 shows Pearson and Spearman correlations for scaled and normalized instantaneous wind speeds versus observed storm surges. Bias calculations have also been performed using landfall intensity, 12-hour, pre-landfall intensity, and a 24-hour, pre-landfall average intensity. Bias is defined here as the ratio of the forecast value to the observed value, and for each of the three cases, the bias is 1.20, 1.18, and 1.00, respectively. Therefore, in addition to providing the highest correlations, the 24-hour, pre-landfall average intensity reduces the forecast bias by about 17 percent. Therefore, this sample of landfalling U.S. hurricanes indicates that using cyclone intensity 12 hours before landfall is just as good of an indicator of maximum storm surge as using a 24-hour, pre-landfall intensity average. As far as statistical significance of the

derived correlations, all correlations are statistically significant at the 99 percent confidence interval. Therefore, there is a less than 1 percent chance that the relationship between scaled, average wind speed and storm surge is insignificant.

These results also indicate something more fundamental about the way meteorologists and oceanographers understand storm surge generation. Numerical models and other storm surge indices use landfall intensity as the intensity most important for prediction of potential storm surge heights. Naturally, if a tropical cyclone impacts land after having maintained the same intensity for 3 days, then landfall intensity would be an appropriate metric. However, for tropical cyclones that significantly weaken or strengthen within a short period prior to landfall, these results indicate that it is vital to consider more than just landfall intensity in order to produce a better prediction of possible storm surge. Therefore, it may be important to reconsider the intensity metric to use in numerical models and other storm surge indices in order to more accurately predict storm surge heights.

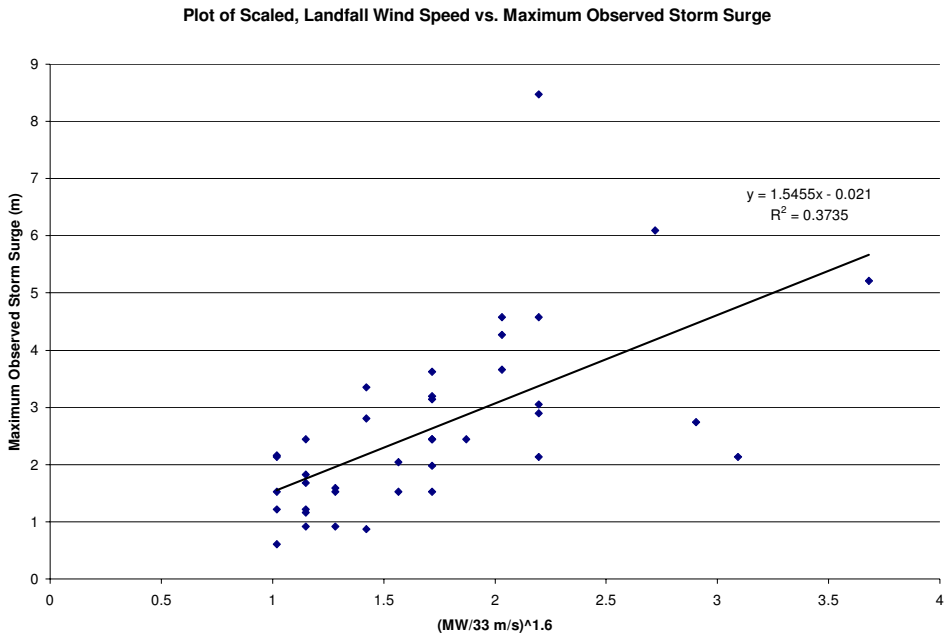

Figure 4.8: Scatter Plot of Scaled, Maximum Wind Speed at Landfall vs. Observed Maximum Surge Heights

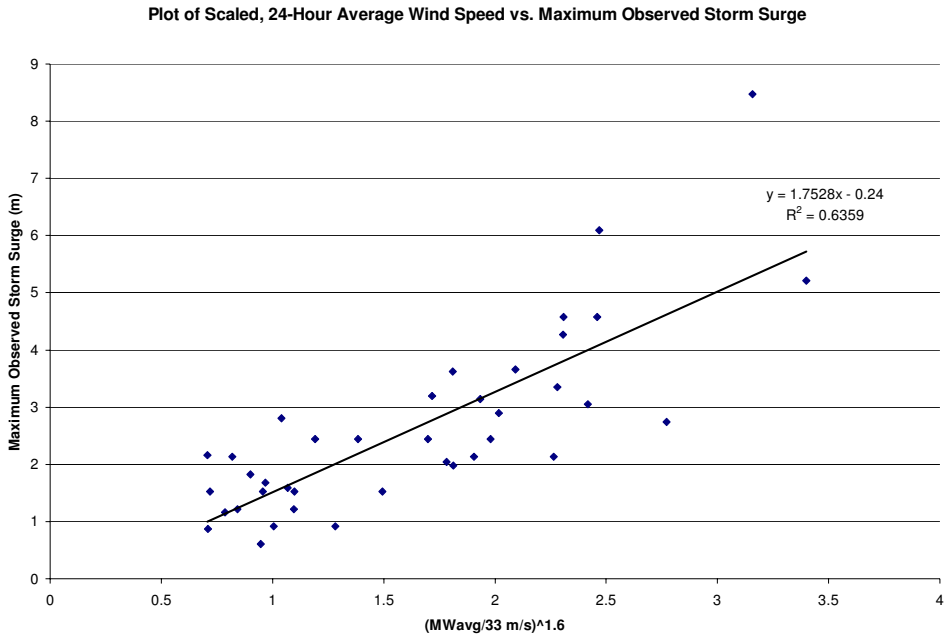

Figure 4.9: Scatter Plot of Scaled, 24-Hour, Pre-Landfall Wind Speed Average vs. Observed Maximum Surge Heights

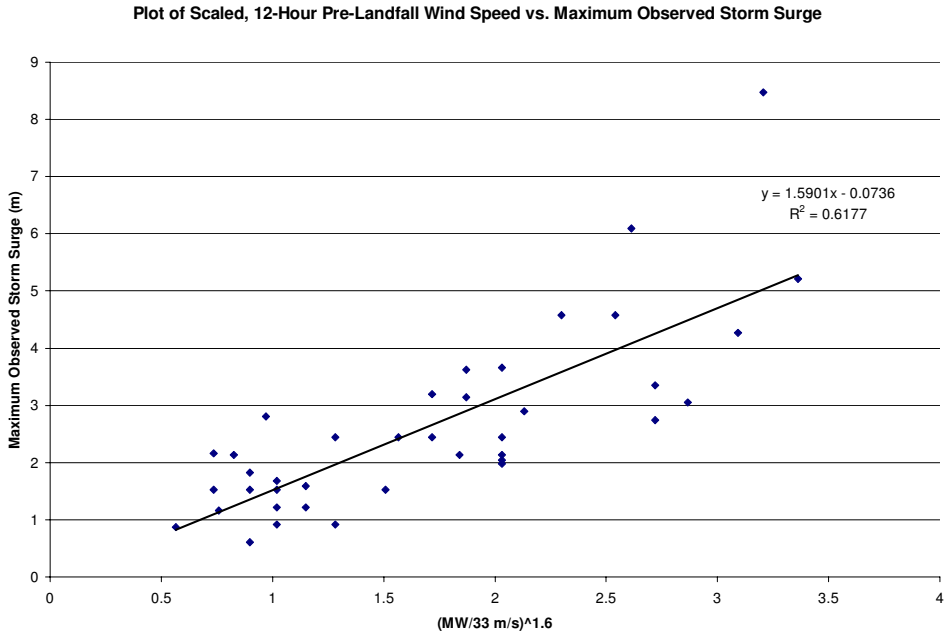

Figure 4.10: Scatter Plot of Scaled, 12-Hour, Pre-Landfall Instantaneous Wind Speed vs. Observed Maximum Surge Heights

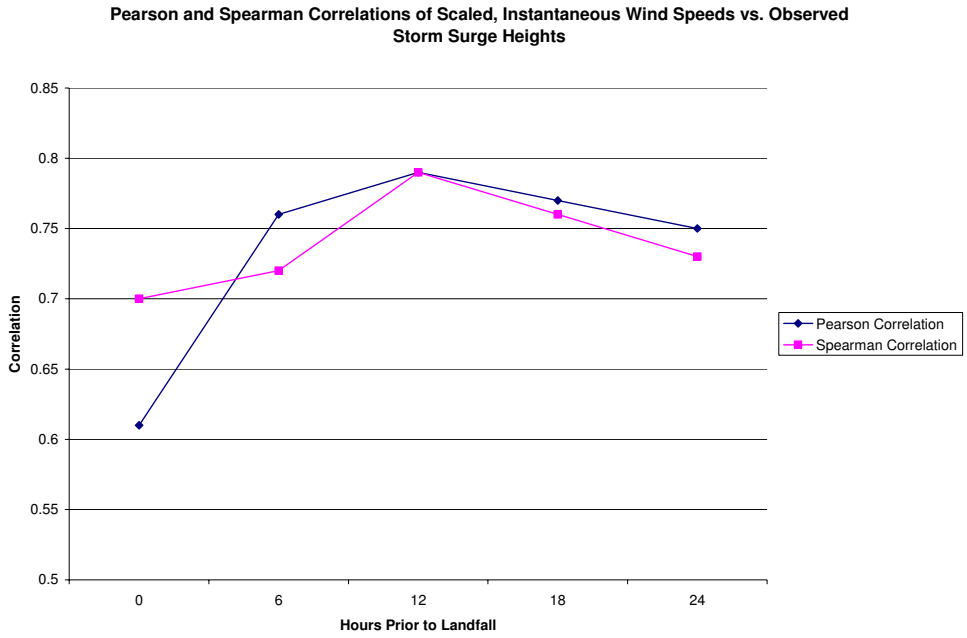

Figure 4.11: Pearson and Spearman Correlations of Scaled, Instantaneous Wind Speeds vs. Observed Storm Surge Heights

The natural question at this point is why would pre-landfall intensity have such an impact on storm surge heights at the time of landfall. To answer the question, it is necessary to return to what causes storm surge in the first place. There are two major factors: changes in atmospheric pressure and wind stress. The contribution to surge from the inverse barometric effect may explain a small portion of the storm surge when pre-landfall intensity is a significant factor. Therefore, the most likely explanation for why pre-landfall intensity is important involves the transfer of momentum from the air to the ocean and subsequent use of that momentum to generate storm surge. That momentum could well be distributed through a variety of processes such as wind-driven surge, Ekman transport, wave run-up, or wave stress. The general equation that describes how the atmosphere transfers momentum to the ocean is the following:

$$\tau = C_d \rho_a U_{10}^{\ 2}, \qquad (4.1)$$

where τ is wind stress; C_d is the drag coefficient; ρ_a is air density, and U_{10} is the 10-meter wind speed. First, it is necessary to confirm that stronger tropical cyclones would impart a greater wind stress to the ocean. Air density is not going to change appreciably since baroclinicity is rare near tropical cyclones. Since wind stress is proportional to the square of the wind speed, a higher wind speed would produce a greater wind stress. The only other factor to consider is the drag coefficient, which is discussed extensively in Chapter 2.

Assuming that an increase in wind speed will always lead to an increase in total momentum available to the ocean, quantifying the percentage of momentum that is distributed between developing a mature wave field and the ocean current is vital. Edson (1998) and Moon (2004) show that the percentage of total momentum distributed to developing a mature wave field is somewhere between 3 and 5 percent while between 95 and 97 percent of the total momentum is imparted to the ocean currents. Therefore, assuming a quickly strengthening tropical cyclone impacts the coast before a mature wave field is developed, the ocean current will not reach the equilibrium associated with the new, higher wind speed. In that case, the maximum possible storm surge associated with the new wind speed cannot be realized. However, 3-5 percent of the total momentum is a very small portion, so that portion could not reasonably account for 10-foot disparities between realized storm surge and predicted storm surge. Therefore, at a given wind speed, the ocean current must require a certain amount of time to reach equilibrium, and if that equilibrium is not achieved before a cyclone crosses the coast, then the observed surge will either be lower or higher than the equilibrium associated with the new wind speed depending on whether the cyclone was initially much weaker or much stronger. From examining the validation database, this time requirement is based on the amount of intensity and size change. Therefore, using an average, pre-landfall wind speed for storm surge prediction is wise until additional research can be conducted to determine the amount of time needed for the ocean current to reach equilibrium under a variety of circumstances.

4.4 Radius of Maximum Winds

Deriving the appropriate power-law relationship between storm surge and radius of maximum winds involves employing the same methods used when deriving the power-law relationship between storm surge and maximum wind speed. Many sensitivity experiments are conducted over a range of radii of maximum winds while holding MW, TS, MWD, and SL constant. Subsequently, the same range of radii is examined at other constant values of the previously mentioned variables to assure that the derived relationships are appropriate. Figures 4.12-4.18 show logarithmic plots of radius of maximum wind versus storm surge. The slope of the regressed line represents the accepted power-law relationship between RMW and storm surge in each of the presented situations. For all experiments conducted, the slopes range from 0.13-0.44. Since R^2 values are either equal to or very close to 1 in all experiments, the power-law relationships are accepted as valid. Using multiple linear regression, the appropriate power law relating RMW and maximum storm surge is 0.33. Therefore, the RMW term in the storm surge index is $(RMW/RMW_o)^{0.33}$, where RMW_o is a normalizing constant of 10 km.

For purposes of evaluating the usefulness of the RMW term in the storm surge index, a scaled and normalized 24-hour average of RMW is used for the same reasons presented in Section 4.3. A larger RMW occupies a larger surface area and imparts more momentum to the ocean over a larger area. Surprisingly, however, the Pearson correlation of a scaled RMW average and observed storm surge is only 0.07. Using landfall RMW, the Pearson correlation is slightly lower. The low correlations using both landfall and pre-landfall RMW are probably are result of the lack of data, especially when considering the calculations are made when all other factors are held constant. With a larger database, it would be possible to examine varying RMW values at the same wind speed to determine the effect of the RMW on storm surge. The Pearson correlation between RMW and storm surge is not significant at the 90 percent confidence level; however, when viewed in light of other factors (constant wind speed, etc…), there may exist a statistically significant relationship between RMW and storm surge.

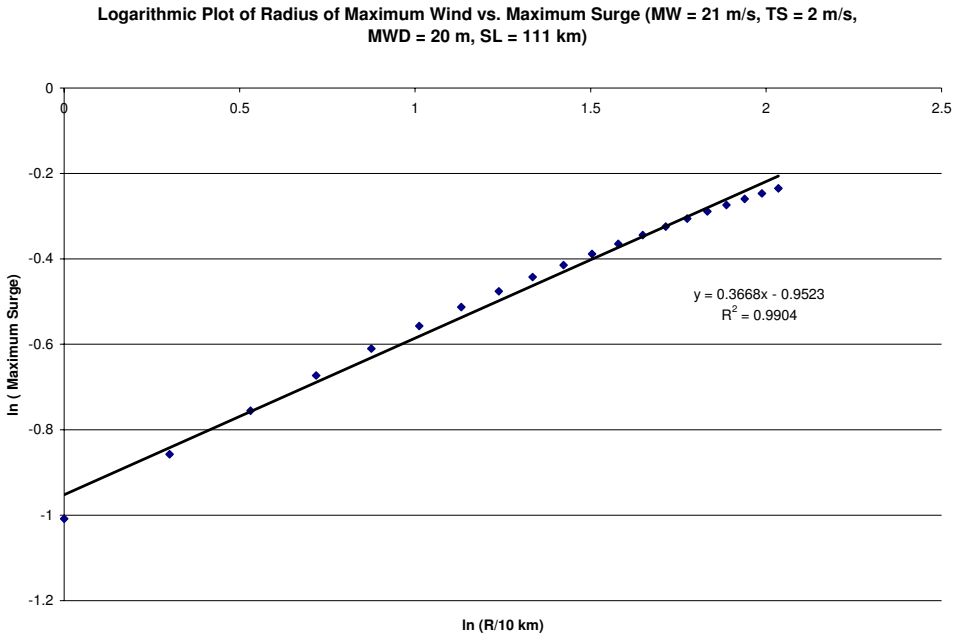

Figure 4.12: Logarithmic Plot of Radius of Maximum Wind vs. Maximum Surge (MW = 21 ms^{-1}, TS = 2 ms^{-1}, MWD = 20 m, SL = 111 km)

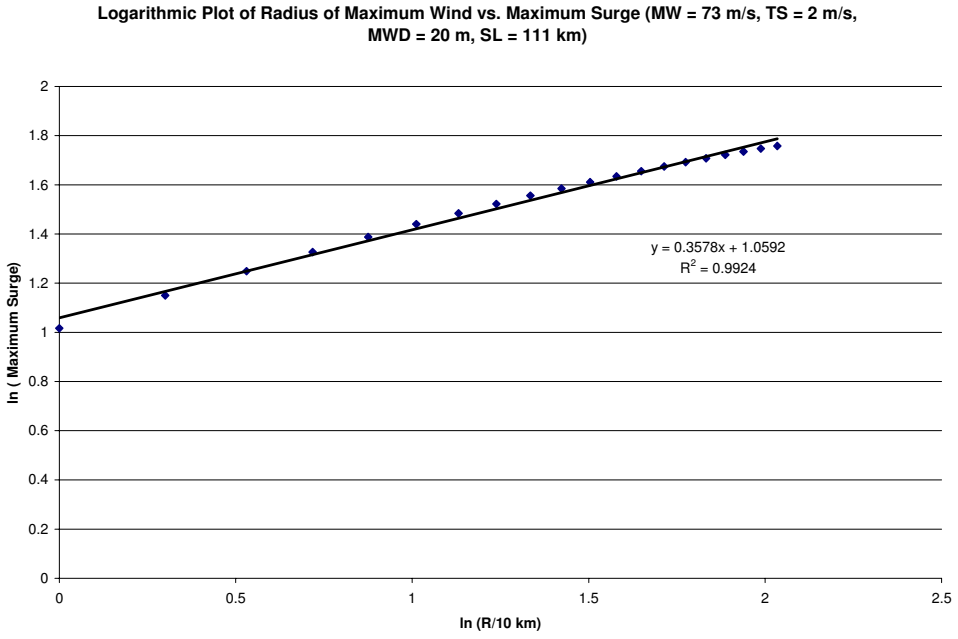

Figure 4.13: Logarithmic Plot of Radius of Maximum Wind vs. Maximum Surge (MW = 73 ms^{-1}, TS = 2 ms^{-1}, MWD = 20 m, SL = 111 km)

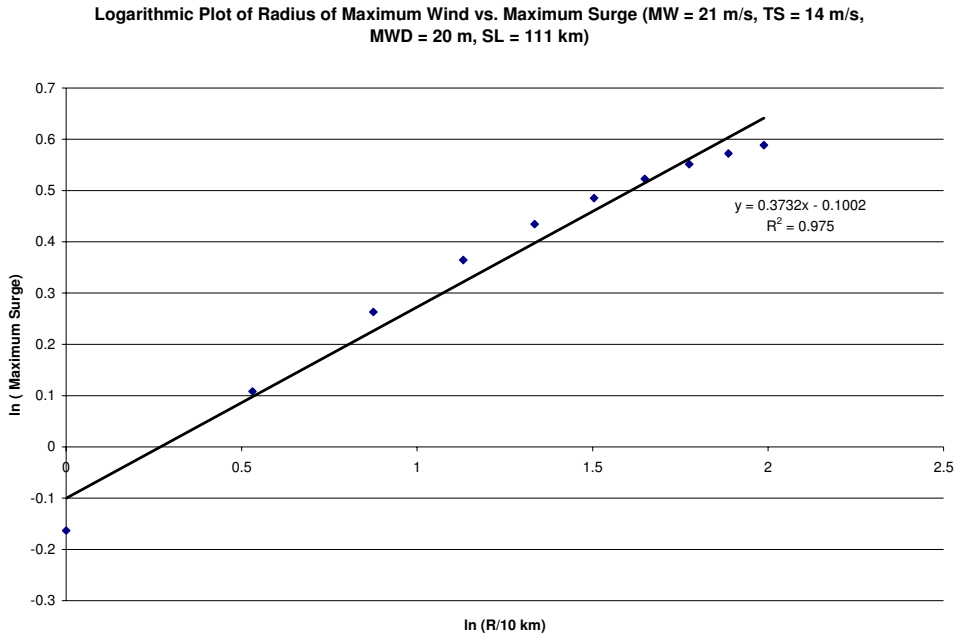

Figure 4.14: Logarithmic Plot of Radius of Maximum Wind vs. Maximum Surge (MW = 21 ms^{-1}, TS = 14 ms^{-1}, MWD = 20 m, SL = 111 km)

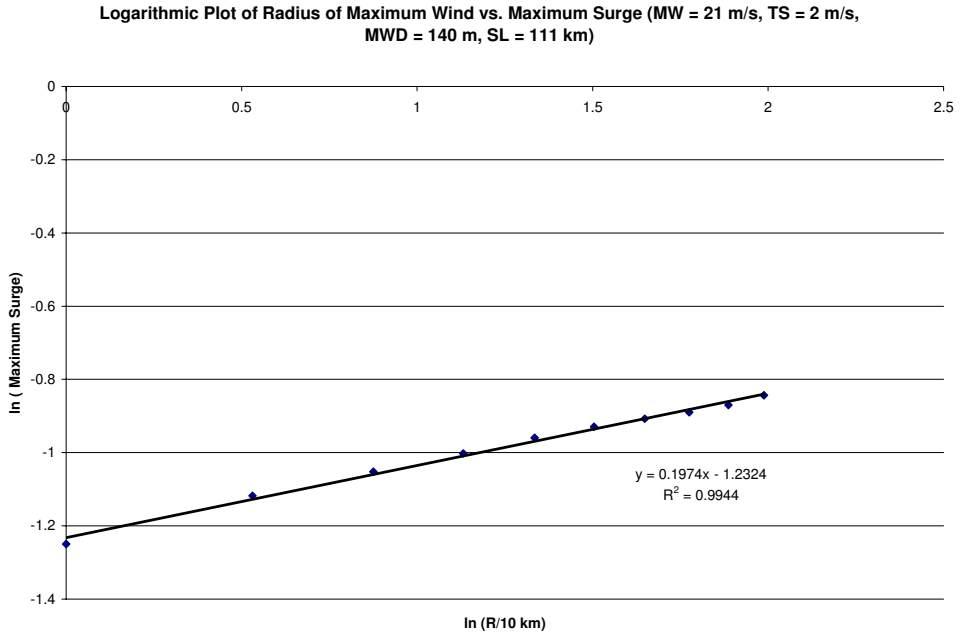

Figure 4.15: Logarithmic Plot of Radius of Maximum Wind vs. Maximum Surge (MW = 21 ms^{-1}, TS = 2 ms^{-1}, MWD = 140 m, SL = 111 km)

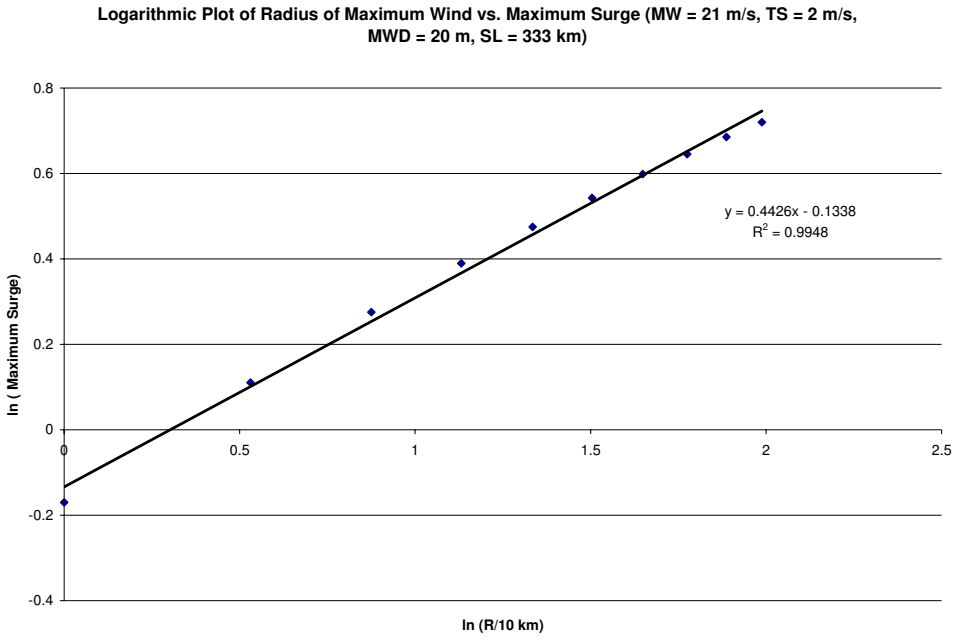

Figure 4.16: Logarithmic Plot of Radius of Maximum Wind vs. Maximum Surge (MW = 21 ms^{-1}, TS = 2 ms^{-1}, MWD = 20 m, SL = 333 km)

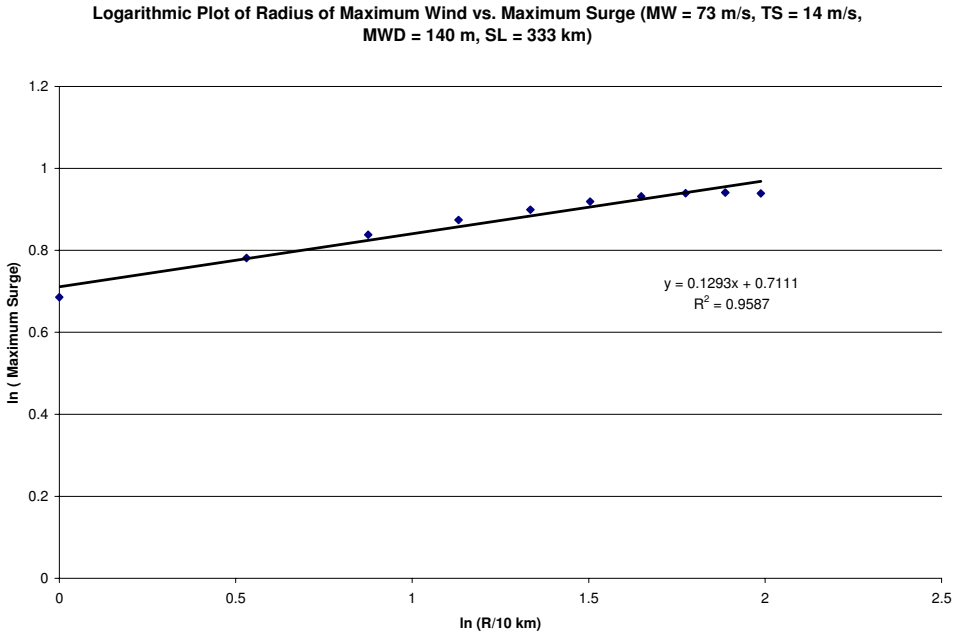

Figure 4.17: Logarithmic Plot of Radius of Maximum Wind vs. Maximum Surge (MW = 73 ms^{-1}, TS = 14 ms^{-1}, MWD = 140 m, SL = 333 km)

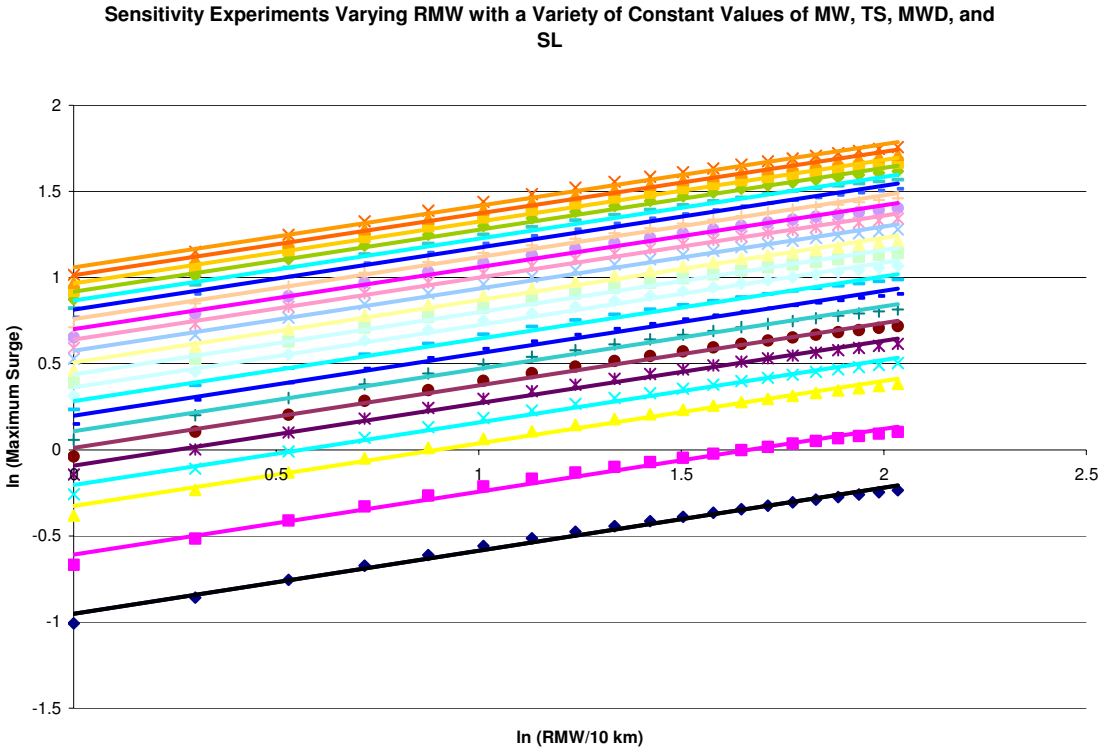

Figure 4.18: Sensitivity experiments varying RMW with a variety of constant values of MW, TS, MWD, and SL

The relatively small influence of RMW size on observed storm surge is somewhat puzzling. Undoubtedly, an increase in RMW size would have a significant impact on the breadth of surge distribution, but surge modelers have claimed for decades that the RMW is a key parameter in determining maximum surge height. In fact, one NHC forecaster recently stated that RMW size is just as important in generating storm surge as maximum wind speed (Knabb 2008, personal communication, in discussing the results of one storm simulation with varying RMWs). However, both the model results and data analysis performed here do not uphold these results. The derived power-law relationship does indicate that if the RMW significantly increases or decreases in size, then that factor would have an impact on expected surge heights, and if RMW size change is viewed with respect to changes in other pertinent variables, the importance of RMW size becomes clearer. However, relative to wind speed, RMW size is not as important in storm surge generation based on the simulations for this research.

4.5 Translation Speed

Using the same methods for sensitivity testing that were used in deriving appropriate power-law relationships for MW and RMW, sensitivity tests are performed to determine how storm surge is affected by changes in TS. Unlike with MW and RMW, logarithmic plots of TS versus storm surge demonstrate a parabolic relationship between the two variables, not a linear relationship. To force a power-law relationship in this instance would violate the purpose of power-law theory. Therefore, it is determined that the appropriate method for determining the relationship between TS and storm surge is through quadratic curve fits.

While examining a variety of curve fits under various circumstances, an interesting trend is noted. While the plots of TS vs. storm surge are inverse parabolas in all instances, the point at which the TS changes from being complimentary to storm surge to detrimental to storm surge shifts to the right (greater translation speed) as the RMW increases. This trend is noted in all cases, and it should be noted that such a dependence is not seen when examining other variables. Figures 4.18-4.24 are presented in pairs to show how this dependence on RMW evolves. These findings also seem to confirm some of the findings related to pre-landfall wind speed as the better predictor of storm surge since it is natural to expect that the ocean needs a certain amount of time to reach equilibrium at a given wind speed. Assuming all variables except RMW and TS are constant, a cyclone with a small RMW would need to move slower in order for the ocean to reach equilibrium compared to a cyclone with a large RMW. A cyclone with a large RMW would have its maximum winds covering a wider swath on the right hand side of the storm relative to forward motion, as opposed to a cyclone with a small RMW. Therefore, assuming that two cyclones are the same except for RMW, the storm with the smaller RMW has to move slower in order for the ocean to reach equilibrium with its maximum wind speed. The cyclone with the larger RMW can move faster since its swath of maximum winds covers a larger area. These findings are important because they move from looking at a tropical cyclone in an earth-relative frame (where an increase/decrease in translation would, theoretically, increase/decrease wind speed on the right hand side of a symmetric cyclone relative to forward motion) to looking at how residence time of a cyclone over a particular area of ocean affects storm surge. The initial increase in storm

surge with an increase in translation speed (noted on all graphs) is a function of the decrease in speed of the bottom of the water column (interaction with continental shelf) while the top of the water column continues moving toward the shore at a constant speed. This faster the water column is moving initially, the higher the column will be forced to rise once encountering an increase in bottom friction.

Therefore, for purposes of evaluating the usefulness of the TS term in the storm surge index, an average of parabolic curve fits is compiled based on RMW. Table 4.3 outlines the quadratic expressions used for various ranges of RMW. Based on the same response time arguments devised in Section 4.3, an average translation speed is used for determining the usefulness of the translation speed term in the storm surge index. The Pearson correlation of the TS term and observed storm surge is 0.32. This correlation indicates that there is a statistically significant relationship between translation speed and storm surge at the 95 percent confidence level.

Table 4.3: Parabolic Curve Fits Associated With Ranges of Radii of Maximum Wind. TS_o is a normalization constant equal to 5 ms^{-1}.

Range of RMW	Expression
7-13 km	$-0.0130(TS/TS_o)^2+0.1839(TS/TS_o)+1.2802$
14-20 km	$-0.0092(TS/TS_o)^2+0.1431(TS/TS_o)+2.8795$
21-27 km	$-0.0086(TS/TS_o)^2+0.1632(TS/TS_o)+2.5962$
28-34 km	$-0.0085(TS/TS_o)^2+0.1632(TS/TS_o)+2.5962$
35-41 km	$-0.0077(TS/TS_o)^2+0.1532(TS/TS_o)+2.7478$
42-48 km	$-0.0085(TS/TS_o)^2+0.1726(TS/TS_o)+2.4215$
49-55 km	$-0.0075(TS/TS_o)^2+0.1532(TS/TS_o)+2.7478$
56-62 km	$-0.0069(TS/TS_o)^2+0.1431(TS/TS_o)+2.8795$
63-69 km	$-0.0062(TS/TS_o)^2+0.1333(TS/TS_o)+2.9950$
70-76 km	$-0.0056(TS/TS_o)^2+0.1243(TS/TS_o)+3.0948$

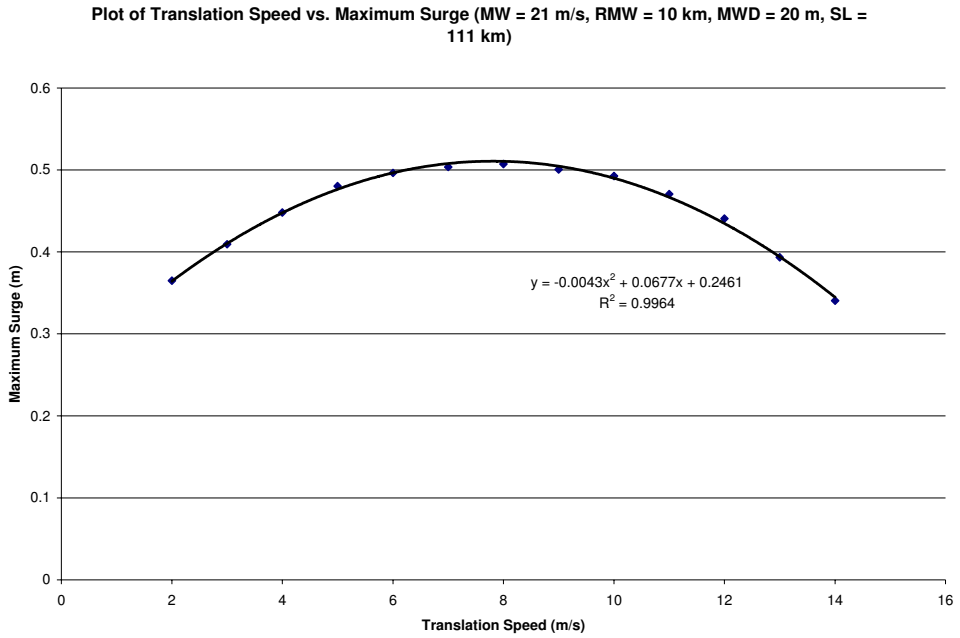

Figure 4.19: Plot of Translation Speed vs. Maximum Surge (MW = 21 ms^{-1}, RMW = 10 km, MWD = 20 m, SL = 111 km)

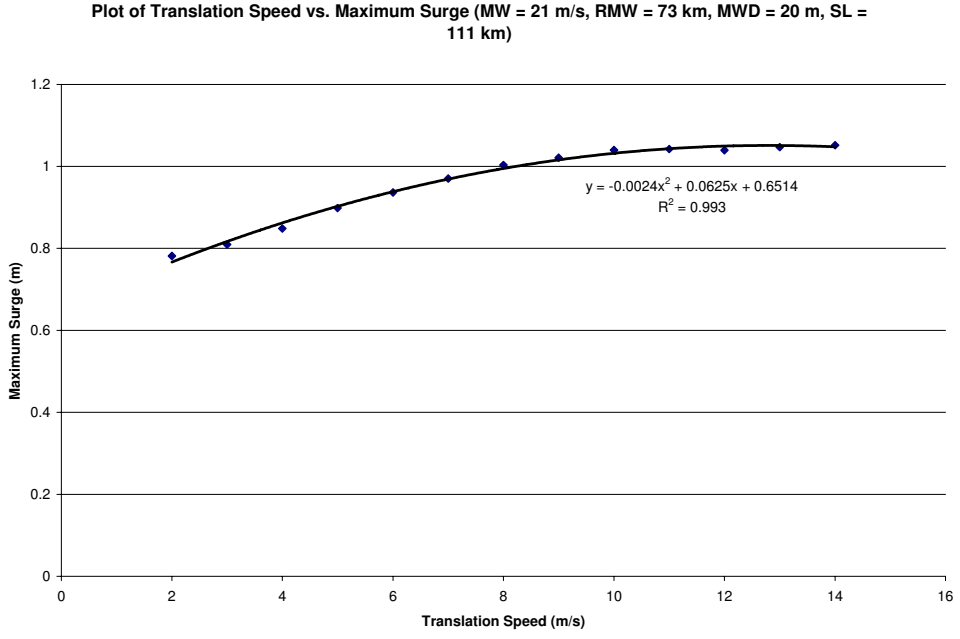

Figure 4.20: Plot of Translation Speed vs. Maximum Surge (MW = 21 ms^{-1}, RMW = 73 km, MWD = 20 m, SL = 111 km)

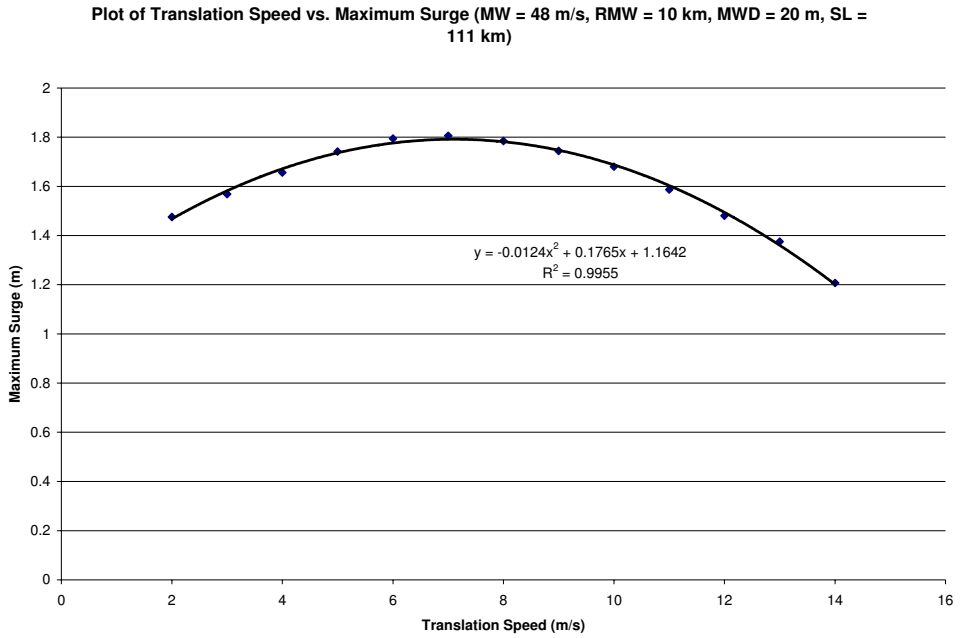

Figure 4.21: Plot of Translation Speed vs. Maximum Surge (MW = 48 ms^{-1}, RMW = 10 km, MWD = 20 m, SL = 111 km)

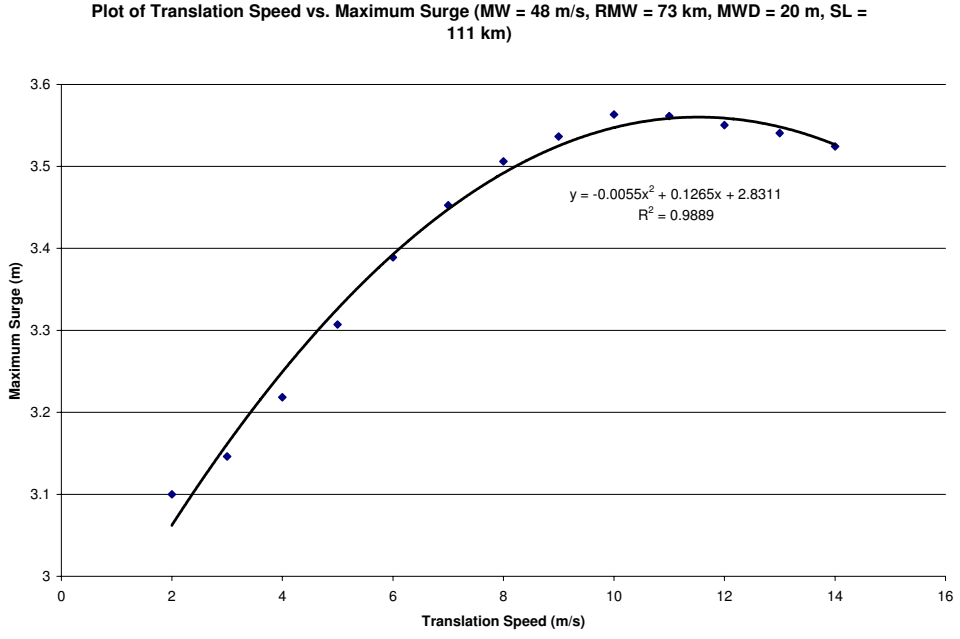

Figure 4.22: Plot of Translation Speed vs. Maximum Surge (MW = 48 ms^{-1}, RMW = 73 km, MWD = 20 m, SL = 111 km)

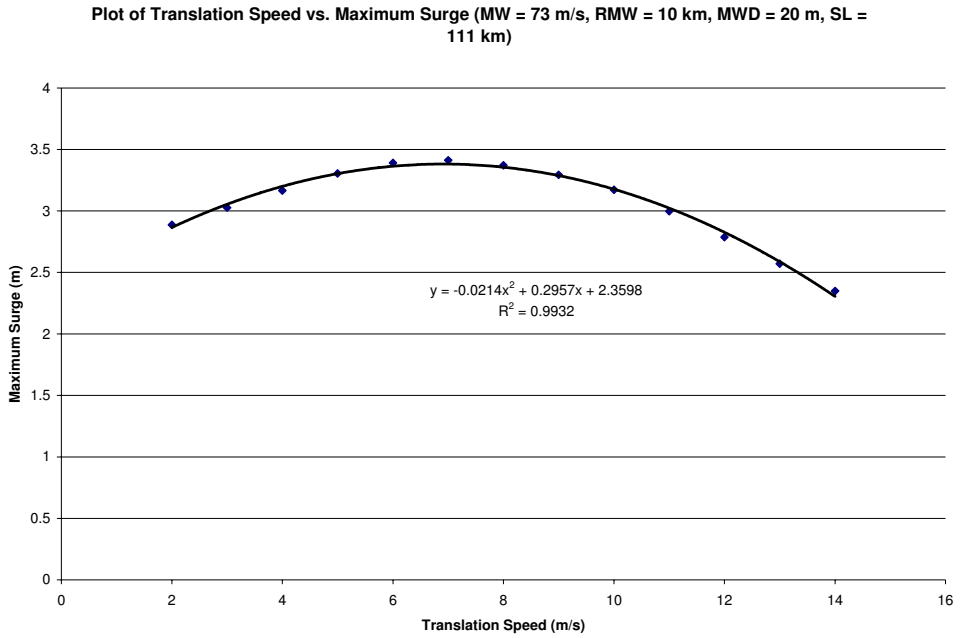

Figure 4.23: Plot of Translation Speed vs. Maximum Surge (MW = 73 ms^{-1}, RMW = 10 km, MWD = 20 m, SL = 111 km)

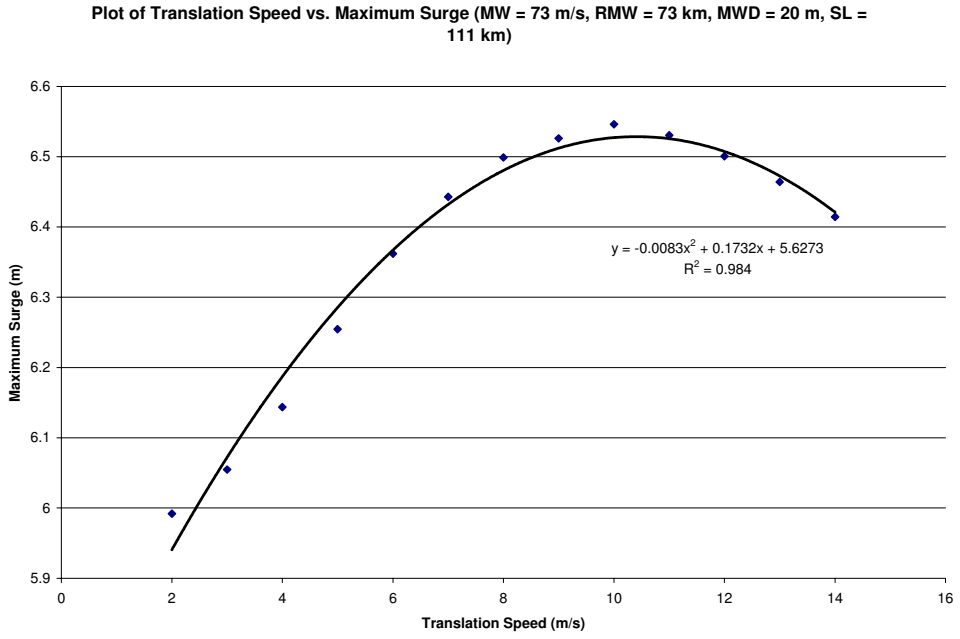

Figure 4.24: Plot of Translation Speed vs. Maximum Surge (MW = 73 ms^{-1}, RMW = 73 km, MWD = 20 m, SL = 111 km)

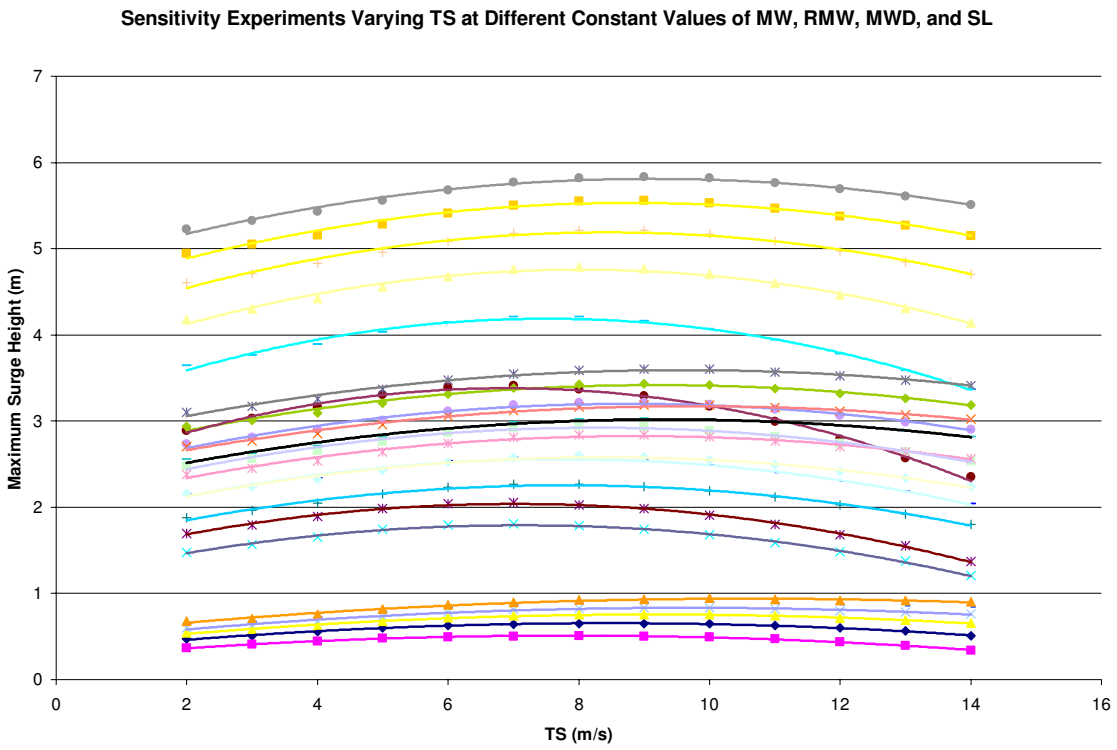

Figure 4.25: Sensitivity Experiments Varying TS at Different Constant Values of MW, RMW, MWD, and SL

4.6 Maximum Water Depth

In an effort to correctly capture the effect of continental shelf slope on storm surge, maximum water depth at the continental shelf break and continental shelf length are considered in the storm surge index. In reality, most continental shelves have slopes that vary at different points along the shelf. Furthermore, water depths do not necessarily decrease at regular intervals from the shelf break to the shore. However, for the purpose of this research, water depth at the continental shelf break (maximum water depth) and shelf length are used to describe bathymetry.

Unlike with TS, storm surge and maximum water depth do exhibit a power-law relationship. Deriving the appropriate power-law relationship between storm surge and maximum water depth involves employing the same methods used when deriving the power-law relationship between storm surge and maximum wind speed/radius of maximum winds. Many sensitivity experiments are conducted over a range of maximum water depths while holding MW, RMW, TS, and SL constant. Subsequently, the same

range of depths is examined at other constant values of the previously mentioned variables to assure that the derived relationships are appropriate. Figures 4.25-4.31 show logarithmic plots of maximum water depth versus storm surge. The slope of the regressed line represents the accepted power-law relationship between RMW and storm surge in each of the presented situations. For all experiments conducted, the slopes range from -0.13 - -0.61, and since R^2 is either equal to or very close to 1 in all experiments, the power-law relationships are accepted as valid. The multiple linear regression of storm surge versus MW, RMW, TS, and SL as described in Section 4.2 indicates an appropriate power-law relationship of -0.27. Therefore, the maximum water depth term in the storm surge index is $(MWD/MWD_o)^{-0.27}$, where MWD_o is a normalizing constant of 20 m.

For purposes of evaluating the usefulness of the MWD term in the storm surge index, a scaled and normalized MWD is used, depending on the MWD at the point where all database storms crossed the continental shelf break. Unlike with MW, RMW, and TS, a single value of MWD is used in the index since MWD is assumed not to change over time. Furthermore, MWD is not appreciably different at most places on the globe. In most places, MWD is very close to 140 m, and for all database storms MWD ranges between 120 m and 150 m. When this term is incorporated into the storm surge index, the Pearson and Spearman correlations do not change compared to the correlations derived when MW, RMW, and TS are used in the index. This outcome is not a surprise when considering how little MWD varies overall.

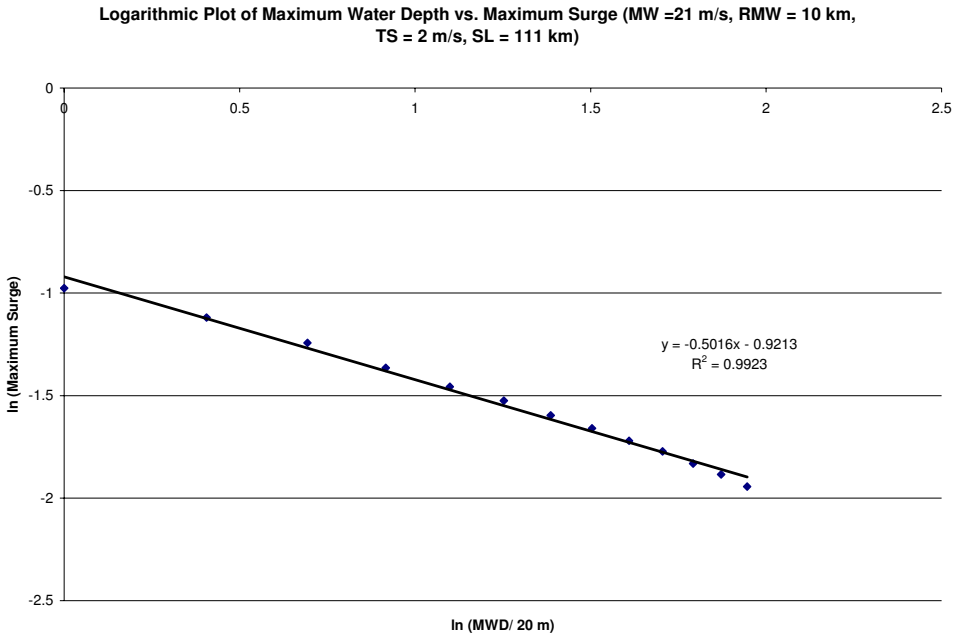

Figure 4.26: Logarithmic Plot of Maximum Water Depth vs. Maximum Surge (MW = 21 ms^{-1}, RMW = 10 km, TS = 2 ms^{-1}, SL = 111 km)

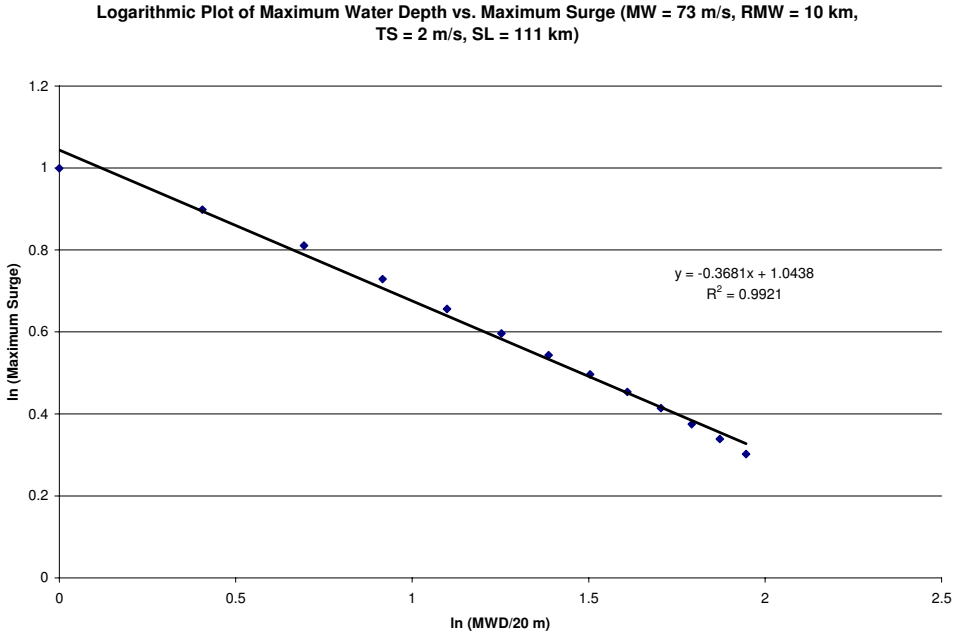

Figure 4.27: Logarithmic Plot of Maximum Water Depth vs. Maximum Surge (MW = 73 ms^{-1}, RMW = 10 km, TS = 2 ms^{-1}, SL = 111 km)

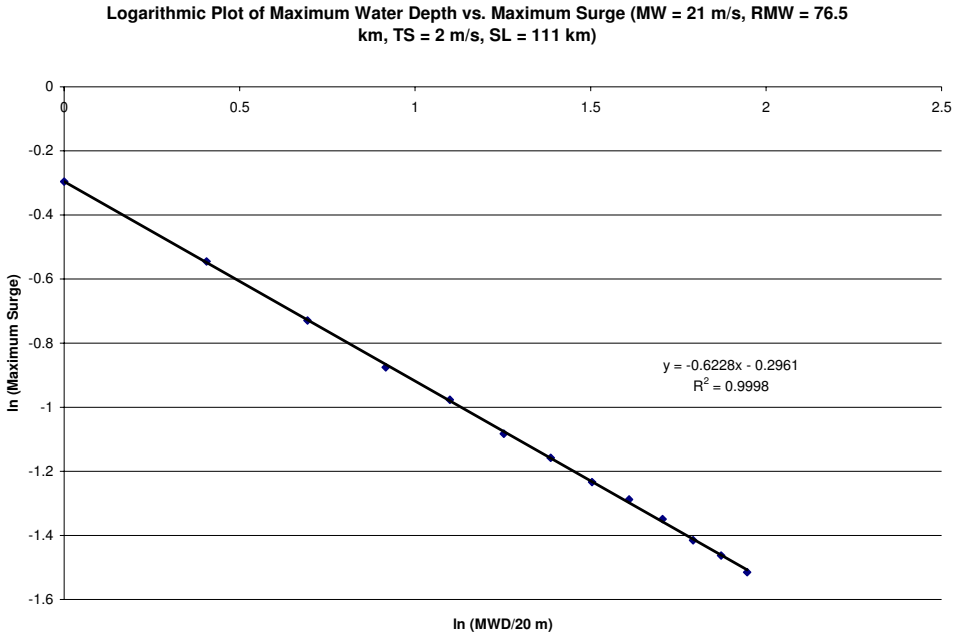

Figure 4.28: Logarithmic Plot of Maximum Water Depth vs. Maximum Surge (MW = 21 ms^{-1}, RMW = 76.5 km, TS = 2 ms^{-1}, SL = 111 km)

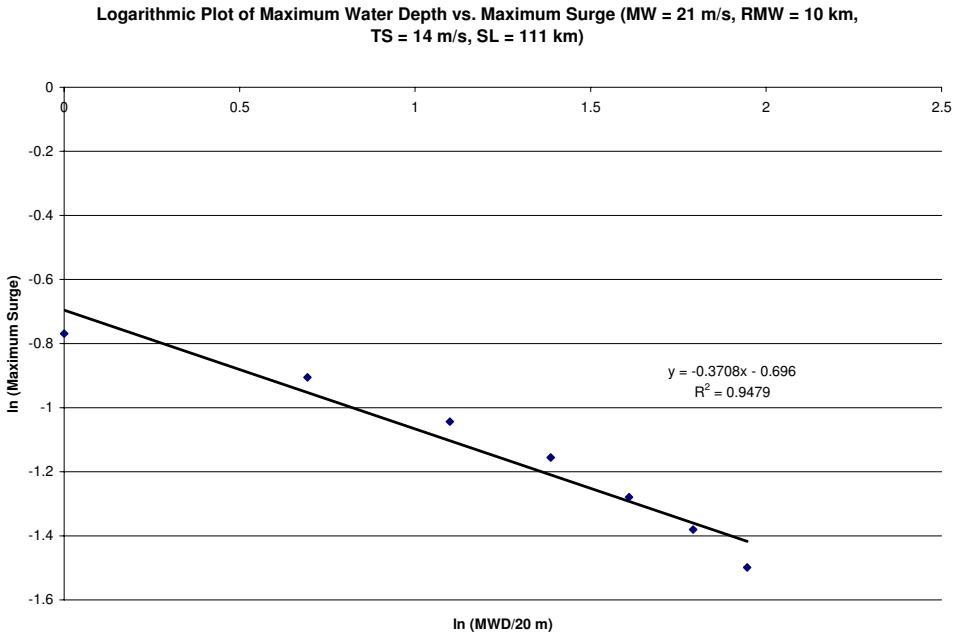

Figure 4.29: Logarithmic Plot of Maximum Water Depth vs. Maximum Surge (MW = 21 ms^{-1}, RMW = 10 km, TS = 14 ms^{-1}, SL = 111 km)

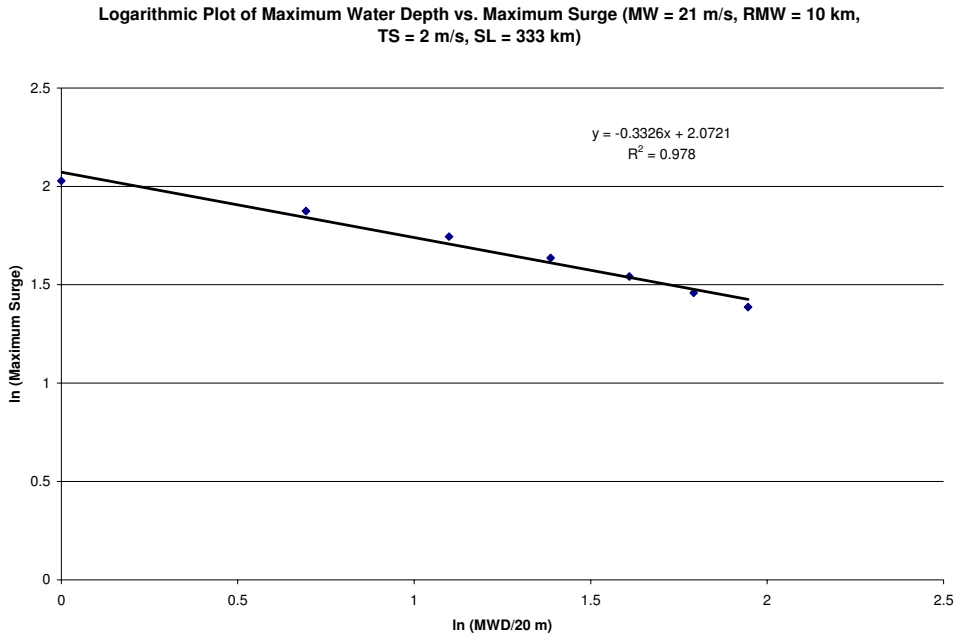

Figure 4.30: Logarithmic Plot of Maximum Water Depth vs. Maximum Surge (MW = 21 ms^{-1}, RMW = 10 km, TS = 2 ms^{-1}, SL = 333 km)

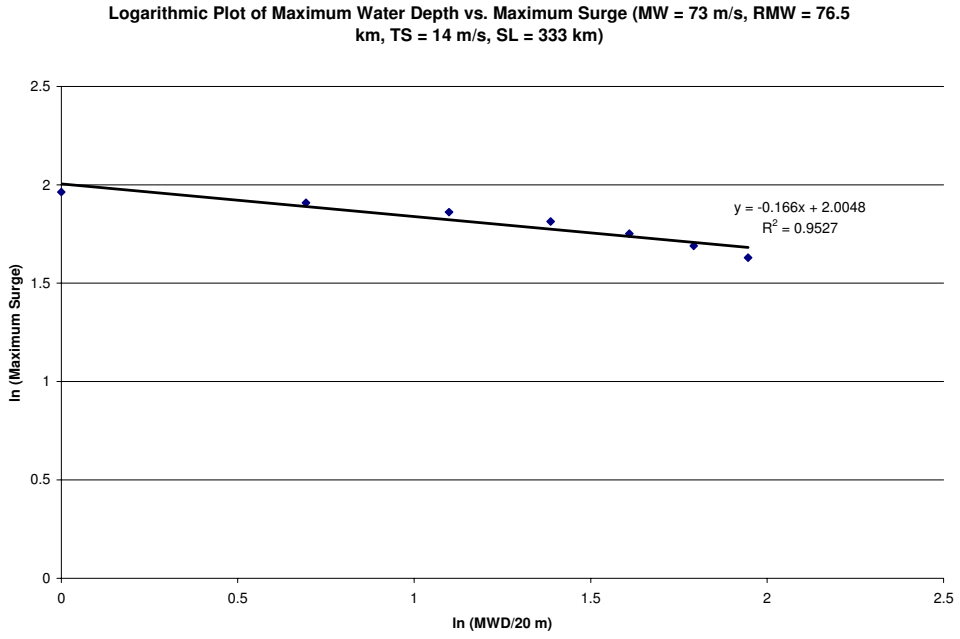

Figure 4.31: Logarithmic Plot of Maximum Water Depth vs. Maximum Surge (MW = 73 ms^{-1}, RMW = 76.5 km, TS = 14 ms^{-1}, SL = 333 km)

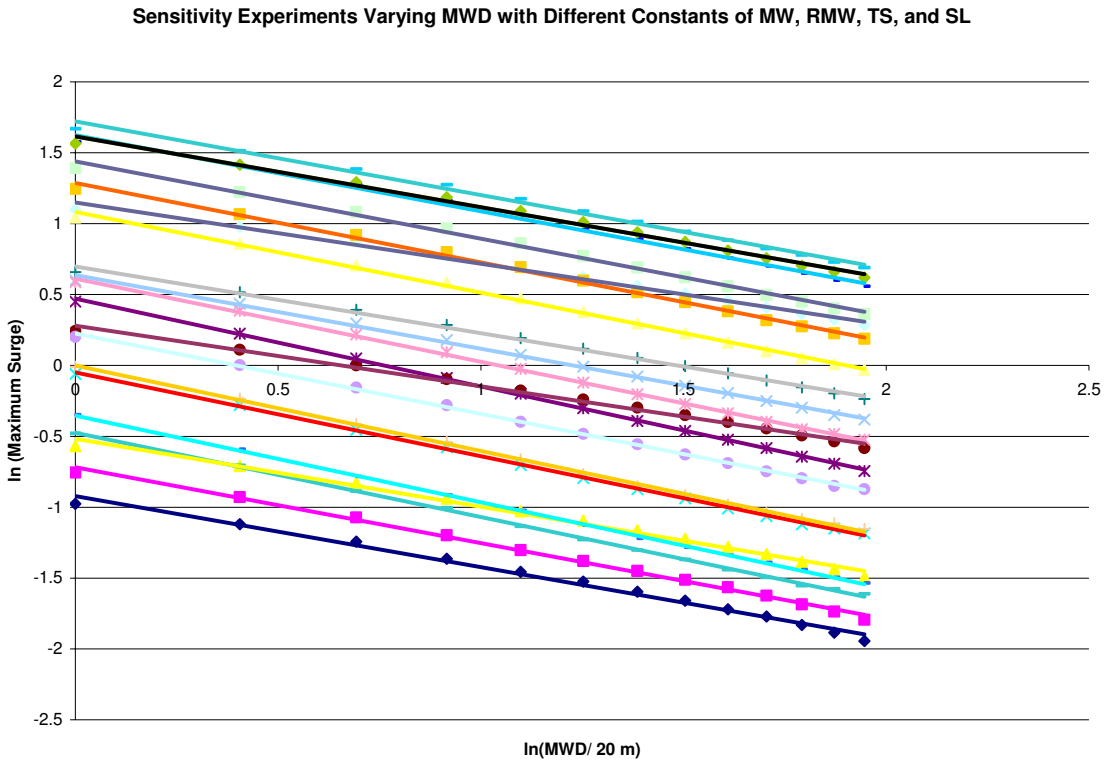

Figure 4.32: Sensitivity Experiments Varying MWD with Different Constants of MW, RMW, TS, and SL

4.7 Shelf Length

The second part in correctly describing bathymetry along a portion of the coast involves incorporating continental shelf length into the storm surge index. Therefore, since maximum water depth and shelf length are known, it is fairly straightforward to describe the general bathymetric characteristics along a coastline. As with other variables where a power-law relationship has been noted, multiple sensitivity tests are conducted over a variety of continental shelf lengths at different constant values of MW, RMW, TS, and MWD. Figures 4.32-4.38 show a variety of experiments where SL is varied and different constant values of MW, RMW, TS, and MWD are assumed. As with other variables, linear regression is performed and variance values are examined to determine how much of the variance in storm surge is explained through the different power-law relationships. The multiple linear regression indicates that the appropriate scaling parameter relating shelf length and storm surge is 0.33. Therefore, continental shelf

length in the storm surge index is represented by $(SL/SL_o)^{0.33}$, where SL_o is a normalizing constant of 28 km.

For purposes of evaluating the usefulness of the SL term in the storm surge index, a scaled and normalized SL is used. The Pearson correlation of the shelf length term and the observed database storm surges is 0.22, a statistically insignificant correlation and the 90 percent confidence level. However, this result is not a surprise considering that even though continental shelf characteristics are important in determining localized storm surge in a particular cyclone, there have been instances of cyclones traversing regions with a steep continental shelf and producing very high storm surges (Andrew 1992). On the other hand, there have also been cases where cyclones traverse regions with gently sloping continental shelves and produce relatively small storm surges (Charley 2004; Wilma 2005). Therefore, even though continental shelf characteristics are a factor in determining how high a storm surge will be, it is not a simple cause/effect relationship. Furthermore, as with RMW and TS, other factors are important in the evaluation of the significance of bathymetry to maximum storm surge, like MW. Therefore, disregarding the effect of bathymetry in storm surge prediction would be detrimental to surge forecasts even though the correlation between the two variables is statistically insignificant by itself.

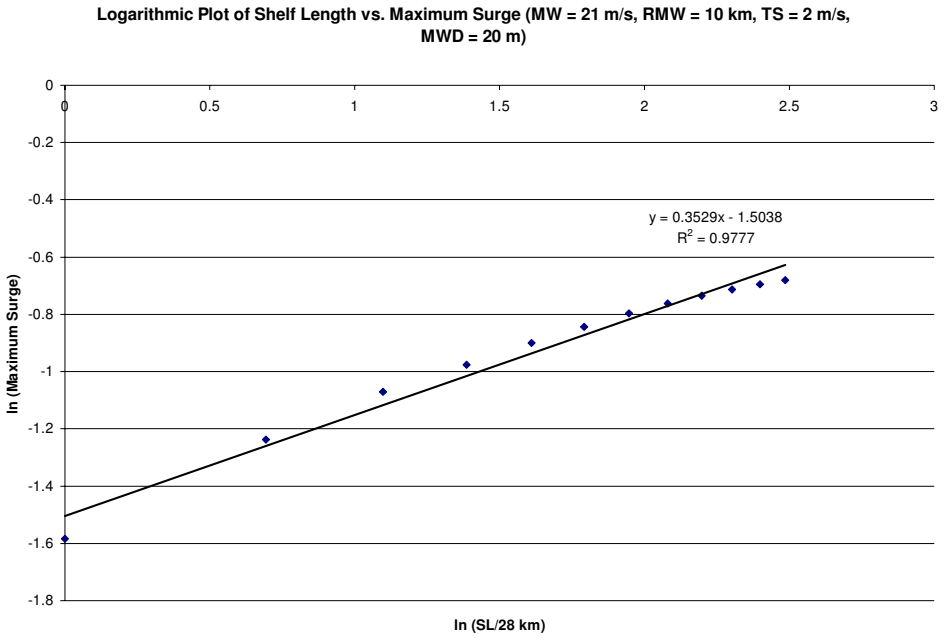

Figure 4.33: Logarithmic Plot of Shelf Length vs. Maximum Surge (MW = 21 ms^{-1}, RMW = 10 km, TS = 2 ms^{-1}, MWD = 20 m)

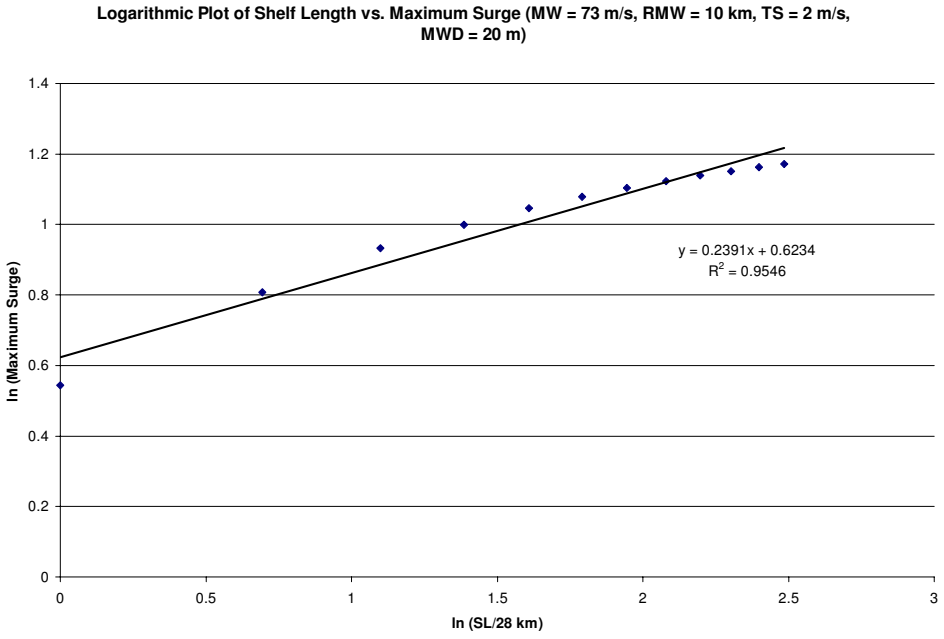

Figure 4.34: Logarithmic Plot of Shelf Length vs. Maximum Surge (MW = 73 ms^{-1}, RMW = 10 km, TS = 2 ms^{-1}, MWD = 20 m)

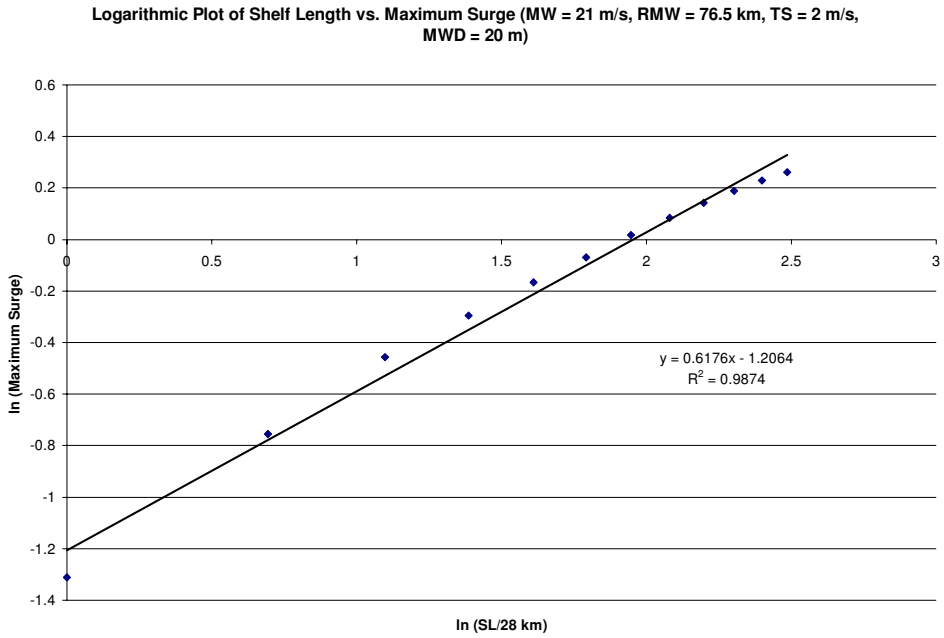

Figure 4.35: Logarithmic Plot of Shelf Length vs. Maximum Surge (MW = 21 ms^{-1}, RMW = 76.5 km, TS = 2 ms^{-1}, MWD = 20 m)

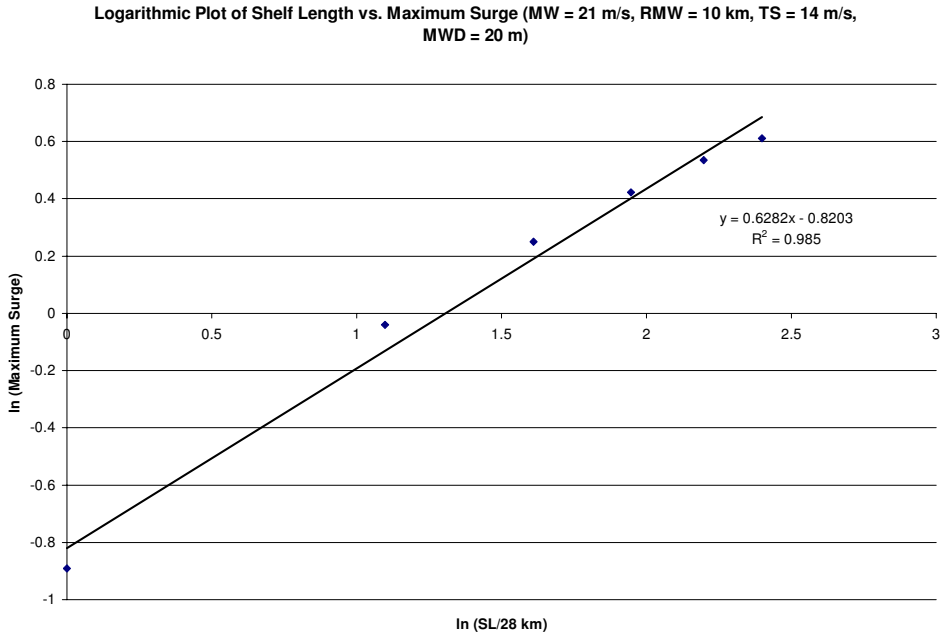

Figure 4.36: Logarithmic Plot of Shelf Length vs. Maximum Surge (MW = 21 ms^{-1}, RMW = 10 km, TS = 14 ms^{-1}, MWD = 20 m)

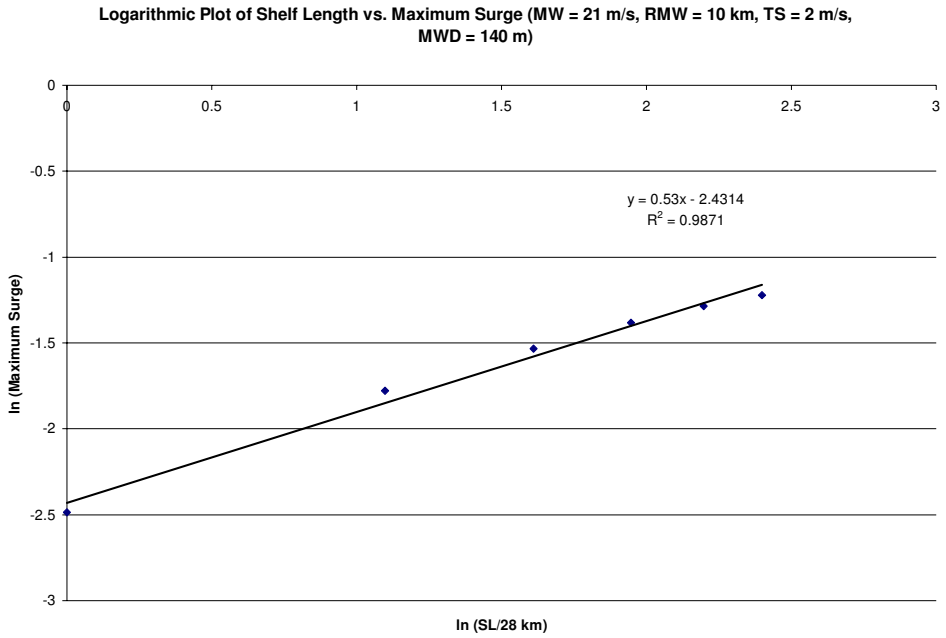

Figure 4.37: Logarithmic Plot of Shelf Length vs. Maximum Surge (MW = 21 ms^{-1}, RMW = 10 km, TS = 2 ms^{-1}, MWD = 140 m)

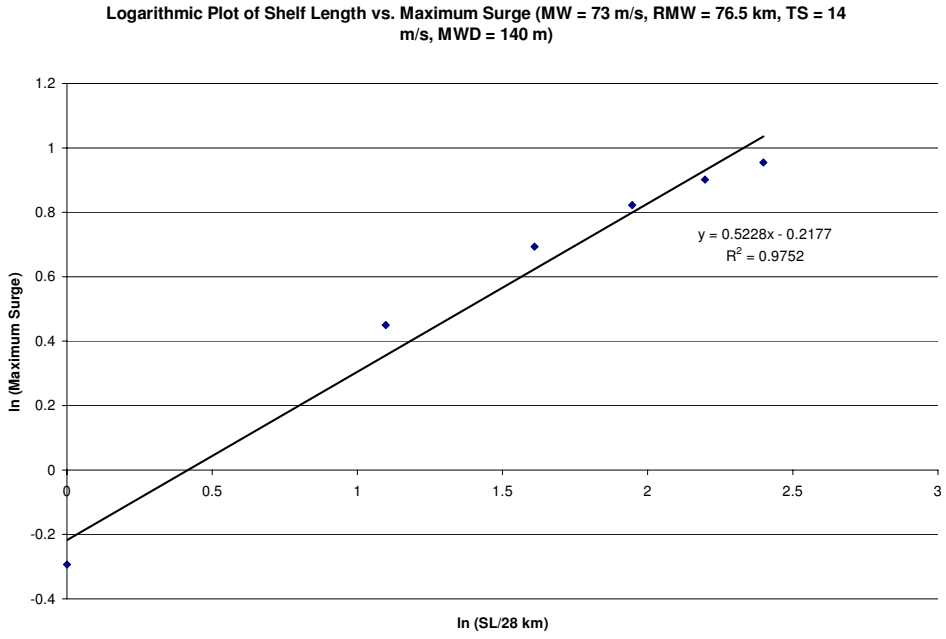

Figure 4.38: Logarithmic Plot of Shelf Length vs. Maximum Surge (MW = 73 ms^{-1}, RMW = 76.5 km, TS = 14 ms^{-1}, MWD = 140 m)

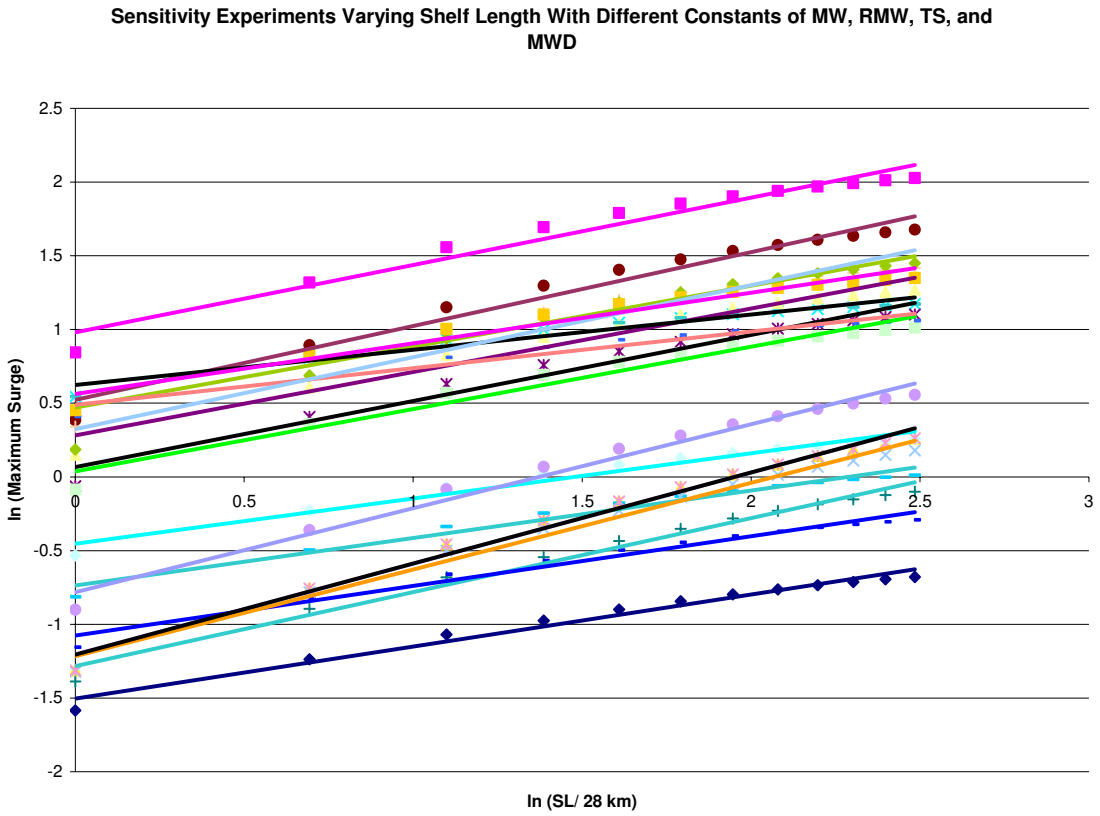

Figure 4.39: Sensitivity Experiments Varying Shelf Length with Different Constants of MW, RMW, TS, and MWD

4.8 Pressure

Until now, the purpose of this research has been to use a numerical model to develop simulations of how storm surge would vary with changes in key variables like MW, RMW, TS, MWD, and SL. In these simulations, it is assumed that wind speed is the driving force behind storm surge generation. However, Section 1.3 details another method that also contributes to overall storm surge: the increase in water level due to a pressure decrease. It is unnecessary to use the model to see whether an appropriate power-law relationship exists between storm surge and pressure because an inverse barometric correction has already been developed to describe how water level height changes with pressure changes. The following relationship describes the inverse barometric correction (IBC) widely used to remove the influences of pressure on water level height (Aviso 2003):

$$IBC = \frac{-1}{\rho_w g}(P - 1013.25\ hPa), \tag{4.1}$$

where ρ_w is sea-water density, g is the acceleration due to gravity, and P represents the actual air pressure (1013.25 hPa is chosen as a reference value because it represents standard sea-level pressure.). For the purpose of this research, ρ_w is assumed not to change even though small variations in the variable are noted as salinity and temperature change. Furthermore, g is assumed not to change even though the variable does change minimally with latitude. Therefore, an examination of the inverse barometric correction indicates that there is just under a 1 cm increase in water level height for every hPa that the air pressure drops below 1013.25 hPa; this association demonstrates that a power-law relationship exists between air pressure and storm surge heights even though pressure does not contribute significantly to the total surge observed in any given situation. The appropriate power-law relationship in this case is 1 since there is approximately a one-to-one relationship between pressure and water level height. The normalized pressure term in the storm surge index is represented as (P_o/P), where P_o is 1013.25 hPa. Finally, both landfall pressure and a 24-hour, pre-landfall average pressure are considered when correlating between pressure and observed storm surge. Water level redistribution due to pressure changes is achieved by long gravity waves propagating out from the center of the pressure change. Since there is some uncertainty as to how long it would take for this pressure redistribution to take place, both methods are considered.

When calculating a Pearson correlation between landfall pressure and observed storm surge, the correlation is 0.84. The Spearman correlation for the same scenario is 0.77. Furthermore, when calculating the two correlations using the 24-hour, pre-landfall average, the values are 0.87 and 0.78, respectively. Therefore, it appears that even though water-level adjustments due to pressure adjustments are not the main contributor to storm surge, the method in which pressure scales relative to storm surge appears to provide a relatively good idea of possible storm surge with landfalling tropical cyclones. All of the correlations presented are statistically significant at the 99 percent confidence level. Undoubtedly, part of this outcome is due to the cross correlation between pressure and wind speed since an increase in the pressure gradient will result in an increase in wind

speed. Assuming that the ambient pressure is not dropping or rising in tandem with the central pressure of a cyclone, the enhancement of the pressure gradient is correlated with an increase in wind speed while a decrease in the pressure gradient is correlated with a decrease in wind speed. It is reasonable to expect that pressure and wind speed cannot necessarily be treated independently even though their independent contributions to total storm surge in any given situation are due to two very different mechanisms.

4.9 Determination of Final Storm Surge Index

The complete storm surge index derived through this research is represented in the following index:

$$SI = \left(\frac{MW}{MW_o}\right)^{1.60}\left(\frac{RMW}{RMW_o}\right)^{0.33} TS\ term\left(\frac{MWD}{MWD_o}\right)^{-0.27}\left(\frac{SL}{SL_o}\right)^{0.33}\left(\frac{P_o}{P}\right), \qquad (4.2)$$

where SI is the acronym for surge index, and all other variables are presented in the order they were derived in the paper. For this study, the combination of variables that produce the highest correlations is the MW, P, and TS. Using just these three variables, the Pearson correlation is 0.89, and the Spearman correlation is 0.82. However, all variables contribute key information that cannot be ignored in any one case even though in this study the correlations are maximized using the three previously mentioned variables. In fact, calculation of the bias using just the three terms that result in the highest correlations show that the bias is 1.23. However, including the bathymetry and RMW terms decreases the bias to 1.12.

Before declaring that Equation 4.2 represents the final storm surge index, it is necessary to determine whether all terms in the index are statistically significant and whether each term adds more than just noise to the final result. Determining statistical significance in this case requires a forward stepwise regression for the entire model. The only term that is not included in the stepwise regression is the pressure term because its power-law relationship was derived independent of model simulations. It is assumed that because of the high correlation between pressure and storm surge, the term is statistically significant. At every step during the regression, p-values, t-statistics, and f-statistics were examined to determine whether the addition of a particular term increased the amount of

variance explanation using the model. Even though R^2 values for RMW/simulated storm surge and MWD/simulated storm surge are less than 0.1, the stepwise regression does not reject these variables. In fact, p-values for all variables in all instances are close to or equal to 0. Furthermore, t-statistics for all variables are always greater than 8 or less than -10, which would indicate that the inclusion of the variables in the index is appropriate. Finally, the f-statistics for all considered models range from 588 to 10353. All of the f-statistics indicate that the individual models are statistically significant. Table 4.4 shows various statistical parameters associated with the final model, including all of the model-simulated terms in Equation 4.2.

Table 4.4: Various Statistical Parameters associated with the Parameters Determined to be Statistically Significant to the Surge Index Model

	Coefficient	Standard Error	T-Statistic	P-Value
MW	1.60	0.009	173.3	0
RMW	0.33	0.006	57.3	0
TS	----------	0.004	25.1	0
MWD	-0.27	0.005	-57.9	0
SL	0.33	0.007	46.6	0

Five of the six surge index terms have been evaluated as being statistically significant through forward stepwise regression; however, since the scaling factor for pressure was no determined through simulations, that term was not included in the regression. Observations indicate that there is a significant relationship between wind speed and a tropical cyclone's central pressure, so it must be determined whether the inclusion of both wind and pressure terms in the index together actually increases variance explanation significantly. Using the 39-storm database, partial correlations are calculated between wind speed/storm surge and pressure/storm surge to determine whether the two variables independently explain a significant amount of storm surge variance. As a reminder, the correlation between landfall wind speed and storm surge is 0.61, and the correlation between landfall pressure and storm surge is -0.84. The partial correlation between wind speed and surge when holding RMW constant is 0.61, the same as the full correlation between wind speed and surge. Surprisingly, however, the partial correlation between wind speed and surge when holding pressure constant is -0.42. Therefore, with the

change in the sign of the correlation, it would appear that wind speed is actually a suppressor variable when included in a model where central pressure is already considered. Considering the partial correlations between pressure and storm surge, holding RMW constant results in a correlation of -0.83. Holding wind speed constant results in a correlation of -0.78. Therefore, removing the effect of wind speed does not affect the correlation between pressure and storm surge as much as removing the effect of pressure affects the correlation between wind speed and storm surge. These results strongly support only including a pressure term in the storm surge index since a significant overlap in variance explanation exists between the two terms. However, due to the limited amount of data used for comparison in these project, both terms are included with the caveat that a larger database of storms may show that the use of both wind speed and pressure in a surge index is redundant based on the results of partial correlations calculated here. For completeness, no other partial correlations are significantly different from their corresponding full correlations, and no other partial correlations demonstrate the sign change seen with taking the partial correlation of wind speed and surge when holding pressure constant

Finally, it would be useful to return to the database storm data and see whether individual linear regressions of MW, RMW, MWD, SL, and P versus observed storm surge would result in scaling parameters similar to the scaling parameters derived using model-generated storm surge heights. Assuming that power-law relationships should exist between the variables and surge, the logarithm of all variables is taken before the linear regressions are conducted. The scaling parameters derived using actual data are 1.55, -0.03, -0.13, 0.17, and 1.06, respectively. Considering the inherent problems with multiple types of errors in observational data sets, it is interesting to note that the scaling parameters derived using observations are relatively similar to the scaling parameters derived using model data. The exception here is the scaling parameter for RMW, which actually shows almost no relationship to storm surge when examining actual data.

CHAPTER 5

ERROR ANALYSIS

5.1 Overview of Possible Errors

The evaluation of the possible errors associated with the newly-derived storm surge index needs to incorporate several different aspects. First, there are inherent errors in the way different variables are measured since the same instrument is not used to measure a particular variable at all times. For example, a tropical cyclone's maximum wind speed can be measured by reconnaissance aircraft, ships, buoys, stepped-frequency microwave radiometer, QuikScat, and the Dvorak technique. All of the various measurement techniques have average errors associated with them, and in a proper error analysis, the strength of the storm surge index will always be limited by the measurement technique associated with the greatest error. Therefore, the average error used for wind speed in a comprehensive error analysis, for example, must take into account the greatest average error associated with the previously mentioned methods of measuring wind speed.

Next, the methods by which variable measurements are recorded have to be considered since rounding off measurements will incorporate a type of random error into the data used. Best track and extended best track data round wind speed to the nearest 5 kts in many places, and the data sets round radii of maximum winds to the nearest 5 nautical miles in many places. Furthermore, pressure recordings are made to the nearest 1 hPa, and there are likely times when the actual pressure is between two whole numbers. Undoubtedly, there are going to be situations where the actual wind speed, radius of maximum wind measurements, and pressure measurements are not going to be truly represented by the rounding. Since the error is random, however, it is possible that the combination of rounding increases and rounding decreases should roughly cancel, a statement that should be evaluated in a thorough data analysis, where one must consider the largest possible error in order to account for all possibilities.

Finally, the storm surge index has been correlated with actual maximum observed storm surge heights associated with the given tropical cyclones. Undoubtedly, there are going to be errors in these measurements due to many factors. First, both random and

systematic errors could exist to different degrees depending on what was used to measure the height of the actual surge. Second, even though scientists attempt to remove the effect of waves and tides from the maximum water level to calculate the storm surge in a given event, there are going to be times when the calculations are done improperly or without enough information to be absolutely confident of the measurement. Third, there are gaps in the coverage of the coastline. This may mean that the reported maximum surge for a given tropical cyclone may not actually be the maximum storm surge because there were no measurements performed in the area that coincided with the highest water levels. Fourth, the maximum storm surge heights, as has been stated, are the maximum storm surge heights reported in the individual storm reports provided by the National Hurricane Center. These tropical cyclone reports are not peer-reviewed articles and are, therefore, subject to error. Fifth, at any time between measurement of surge height and recording of that measurement, transcription errors could have occurred. Overall, there are many factors that have to be evaluated before a sense of the errors in the in situ storm surge data can be determined.

5.2 Calculation of Possible Storm Surge Index Error

Four of the six variables in the storm surge index are considered in this error analysis: maximum wind speed, radius of maximum winds, translation speed, and pressure. Maximum water height and shelf length are not considered because even though the measurements of those variables may have involved some random and/or systematic errors, those variables have been measured and will not be measured again in the future as often as the previous four variables. Therefore, the form of the surge index to be considered for this error analysis is found below:

$$SI = \left(\frac{MW}{MW_o}\right)^{1.60}\left(\frac{RMW}{RMW_o}\right)^{0.33}\left(\frac{P_o}{P}\right)\left(-0.0086\left(\frac{TS}{TS_o}\right)^2 + 0.1632\left(\frac{TS}{TS_o}\right) + 2.5962\right), \quad (5.1)$$

as previously. The expression involving translation speed was chosen based on an average on radius of maximum wind measurements with respect to translation speed, as discussed in Chapter 3.

Error quantification is achieved through taking the root-mean-square error of the previous equation. The general formula for root-mean-square error, tailored for this situation, is:

$$\sqrt{(\frac{\partial SI}{\partial MW_{term}}\delta MW)^2+(\frac{\partial SI}{\partial RMW_{term}}\delta RMW)^2+(\frac{\partial SI}{\partial P_{term}}\delta P)^2+(\frac{\partial SI}{\partial TS_{term}}\delta TS)^2}\ . \quad (5.2)$$

When a partial derivative is not taken with respect to a particular variable, that variable is, naturally, held constant. In those cases, MW = 50 ms^{-1}; RMW = 30 km; P = 970 hPa, and TS = 5 ms^{-1}. Furthermore, as has been stated, the error estimates associated with each variable have been chosen to maximize the possible measurement error. In this situation, δMW = 2.5 ms^{-1}; δRMW = 10 km; δP = 3 hPa, and δTS = 2 ms^{-1}.

The approximated errors for each variable using the root-mean-square approach are shown in Figures 5.1-5.4. Figure 5.1 shows that the error due to changes in MW is approximately 0.35 for marginal hurricanes and about 0.8 for severe hurricanes. Considering the overall values of SI for the database storms, a change in index value of +/- 0.8 would be significant; however, those fluctuations are not unexpected given the nature of the measurement errors and the significant dependence of SI on MW .

Figure 5.2 shows the error due to changes in RMW to be approximately 1.4-1.6 for storms with exceptionally small radii of maximum winds. For storms with radii of maximum winds approaching 80 km, the error is around 0.35. RMW has the ability to contribute to a higher error at small radii of maximum winds than MW ever does no matter what wind speed is being considered. This finding would seem counterintuitive since MW is associated with a much higher power than RMW is in the original equation. However, the finding is correct because of the large measurement error value associated with RMW. Considering the way in which the SI is written, it is possible, based on Figure 5.2, for the index to become 0 for small values of radius of maximum winds when measurement error is considered. Of course, reality would dictate that such an event is impossible.

Figure 5.3 shows the error due to changes in pressure. The errors associated with this term fall into a very small range from -0.026 to -0.022. The negative errors are a function of the inverse proportionality between pressure and storm surge. However, due

to the small errors associated with pressure measurement and the normalization constant used, the relative error of pressure in this situation is not very large. Therefore, as long as there is not a significant error in pressure estimation, the pressure term should result in the least amount of error when considering the four terms in this error analysis.

Figure 5.4 shows the error due to changes in translation speed. In general, the errors associated with changes in translation speed are more significant than the errors associated with changes in pressure, but less significant than the errors associated with changes in MW and RMW. Overall, errors range from about 0.16 to 0.17. Therefore, based on the low measurement error associated with translation speed, translation speed does not account for major error in the calculation of the SI.

Certain constants were chosen for each of the four variables when the variable was not being evaluated. Altering those constants to determine whether the constants chosen significantly impact the error calculations for the four variables indicates that the calculated errors do not significantly change. Therefore, the constants chosen for this analysis generally represent the error bounds associated with each of the four variables.

Using the information derived in this error analysis to quantify the error associated with any SI prediction for storms in the database is relatively simple. With the accepted values of MW, RMW, P, and TS, each chart can be evaluated to determine the error for a given wind speed, radius of maximum wind, pressure, and translation speed, respectively. Then, each of those values can be squared and summed. Finally, the square root of the final value gives the root-mean-square error and the positive and negative error bounds for a particular storm surge forecast using the SI. For example, if a hurricane landfalls with a MW = 60 ms^{-1}, RMW = 30 km, P = 945 hPa, and TS = 6 ms^{-1}, the value of the SI for that storm is 9.34. The root-mean-square error in this case would be 0.89. Therefore, a more accurate representation of the SI value in this case would be 9.34 +/- 1.00.

If one were to implement the index in a true real-time format, the procedure for reporting error bounds would generally remain the same. One significant difference, however, is that in addition to variable measurement and reporting errors, one would have to consider average forecast error of the necessary variables. Therefore, error bounds could be significantly larger when considering average forecast error, depending

on the length of forecast involved. For example, assume that emergency preparedness officials in a city are concerned about potential storm surge from a hurricane in 96 hours, and assume that the forecast track of this hurricane is perfect. Average National Hurricane Center intensity error at 96 hours is 10 ms^{-1}. Therefore, δMW would be 12.5 ms^{-1} in this case when also incorporating measurement error. An estimate of forecast error concerning pressure would be 15 hPa, and incorporating the pressure measurement error of 3 hPa would increase the δP to 18 hPa. Futhermore, it is reasonable to assume that forecasts of RMW could have 25 km errors at this time frame. Incorporating the 10 km measurement error discussed previously would result in a δRMW of 35 km. Finally, forecasts of translation speed could reasonably have 5 ms^{-1} errors, and incorporating the measurement error, δTS would be 7 ms^{-1}. Using the same MW, RMW, P, and TS parameters in the previous example, the SI including the error bounds would be 9.34 +/- 3.76.

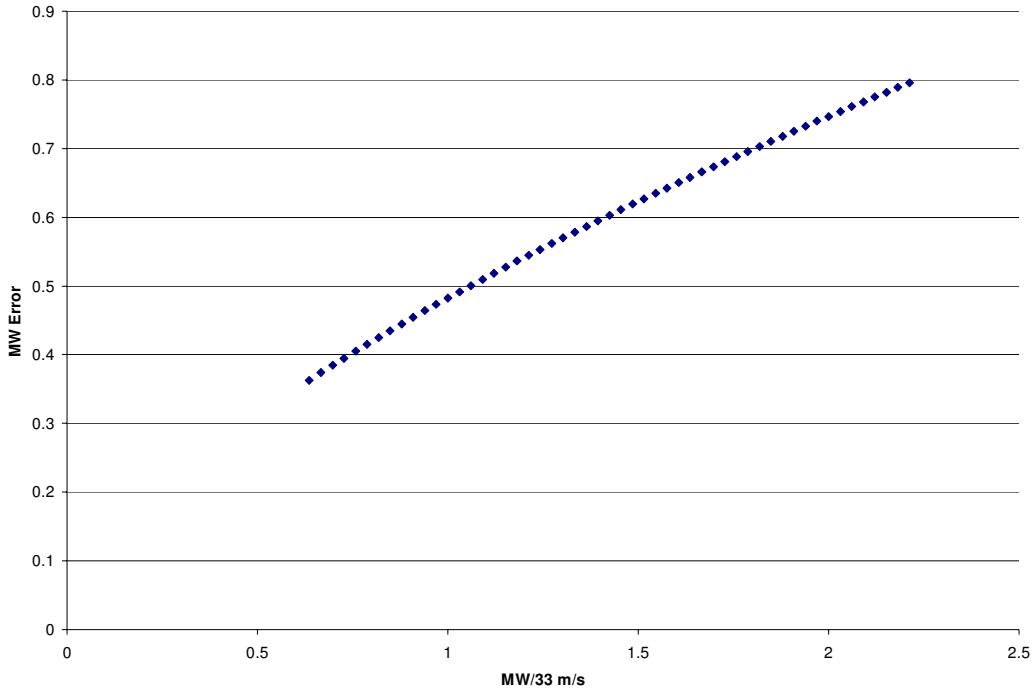

Figure 5.1: Error Due to Changes in MW (RMW=30 km, Pressure = 970 hPa, Translation Speed = 5 ms^{-1})

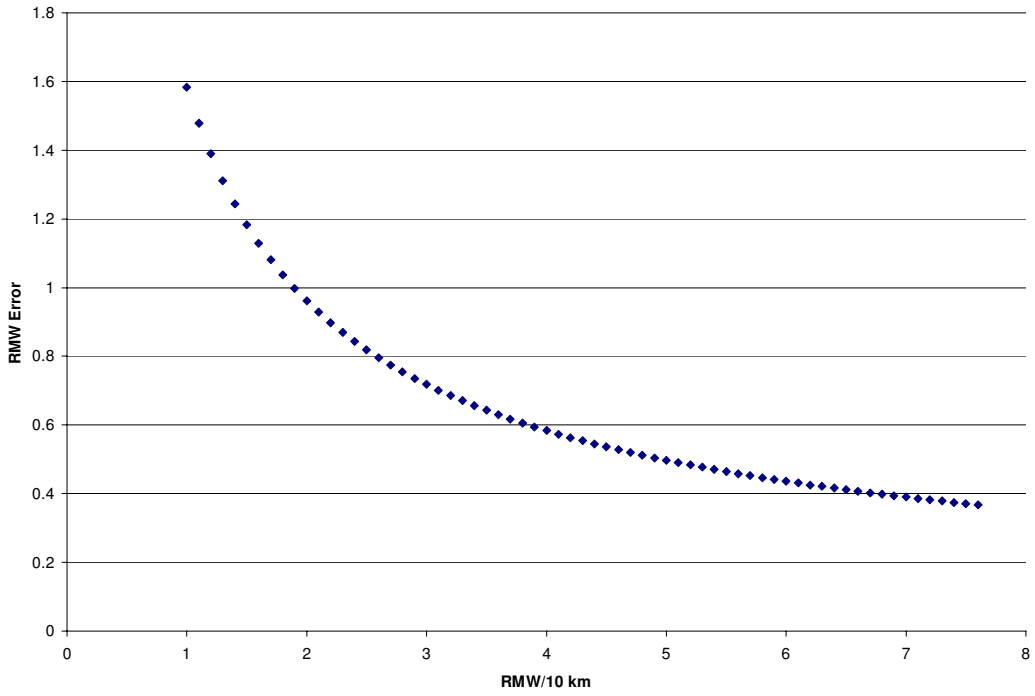

Figure 5.2: Error Due to Changes in RMW (MW = 50 ms^{-1}, Pressure = 970 hPa, Translation Speed = 5 ms^{-1})

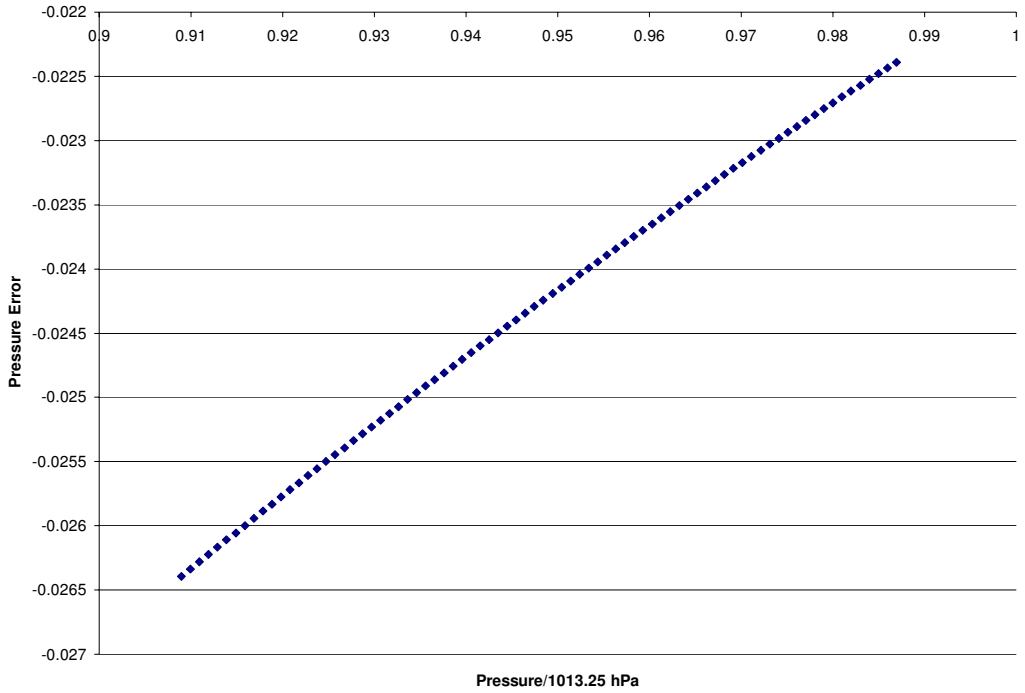

Figure 5.3: Error Due to Changes in Pressure (MW = 50 ms^{-1}, RMW = 30 km, TS = 5 ms^{-1})

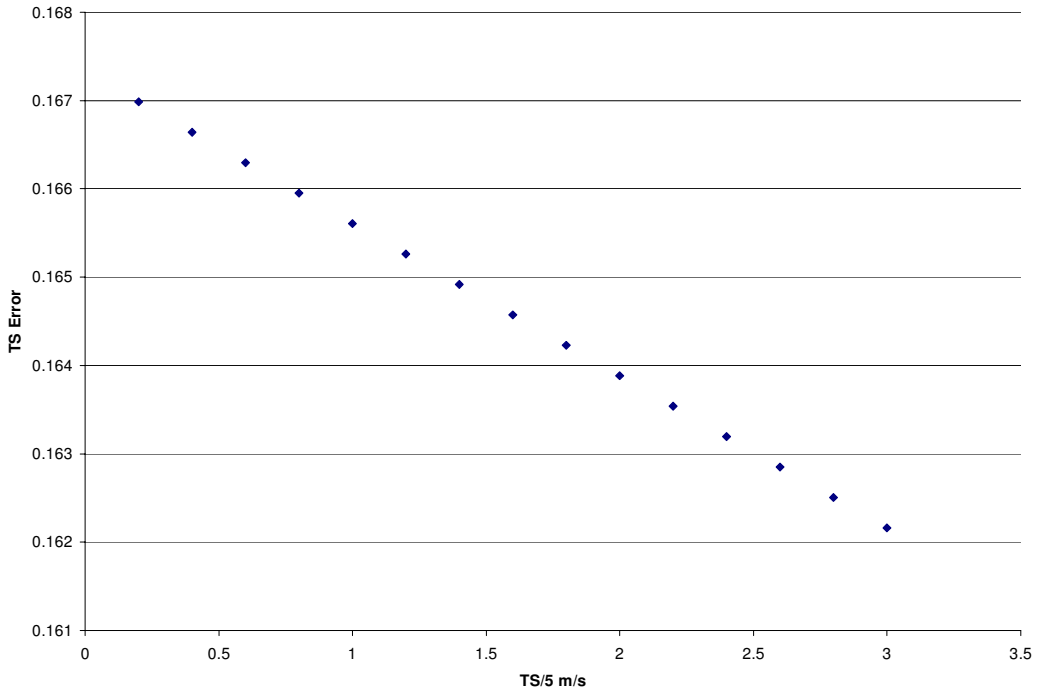

Figure 5.4: Error Due to Changes in Translation Speed (MW = 50 ms^{-1}, RMW = 30 km, Pressure = 970 hPa)

CHAPTER 6

CONCLUSIONS

6.1 Scientific Value of Dissertation

A new analysis of the storm surge sensitivity to various environmental and topographical features has been created. This represents the first attempt at a numerical qualification of storm surge sensitivity to changes in many different variables, including wind speed, radius of maximum winds, translation speed, and bathymetry. Furthermore, unlike many index-based, storm surge forecasting methods that have been presented in the scientific literature, this research also represents the first time anyone has performed a comprehensive evaluation of an index's performance with respect to previous events. Included with the index validation is a complete analysis of possible errors associated with the index as it is presented in the dissertation along with recommendations for how such an index should be used in a real-time format.

Second, this dissertation also attempts to explain why many storms that weaken/strengthen within several hours of landfall tend to exceed/lag available storm surge predictions. An extensive correlation analysis of database tropical cyclones has been performed and shows that landfall intensity and observed maximum storm surge have a significantly lower correlation than 12-hour, pre-landfall intensity and observed maximum storm surge or 24-hour, pre-landfall average intensity and observed maximum storm surge. In a surprising finding, the correlation analysis shows that landfall intensity actually has the smallest correlations with observed storm surge. These results are further supported by numerical simulations that indicate translation speed of tropical cyclones is constructive to storm surge at lower translation speeds; however, depending on the size of the radius of maximum winds, translation speed actually is destructive to storm surge once a certain forward speed is attained. When a tropical cyclone has a small radius of maximum winds, the translation speed at which storm surge is destructively impacted is lower than when the radius of maximum winds is large.

Finally, this dissertation attempts to explain why pre-landfall intensity is a better indicator than landfall intensity of maximum storm surge. Starting with the knowledge that oceanic momentum input is primarily responsible for storm surge, as has been

accepted in other storm surge indices from Kantha (2006) to Hebert (2008), an argument is developed that for quickly strengthening cyclones just prior to landfall, additional momentum input is divided between two regimes: wave maturation and the ocean current. Other research has shown that the majority of this additional input goes into wave maturation and a smaller portion goes into the ocean current until wave maturation is reached. While the exact percentage of momentum distributed into each regime is currently unknown, there is no doubt that if a cyclone impacts the coast before equilibrium is reached with the ocean current at a given wind speed, then storm surge will not be maximized. For a quickly weakening cyclone, no additional momentum is imparted to the wave field, and the wave field gradually subsides to reach equilibrium with the lower wind speed. However, momentum imparted to the ocean current at the times when wind speeds were much higher does not immediately disappear. Instead, the ocean current, just as the wave field, eventually reaches a new equilibrium at the lower wind speed. However, no research to date has evaluated the time scale of the development of the storm surge in non-coastal regions, and it is impossible to quantify the effects of the waves, changes in momentum, and currents on the set-up of the storm surge itself. In addition, the theoretical arguments that have been advanced take as an axiom that atmospheric momentum is transferred to the ocean proportional to V^2 and ,thus, that there is a quadratic relationship between wind speed and storm surge. To assume such a relationship would be to assume that all momentum imparted to the ocean is used to generate storm surge, which is not supported through hundreds of numerical simulations or common sense. However, this highlights our lack of knowledge regarding the role of waves and currents and time scales in the development of the oceanic storm surge. Research on the open ocean storm surge response is needed to address the issues which this research has identified fully.

6.2 Societal Value of Dissertation

For the general public, the research encompassed by this dissertation has two main societal impacts. First, many countries around the world that are prone to significant tropical cyclones do not have access to intricate storm surge models, and many countries do not have any method for storm surge prediction except for a basic climatology or

analog forecast based on memories or stories passed down from one generation to another. This storm surge index can be used in a forecast mode, and since a database of previous tropical cyclone index values has already been compiled, a more detailed analog forecast can be generated based on storms that have similar index values. This type of forecasting would be incredibly beneficial for many countries that routinely experience significant loss of life from landfalling tropical cyclones because now those countries would have an estimate as to the height of storm surge with a cyclone. Based on knowledge of elevation, people can determine whether they are located high enough to avoid drowning in a significant storm surge.

Second, since the storm surge index represents the sensitivity of storm surge to changes in many variables, one can use the index to determine how storm surge may change with large climatic shifts hundreds of years in the future. For example, the issue of whether the Earth's average temperature is increasing is pervasive in the media, the public, and in an array of scientific fields. Some of the proposed changes in tropical cyclones in a warmer world may include increased intensity, lower pressures, and increased sea levels. Using the storm surge index, one can determine how strengthening a storm by 2 m/s would impact the expected surge from a landfalling tropical cyclone. If 100 years from now most of South Florida is under water, or the Louisiana Bayou is in the Gulf of Mexico, the storm surge index can quantify how increasing maximum water levels or lengthening the continental shelf can affect the expected storm surge for a tropical cyclone. Therefore, this new index is useful in both the meteorological and climatology fields.

6.3 Future Work

There are many opportunities for future work with this research and with in other fields related to this research. First, it would be useful to use another model(s) and another vortex parameterization(s) to make sure the results found using the modified version of the Princeton Ocean Model are not specific only to that model. Second, it would also be useful to determine whether additional variables could or should be included in the analysis. Shape of the coastline is one of the variables that is excluded from this study, and it would be interesting to do a cost-benefit analysis to determine

whether adding additional terms would be helpful in obtaining a more accurate index. Third, a more detailed study in quantifying lag time between oceanic momentum input and wave/ocean current equilibrium would be extremely useful. Finally, any improvements in numerical surge models based on the findings in this research would greatly benefit the scientific community and general public. At some point, it is the hope of everyone except surge forecasters that a numerical model will include enough knowledge about storm surge and atmospheric physics that surge forecasts are correct 100 percent of the time. Of course, when that day arrives, the storm surge index derived in this paper will become obsolete; hopefully, that day arrives sooner rather than later.

REFERENCES

Avila, L., 1998: Preliminary Report: Hurricane Bonnie <http://www.nhc.noaa.gov/1998bonnie.html>.

Avila, L., 1999: Preliminary Report: Hurricane Irene <http://www.nhc.noaa.gov/1999irene.html>.

AVISO and PO.DAAC User Handbook, IGDR and GDR Jason Products, CNES/NASA, JPL D21352(PODAAC), Edition 2.0, April, 2003.

Beven, J., 2003: Tropical Cyclone Report: Hurricane Claudette <http://www.nhc.noaa.gov/2003claudette.shtml?>.

Beven, J., and H. Cobb, 2004: Tropical Cyclone Report: Hurricane Isabel <http://www.nhc.noaa.gov/2003isabel.shtml>.

Beven, J., 2004: Tropical Cyclone Report: Hurricane Frances <http://www.nhc.noaa.gov/2004frances.shtml?>.

Beven, J., 2006: Tropical Cyclone Report: Hurricane Dennis <http://www.nhc.noaa.gov/pdf/TCR-AL042005_Dennis.pdf>.

Blake, E., 2007: Tropical Cyclone Report: Hurricane Humberto <http://www.nhc.noaa.gov/pdf/TCR-AL092007_Humberto.pdf>.

Clauset, A., C. R. Shalizi and M. E. J. Newman, 2007: Power-law distributions in empirical data. *SIAM* (in review).

Demuth, J., M. DeMaria, and J.A. Knaff, 2006: Improvement of advanced microwave sounder unit tropical cyclone intensity and size estimation algorithms. *J. Appl. Meteor.*, 45, 1573-1581.

Donelan, M.A., B. K. Haus, N. Reul, W. J. Plant, M. Stiassnie, H. C. Graber, O. B. Brown, and E. S. Saltzman, 2004: On the Limiting Aerodynamic Roughness of the Ocean in Very Strong Winds. *Geo. Res. Letters*, vol 31, L18306, doi:10.1029/2004GL019460.

Edson, J.B., and C.W. Fairall, 1998. Similarity relationships in the marine atmospheric surface layer for terms in the TKE and scalar variance budgets. *J. Atmos. Sci.*, 55: 2311-2328.

Emanuel, K., S. Ravela, E. Vivant and C. Risi. 2006: A Statistical-Deterministic Approach to Hurricane Risk Assessment**.** *Bull. Amer. Meteor. Soc.,* **87**, 299–314.

Franklin, J., D. Brown, and E. Blake, 2005: Tropical Cyclone Report: Hurricane Gaston <http://www.nhc.noaa.gov/2004gaston.shtml?>.

Gerrish, H., 1986: Preliminary Report: Hurricane Bonnie <http://www.nhc.noaa.gov/archive/storm_wallets/atlantic/atl1986-prelim/bonnie/>.

Gerrish, H., 1989: Preliminary Report: Hurricane Chantal <http://www.nhc.noaa.gov/archive/storm_wallets/atlantic/atl1989-prelim/chantal/>.

Guiney, J., 1988: Preliminary Report: Hurricane Florence <http://www.nhc.noaa.gov/archive/storm_wallets/atlantic/atl1988-prelim/florence/>.

Guiney, J., 1998: Preliminary Report: Hurricane Georges <http://www.nhc.noaa.gov/1998georges.html>.

Harris, D.L., 1963. Characteristics of the Hurricane Storm Surge, Technical Paper No. 48, United States Weather Bureau, Washington, D.C., 139 p.

Hebert, C., 2008: Hurricane Severity Index. ImpactWeather.

Holland, G. J., 1980: An analytic model of the wind and pressure profiles in hurricanes. *Mon. Wea. Rev., **108**,* 1212-1218.

Hunter, M., 2006: "Deaths of Evacuees push toll to 1,577." *New Orleans Times Picayune*. 19 May 2006.

Jarvinen, B. J. and C. J. Neumann, 1985: An evaluation of the SLOSH storm surge model. Bull. Amer. Meteor. Soc., **66**, 1408-1411.

Johnson, Richard. *Miller and Freund's Probability and Statistics for Engineers*. Upper Saddle River: Prentice Hall, 2000.

Jones et al., 1993: Evaluation / review of the ODA-financed relief and rehabilitation programmes in Bangladesh following the cyclone of April 1991. Technical Report.

Jordan II, M.R. and C.A. Clayson, 2008a: Evaluating the Usefulness of a New Set of Hurricane Classification Indices. *Mon. Wea. Review*, (in press).

Jordan II, M.R. and C.A. Clayson, 2008b: A New Approach to Using Wind Speed for Prediction of Tropical Cyclone Generated Storm Surge. *Geo. Res. Letters*, (in review).

Kabir, M., B. Saha, J. Hye, 2005: Cyclonic Storm Surge Modelling for Design of Coastal Polder. Institute of Water Modelling.

Kantha, L. H., 2003: On an improved model of the turbulent PLB. *J. Atmos. Sci*., **60**, 2239-2246.

Kantha, L. H., 2006: Time to Replace the Saffir-Simpson Hurricane Scale? *EOS Transactions of the American Geophysical Union,* 87:3,6.

Kantha, L. H., and C. A. Clayson, 1994: An improved mixed layer model for geophysical applications. *J. Geophys. Res*., **99**, 25,235-25,266.

Kantha, L. H., and C. A. Clayson, 1999, Numerical Models of Oceans and Oceanic Processes, *Academic Press*

Kantha, L. H., and C.A. Clayson, 2000: *Numerical Models of Oceans and Oceanic Processes.* International Geophysics Series, Volume 66. Academic Press, pp. 940.

Kantha, L., Rojsiraphaisal, T., and J. Lopez, 2007. The North Indian Ocean circulation and its variability as seen in a numerical hindcast of the years 1993 to 2004. *Progress in Oceanography*, pp 53, (in press).

Knabb, R., J. Rhome, and D. Brown, 2006: Tropical Cyclone Report: Hurricane Katrina <http://www.nhc.noaa.gov/pdf/TCR-AL122005_Katrina.pdf>.

Knabb, R., D. Brown, and J. Rhome, 2006: Tropical Cyclone Report: Hurricane Wilma <http://www.nhc.noaa.gov/pdf/TCR-AL252005_Wilma.pdf>.

Knabb, R., 2008: Personal communication

Lawrence, M., 1989: Preliminary Report: Hurricane Hugo <http://www.nhc.noaa.gov/archive/storm_wallets/atlantic/atl1989-prelim/hugo/>.

Lawrence, M., 1996: Preliminary Report: Hurricane Bertha <http://www.nhc.noaa.gov/archive/storm_wallets/atlantic/atl1996-prelim/bertha/>.

Lawrence, M., 2003: Tropical Cyclone Report: Hurricane Lili <http://www.nhc.noaa.gov/2002lili.shtml>.

Lawrence, M., and H. Cobb, 2005: Tropical Cyclone Report: Hurricane Jeanne <http://www.nhc.noaa.gov/2004jeanne.shtml?>.

Mayfield, M., 1989: Preliminary Report: Hurricane Jerry <http://www.nhc.noaa.gov/archive/storm_wallets/atlantic/atl1989-prelim/jerry/>.

Mayfield, M., 1991: Preliminary Report: Hurricane Bob <http://www.nhc.noaa.gov/archive/storm_wallets/atlantic/atl1991-prelim/bob/>.

Mayfield, M., 1995: Preliminary Report: Hurricane Opal <http://www.nhc.noaa.gov/archive/storm_wallets/atlantic/atl1995-prelim/opal/>.

Mayfield, M., 1996: Preliminary Report: Hurricane Fran <http://www.nhc.noaa.gov/archive/storm_wallets/atlantic/atl1996-prelim/fran/>.

Mayfield, M., 1998: Preliminary Report: Hurricane Earl <http://www.nhc.noaa.gov/1998earl.html>.

Moon, I.-J., T. Hara, I. Ginis, S. E. Belcher, and H. Tolman, 2004. Effect of surface waves on air-sea momentum exchange : I. Effect of mature and growing seas. *J. Atoms. Sci*., 61(19), 2321-2333.

Pasch, R., 1996a: Preliminary Report: Hurricane Allison <http://www.nhc.noaa.gov/archive/storm_wallets/atlantic/atl1995-prelim/allison/>.

Pasch, R., 1996b: Preliminary Report: Tropical Storm Josephine <http://www.nhc.noaa.gov/archive/storm_wallets/atlantic/atl1996-prelim/josephine/>.

Pasch, R., 1997: Preliminary Report: Hurricane Danny <http://www.nhc.noaa.gov/1997danny.html>.

Pasch, R., T. Kimberlain, and S. Stewart, 1999: Preliminary Report: Hurricane Floyd <http://www.nhc.noaa.gov/1999floyd.html>.

Pasch, R., D. Brown, and E. Blake, 2005: Tropical Cyclone Report: Hurricane Charley <http://www.nhc.noaa.gov/2004charley.shtml?>.

Pasch, R., E. Blake, D. Brown, and D. Roberts, 2006: Tropical Cyclone Report: Hurricane Wilma <http://www.nhc.noaa.gov/pdf/TCR-AL282005_Gamma.pdf>.

Powell, M. D., S. H. Houston, L. R. Amat, and N Morisseau-Leroy, 1998: The HRD real-time hurricane wind analysis system. *J. Wind Engineer. and Indust. Aerodyn.* 77&78, 53-64.

Powell, M.D. and T. A. Reinhold, 2007 : "Tropical Cyclone Destructive Potential by Integrated Kinetic Energy.", *Bull. Amer. Meteo. Soc.*,vol. 88 no. 4, pp.513-526.

Rappaport, E., 1993: Preliminary Report: Hurricane Andrew <http://www.nhc.noaa.gov/archive/storm_wallets/atlantic/atl1992-prelim/andrew/>.

Rappaport, E., 1995: Preliminary Report: Hurricane Erin <http://www.nhc.noaa.gov/archive/storm_wallets/atlantic/atl1995-prelim/erin/>.

Russo, Edward. Estimating Storm Surge Amplitudes for the Gulf of Mexico and Atlantic Coastlines of the United States. *Institute of Electrical and Electronics Engineers*. 1998, 1301-1305.

Smith, S., 2006: Carville Hurricane Index. ReAdvisory.

Stewart, S., 2005: Tropical Cyclone Report: Hurricane Ivan <http://www.nhc.noaa.gov/2004ivan.shtml>.

Stewart, S., 2006: Tropical Cyclone Report: Hurricane Cindy <http://www.nhc.noaa.gov/pdf/TCR-AL032005_Cindy.pdf>.

Toner, M., Kirwan, A. D. Jr., Kantha, L., and J.-K. Choi, 2001: Can general circulation models be assessed and enhanced with drifter data? *J. of Geophys. Res.*, 106, 19,653-19,679.

Toner, M., Kirwan, A. D. Jr., Poje, A. C., Kantha, L. H., Muller-Karger, F. E. and C.K.R.T. Jones, 2003: Chlorophyll dispersal by eddy-eddy interactions in the Gulf of Mexico. *J. of Geophys. Res.*, 108(C4), 3105, DOI:10.1029/2002JC001499.

BIOGRAPHICAL SKETCH

Mark Rickman Jordan II was born on August 26, 1982, in Charleston, South Carolina. In 2000, Jordan graduated from Bishop England High School in Charleston, SC, with honors and began college at the University of North Carolina-Asheville in Asheville, North Carolina. While in college, Jordan was a member of Phi Eta Sigma and was President of the university's chapter of the American Meteorological Society. In December 2003, Jordan graduated Summa cum Laude from the University of North Carolina-Asheville with a degree in Atmospheric Sciences. Jordan subsequently began graduate school in January 2004 at Florida State University. He received his M.S. in Meteorology in December 2005 under the direction of Dr. T.N. Krishnamurti. In January 2006, Jordan began work on his Ph.D. under the direction of Dr. Carol Anne Clayson. While completing research for the Ph.D., Jordan taught several undergraduate courses, including Introduction to the Atmosphere, Weather Analysis and Forecasting, and Current Weather Discussion. In August 2008, Jordan will graduate from Florida State University with a Ph.D. in Meteorology.